Evaluation of southern African maize germplasm for phytoalexin accumulation following inoculation by *Fusarium verticillioides*

Amy Veenstra

Thesis presented for the degree of Master of Science

in the Department of Molecular and Cell Biology, Faculty of Science

University of Cape Town

August 2017

Supervisors: Dr Shane Murray and Dr Suhail Rafudeen

Plagiarism declaration

I, Amy Veenstra, know the meaning of plagiarism and declare that all of the work in this thesis, save for that which is properly acknowledged, is my own. Any work that was not performed by me has been referenced using the Harvard-UCT referencing style

Signed: Signed by candidate Date: 14 August 2017

Acknowledgements

I would like to acknowledge the University of Cape Town and the Maize Trust for providing financial support throughout my Msc. degree. I would also like to acknowledge Dr Lindy Rose from Stellenbosch University for providing maize seed for this study. As phytoalexin accumulation was so important for this research, I am deeply grateful to Dr Shawn Christensen at the United States Department of Agriculture (USDA) for performing the analysis for me.

It has been such a pleasure to be a part of the MCB department and to meet so many wonderful people. Specifically, I would like to thank Humaira Lambarey for being so helpful in showing me how to work with *Fusarium verticillioides* and perform inoculations, and Sara Wighard for all of the help that she gave me in the lab. I am so grateful to have worked alongside Naadirah Moola, who was by my side in so many stressful situations. Finally, thank you to Dr Jeanne Korsman for being my go-to for any questions, big or small! I am grateful to have worked with you all and to call you my friends.

Thank you to Dr Suhail Rafudeen, my co-supervisor. Your advice on all aspects of my project has been invaluable. To my supervisor, Dr Shane Murray, thank you for everything! I am so grateful to have worked under such an encouraging, supportive, available and passionate supervisor. I have learnt so much and I am deeply grateful.

To my friends, who put up with me and supported me through the more stressful times of this thesis, thank you, thank you, thank you!! I appreciate it more than I could ever say. Most importantly, thank you to the people that have always been there for me, my family. My big brothers, Simon and Jeremy, and my sister-in-law, Joh-Nell, I look up to you more than you could ever know. To mom and dad, I love you so very much. There are no words to describe how grateful I am for the sacrifices you have made to give all of your children what we need, both physically and emotionally. Thank you for encouraging, supporting and loving me always.

Abstract

Maize is a socially and economically important crop in Africa (and worldwide) that is severely affected by many fungal pathogens. The pathogen *Fusarium verticillioides* causes Fusarium ear rot in maize, a disease that greatly reduces quantity and quality of annual maize yields. The pathogen produces mycotoxins called fumonisins, which have been linked to adverse health effects in both humans and animals. Maize produces terpenoid phytoalexins, which are antimicrobial compounds that directly reduce the growth of many fungal pathogens including *F. verticillioides*. Two families of maize phytoalexins, termed kauralexins and zealexins, have been characterized. Key genes putatively involved in the biosynthetic pathway of these phytoalexins have been identified from the rice model and subsequent studies on maize. This research aimed to evaluate the correlation between phytoalexin accumulation and fungal growth in diverse southern African maize lines in response to *F. verticillioides* inoculation. Maize lines were inoculated with *F. verticillioides* using a seed soak inoculation method and grown *in vitro* for up to two weeks. The harvested tissue was analysed for fungal growth using quantitative PCR, putative phytoalexin biosynthetic gene expression using RT-qPCR and phytoalexin accumulation using gas-chromatography mass spectrometry.

Furthermore, an endophyte growing in one of the maize lines was isolated and identified as *Trichoderma asperellum*. *Trichoderma* spp. are used as biocontrol agents against many fungal pathogens, although research on the specific antagonistic effect of *T. asperellum* on *F. verticillioides* is limited. Phytoalexin accumulation in maize containing endophytic *T. asperellum* was compared to maize inoculated with *F. verticillioides. In vitro* competition assays were performed to analyse the antagonistic effect of *T. asprellum* on *F. verticillioides*.

Results from this study show that inoculation of maize lines with *F. verticillioides* induces the accumulation of total phytoalexins, and more specifically the accumulation of total kauralexins. Putative phytoalexin

biosynthetic genes are also up-regulated in response to inoculation. Maize growing with a *T. asperellum* endophyte accumulated phytoalexins to the same levels as *F. verticillioides*, suggesting that *T. asperellum* induces a defence response that 'primes' the plant for further infection. *In vitro* competition assays between *F. verticillioides* and *T. asperellum* showed that *T. asperellum* significantly inhibits *F. verticillioides* growth.

These results will aid in the identification of maize lines that can be bred with increased resistance to *F. verticillioides* with the goal to reduce *F. verticillioides* incidence in southern Africa. Furthermore, analysis of the efficacy of *T. asperellum* as an antagonist against *F. verticillioides* may provide another method for disease reduction in the field.

List of abbreviations

°C	degrees celsius
ABA	abscisic acid
An2	Anther ear 2
BCA	biological control agent
bp	base pairs
CPP	copalyl diphosphate
CPS	copalyl diphosphate synthase
C_t	cycle threshold
CYP	cytochrome P450
DNA	deoxyribonucleic acid
dpi	days post inoculation
EF1α	elongation factor 1α
FB_1	Fumonisin B_1
FC	fold change
FER	Fusarium ear rot
FPP	farnesyl diphosphate
Fv	*Fusarium verticillioides*
GA	gibberellic acid
GC/MS	gas-chromatography mass-spectrometry
GGPP	geranylgeranyl diphosphate
GST3	glutathione S-transferase III
ITS	internal transcribed spacer
JA	jasmonic acid
KO	kaurene oxidase
KS/L	kaurene synthase/-like
LUG	leunig
MeJA	methyl-jasmonate
MEP	membrane protein PB1A10.07c
MS	Murashige and Skoog
$ng.\mu g^{-1}$	nanograms per microgram
$ng.\mu l^{-1}$	nanograms per microlitre
NTC	no template control
PCR	polymerase chain reaction
PDA	potato dextrose agar
qPCR	quantitative polymerase chain reaction
QTL	quantitative trait locus
RIL	recombinant inbred line
RNA	ribonucleic acid
Rpol	DNA-directed RNA polymerase
RT-qPCR	reverse transcription polymerase chain reaction
SA	salicylic acid
SD	standard deviation
spp.	species
TPS	terpene synthase
TSS	transcription start site
Zm	*Zea mays*
$\mu g.gFW^{-1}$	micrograms per gram fresh weight

List of figures

List of tables

Table of Contents

CHAPTER 1

LITERATURE REVIEW

1.1 Maize introduction

Zea mays (maize) is a cereal crop of great economic importance throughout the world. It is both a direct and indirect food source. The United States of America (USA) is the world's largest producer of maize, followed by China (United States Department of Agriculture, Foreign Agricultural Service, 2017). Maize produced in the USA is mainly used for livestock feed, with a smaller percentage used as a food source (World of Corn, 2017). Sub-Saharan Africa is responsible for six percent of maize production and consumption worldwide (United States Department of Agriculture, Foreign Agricultural Service, 2017).

Although Sub-Saharan Africa is a relatively small player in the global maize industry, maize is the most important crop in the region, as it is the staple food for 50% of the population (MAIZE, 2016). Maize production increased by ~50% between 2004 and 2014 in Southern Africa (Food and Agriculture Organization of the United Nations, 2017). Despite observed increases in production, Sub-Saharan Africa, and particularly central African countries, are at high risk in terms of food insecurity, based on analysis looking at population hunger and reliance on agriculture for their gross domestic production (GDP) (Chakraborty & Newton, 2011). Therefore, maize production needs to increase significantly in order to determine food and economic security in these areas.

Maize production is limited by many different biotic and abiotic stresses. Maize loss predictions due to drought have been estimated at various levels, ranging from 20% by some estimates to 50% by others (Schlenker & Lobell, 2010). Biotic stress, including weeds, animal pests, and pathogens, was shown to reduce maize yields by 31% between 2001 and 2003 (Oerke, 2006). Other estimates indicate that 10-16% of global harvest is lost to plant diseases annually (Strange & Scott, 2005), with an additional 6-12% lost to postharvest diseases and spoilage during storage (Chakraborty & Newton,

2011). Crop production as a whole, of both maize and other important food crops, is threatened by these biotic and abiotic factors.

1.2 Fungal pathogens in maize

Fungal pathogens are biotic stresses that are able to cause significant damage to crop production. Fungal spores are easily spread by water or wind, they often have a short latency period and sporulate prolifically, and they often produce phytotoxic compounds that greatly weaken the plant structure (Strange & Scott, 2005).

Maize is susceptible to a large number of fungal genera, including *Aspergillus, Ustilago* and *Fusarium* (Schmelz et al., 2014). Depending on the fungus, the mode of nutrition and mechanism of infection will differ. Fungi can be classified as biotrophs, hemi-biotrophs or necrotrophs (Agrios, 1997). Biotrophs infect and derive nutrients from living host tissue, while necrotrophs derive nutrition from dead host cells (Glazebrook, 2005). Many fungi are hemi-biotrophs, acting as biotrophs and necrotrophs at different stages of their life cycle (Glazebrook, 2005).

1.3 *Fusarium verticillioides*, Fusarium Ear Rot and fumonisins

Fusarium graminearum (teleomorph name: *Gibberella zeae*) and *Fusarium verticillioides* (previously described as *F. moniliforme*) are two of the most commonly isolated *Fusarium* species from maize globally, and both are hemi-biotrophic (Logrieco et al., 2002). *F. graminearum* is associated with cool, moist conditions, while *F. verticillioides* favours warmer, dry conditions (Sikhakolli et al., 2012; Maschietto et al., 2017). In Africa, *F. verticillioides* appears to be the most prevalent *Fusarium* spp. (Fandohan et al., 2003).

F. verticillioides can greatly affect maize yield and grain quality. *F. verticillioides* infects maize at all stages of development and can infect all tissues including the roots, stalk and kernel (Munkvold, McGee & Carlton, 1997). The fungus can enter the plant via silk infection as well as wounding from insects (Munkvold, 2003a). *F. verticillioides* can also exist as an endophyte and spread systemically, colonising all parts of the plant (Pamphile & Azevedo, 2002). The definition of an endophyte is constantly under revision,

but endophytes can be loosely defined as microbes that colonise internal structures of plants without causing visible disease symptoms (Hyde & Soytong, 2008). Studies have shown that *F. verticillioides* moves from an infected seed to the seedling, into the stalk, then the ear and finally spreading within the ear and kernels (Munkvold, McGee & Carlton, 1997). However, kernel infection was much higher when infected through the silks compared to the seed or the stalk (Munkvold, McGee & Carlton, 1997). The point of *F. verticillioides* entry, maize growth stage and temperature affect colonisation and systemic movement of *F. verticillioides* (Murillo-Williams & Munkvold, 2008). Fluorescence microscopy studies have shown that systemic movement of *F. verticillioides* following seed inoculation does not occur in the early stages of the *F. verticillioides*-maize interaction (Oren et al., 2003). Maize infected with *F. verticillioides* can have varying levels of disease severity, ranging from asymptomatic to severe disease symptoms (Munkvold & Desjardins, 1997; Pamphile & Azevedo, 2002). Maize visibly infected with *F. verticillioides* may develop Fusarium Ear Rot (FER). FER is detectable by white or light pink mould growing on a few or many kernels on a cob (Munkvold, 2003a).

Although FER is the most significant and prevalent disease caused by *F. verticillioides*, it also causes seedling disease, root rot and stalk rot (Munkvold & Desjardins, 1997). Levels of infection and disease severity differ depending on the entry point of the fungus as well as the developmental stage of the plant, with less mature tissues appearing more susceptible to disease (Reid et al., 2002). Although some kernels infected with *F. verticillioides* may not present with FER and don't necessarily reduce yield, they are still cause for concern due to a loss of grain quality (Munkvold & Desjardins, 1997).

Asymptomatic *F. verticillioides* infected kernels are often unfit for human and livestock consumption due to the production of fungal secondary metabolites called mycotoxins (Fandohan et al., 2003; Dutton, 2009). A variety of mycotoxins are produced by different fungal pathogens, including, but not limited to, trichothecenes, zearalenones and fumonisins (Logrieco et al.,

2002). Mycotoxins produced by different fungi can have many adverse effects on human and animal health (Council for Agricultural Science and Technology, 2003). *F. verticillioides* produces a series of fumonisins (A, B, C and P), of which the B series, and particularly fumonisin B_1 (FB_1), is the most active (Logrieco et al., 2002). Fumonisins are detected in symptomatic and asymptomatic maize, although levels in visibly infected maize are considerably higher (Thiel et al., 1992). Fumonisin-nonproducing strains of *F. verticillioides* have been shown to cause FER with the same level of severity as fumonisin-producing strains, suggesting that fumonisins are not necessary for virulence of *F. verticillioides* (Desjardins & Plattner, 2000). Although fumonisins do not appear to contribute to *F. verticillioides* pathogenicity, their accumulation is undesirable due to the health risks that they are associated with.

Administration of FB_1 to horses and pigs resulted in leukoencephelomalacia (LEM) and pulmonary oedema respectively (Harrison et al., 1990; Thiel et al., 1992). Fumonisins have also been correlated with the occurrence of oesophageal cancer in the former Transkei (Eastern Cape, South Africa) (Sydenham et al., 1990) and FB_1 contaminated corn has been identified in regions of China with high incidences of oesophageal and liver cancer (Sun et al., 2007). Fumonisins have also been suggested to be associated with higher risks of neural tube defects *in utero* due to the mechanism of action of fumonisins, which is to disrupt sphingolipid biosynthesis (Marasas et al., 2004). A number of screening methods can be used to determine whether maize is contaminated with fumonisins.

Immunological assays can be used as a quick and easy tool to screen for fumonisins, although this method is non-specific and does not give an indication of fumonisin quantity (Joint FAO WHO Expert Committee on Food Additives, 2012). High Performance Liquid Chromatography (HPLC) and Mass Spectrometry (MS) are commonly used to detect fumonisins in maize and although this method is specific, it is not ideal as it assumes homogenous contamination throughout the maize, which is not often the case (Levasseur-Garcia et al., 2015). Therefore, HPLC-MS requires a large number of samples

in order to correctly represent the fumonisin content of a harvest, and this is both expensive and time-consuming. Recent studies have shown that near-infrared spectrometry (NIRS) can be used to rapidly screen maize for fumonisin contamination, and if this technology is developed, may be a useful tool for maize quality assessment in future (Levasseur-Garcia et al., 2015). The World Health Organisation (WHO) and Food and Agriculture Organisation (FAO) of the United Nations declared the maximum daily limit of fumonisin intake to be 2μg.kg^{-1} body weight (Joint FAO WHO Expert Committee on Food Additives, 2012). This daily limit is particularly worrying for small-scale subsistence farmers in Sub-Saharan Africa who do not necessarily have the resources to combat fungal diseases, and who rely on maize for their staple diet (Dutton, 2009). A comparison between home-grown and commercially-grown maize in Kenya showed that a higher percentage of home-grown samples were contaminated with fumonisins than commercially grown samples (Mutiga et al., 2015). In the case of small-scale farmers in Africa, regulating fumonisin consumption and screening maize for contamination is not a viable option due to the lack of resources. Developing fast and cost-effective screening tools is important for reducing the consumption of highly contaminated maize, but this would also result in reduced food production as a large percentage may be found unfit for consumption. Therefore, reducing the incidence of *F. verticillioides* and fumonisins is most effective for maintaining grain quality, yield and therefore maintaining food security.

Important factors that affect *F. verticillioides* infection include changing climate conditions (drought stress has been associated with increased levels of *F. verticillioides*), point of fungal entry and developmental stage of the plant (Reid et al., 2002; Munkvold, 2003a). Furthermore, the genetic background of the maize affects disease development (Munkvold, 2003a; Small et al., 2012). Managing these factors is important for managing disease development and fumonisin production in infected maize.

1.4 *F. verticillioides* management strategies

Many traditional agricultural practices such as crop rotation, tillage practices, fertilization practices, planting dates and irrigation systems are employed to

combat crop disease (Munkvold, 2003a). A study showed that *F. verticillioides* growth and fumonisin production increase in kernels as they approach physiological maturity and further increase throughout the season until harvest, suggesting that earlier harvest dates would reduce the amount of contamination in the grain (Bush et al., 2004). Although crop rotation and tillage practices have been shown to reduce levels of *F. graminearum* infection in wheat and barley crops, these practices have not been shown to reduce *F. verticillioides* levels in maize (Munkvold, 2003b). *Fusarium* spp., including *F. verticillioides*, colonise crop residues and are extremely resilient, surviving through winter until the next planting season, making them difficult to manage (Binder, 2007). One of the major dispersal and infection mechanisms of *F. verticillioides* is via insects, which wound the maize and allow for infection (Munkvold, 2003a). Therefore, maize that is able to reduce pest damage, such as transgenic Bt maize, is also able to indirectly reduce *F. verticillioides* and fumonisin contamination (Wu, 2006). This has been observed in Bt maize hybrids that have lower incidences of FER than non-Bt hybrids (Bowers, Hellmich & Munkvold, 2014; Ncube et al., 2017). Thus, insect management would be a helpful, indirect tool for FER management in the field. *F. verticillioides* can also survive and produce mycotoxins post-harvest (Pereyra et al., 2008). It is therefore important to keep grain in cool, dry, aerated storage places to minimise postharvest contamination (Munkvold, 2003b; Binder, 2007). Unfortunately, poor agricultural practices, inadequate storage and transport of grain in Africa is common due to a lack of resources, increasing contamination of grain in this region (Wagacha & Muthomi, 2008).

The most favourable practice to reduce the incidence of *F. verticillioides* is by prevention. Although chemical control, such as fungicides to reduce *F. verticillioides* growth and pesticides to reduce insect wounding, is available, it is not always sufficient and is also unfavourable due to the economic burden for farmers and due to environmental concerns (Wagacha & Muthomi, 2008). Research into biological control, using microorganisms that can outcompete or are pathogenic to disease-causing microorganisms, is increasing and this is becoming a popular method for disease resistance (Wagacha & Muthomi, 2008). Aside from these methods, one of the best ways to combat

F. verticillioides is by enhancing plants' innate defence responses and breeding for more resistant lines (Agrios, 1997). Low incidences of FER have been observed in some South African maize inbred lines (Small et al., 2012). Although these maize lines do not exhibit full resistance to *F. verticillioides*, these lines are partially resistant and show that breeding resistant hybrids is a viable practice for reducing *F. verticillioides* incidences.

1.5 Plant defence responses

Plants have a highly complex immune system that is usually induced in the presence of a biotic stress. The cost of constitutive resistance to plants is high, and therefore the balance between growth and defence is mediated by signalling according to the environment (Karasov et al., 2017). The main plant defence model has two pathways: pathogen recognition via microbial-associated or pathogen-associated molecular patterns (MAMPs or PAMPs) that plants detect using transmembrane pattern recognition receptors (PRRs); and the second via resistance (*R*) gene products that recognise pathogenic avirulence (avr) proteins, also known as effectors (Dangl & Jones, 2001; Jones & Dangl, 2006). The first stage of immunity is PAMP-triggered immunity (PTI) and the second is effector-triggered immunity (ETI) (Jones & Dangl, 2006).

The PRRs involved in PTI are made up of large families of receptor-like kinases (RLKs) and receptor-like proteins (RLPs), and different RLK/RLP families have different roles in plant signalling (Tang, Wang & Zhou, 2017). PRRs form complexes with a number of proteins to initiate an immune defence response (Tang, Wang & Zhou, 2017). A part of this signalling pathway is the production of reactive oxygen species (ROS) downstream of RLKs, which is important in mediating the cellular response to the environment (Kimura et al., 2017). ETI occurs when pathogens survive PTI and produce effectors that assist with pathogen virulence (Jones & Dangl, 2006). ETI usually results in a hypersensitive cell death response (HR) at the point of infection, which is not necessarily advantageous to the plant if the pathogen is necrotrophic (Jones & Dangl, 2006).

Plants produce phytohormones as part of PTI and ETI (Vlot, Dempsey & Klessig, 2009). Phytohormones regulate a variety of functions within the plant including, but not limited to, plant growth and development, reproduction, and pathogen defence (Karasov et al., 2017). Salicylic acid (SA) and jasmonic acid (JA) are two well-studied hormones that have been implicated in plant immune responses for many years. As immune responses come at the cost of growth, many phytohormones are involved in growth and development and are also involved in defence responses (Karasov et al., 2017). Auxins, abscisic acid (ABA), ethylene and gibberellic acid (GA), to name a few, interact with each other, SA and JA to elicit an immune response (Robert-Seilaniantz, Grant & Jones, 2011). SA and JA have antagonistic roles, as SA signalling activates hemibiotrophic and biotrophic resistance while JA signalling, which has a synergistic interaction with ethylene, activates necrotrophic resistance, although hormone interactions and functions differ depending on the host, pathogen, and environment (Vlot, Dempsey & Klessig, 2009; Robert-Seilaniantz, Grant & Jones, 2011; Denancé et al., 2013).

One of the largest groups of proteins induced by maize-pathogen interactions are the pathogenesis-related (PR) proteins. These are mostly induced by maize following pathogen attack, but some are constitutively produced during development (Muthukrishnan et al., 2001). PR proteins and their roles in different tissues are diverse. Chitinases and glucanases are among some of the PR proteins induced in response to fungal infection (Pechanova & Pechan, 2015). PR proteins are usually encoded by more than one gene and act together with different PR protein groups, making it more difficult for pathogens to overcome this defence response (Muthukrishnan et al., 2001). In contrast, *R* gene resistance is based on the effect of a single gene on the defence response (Balint-Kurti & Johal, 2009). Single-gene resistance is qualitative, and although single proteins can provide high-level protection to the plant, they are easily overcome by pathogen mutations, particularly in the field (Balint-Kurti & Johal, 2009). Therefore, polygenic defence, which is associated with quantitative resistance and provides an intermediate but robust form of protection for plants in the field, is more favourable (Balint-Kurti & Johal, 2009).

1.6 Quantitative resistance

Quantitative resistance is the result of polygenic expression of defence-related genes. A number of genes encoding a specific polygenic trait, such as flowering or resistance, can often be found clustered in a region of the genome termed a quantitative trait locus (plural: loci) (QTL) (Poland et al., 2009). One of the limitations of qualitative resistance is that it often results in HR, a cell death response, which is useful in combatting biotrophic infection, but does not work on necrotrophic pathogens (Poland et al., 2009). In this case, quantitative resistance and QTL may be useful in resistance against necrotrophic pathogens, as well as rapidly mutating pathogens. Individual QTL often have small-effects on a phenotype, but because many QTL contributing to a trait may be present in a plant, the effects are often additive (Ding et al., 2008; Maschietto et al., 2017). Although the positions of many QTL have been identified, few QTL have been cloned and therefore the molecular mechanisms underlying QTL are still unknown.

QTL are identified using the progeny of recombinant inbred line (RIL) populations, developed from parents that often have differing traits, as well as nested associated mapping (NAM) populations and genome-wide association (GWA) mapping populations, which allow for many lines to be mapped and studied for QTL analysis (Corwin & Kliebenstein, 2017). Mapping QTL is highly complex due to the diversity of maize genotypes, as well as external factors. The stage of plant development and environmental factors have been shown to affect the QTL mapping process (Ding et al., 2008; Corwin & Kliebenstein, 2017). Interestingly, some QTL mapped to plant developmental stages have also been associated with disease resistance, showing an overlap between the two traits (Maschietto et al., 2017). This may suggest a reason for the difference in disease severity seen at different developmental stages of the plant (Reid et al., 2002). A study looking for QTL associated with FER disease severity and FB_1 accumulation identified a number of QTL that were associated with both traits, suggesting that there is an overlap between the mechanisms underlying these two traits (Maschietto et al., 2017). Furthermore, a meta-analysis of previous QTL studies found a number of QTL associated with FER, Aspergillus ear rot (AER) and Graminearum ear rot

(GER) that were clustered in the same chromosome region, showing once again that QTL can contribute to more than one trait (Xiang et al., 2010).

Some QTL can be described as expression QTL (eQTL) – these are regions of the genome that do not contribute to a trait by genetic variation but by regulating the expression of genes associated with different traits (Michaelson, Loguercio & Beyer, 2009). eQTL can regulate expression of genes located near to the eQTL (*cis*-eQTL) or distant to the gene (*trans*-eQTL) (Hansen, Halkier & Kliebenstein, 2008). A study identified a number of *trans*-eQTL hotspots that coincide with QTL for grey leaf spot (GLS) disease in maize, showing that both variation in gene expression as well as direct genotypic variation contribute to phenotypic variation (Christie et al., 2017).

A combination of transcriptomics studies and QTL mapping are useful in identifying candidate genes contributing to a specific trait, such as disease resistance. Transcriptomics studies such as RNA-sequencing and microarray assays provide information about gene expression, while QTL mapping can identify regions in the genome contributing to a specific trait (Lanubile et al., 2014; Christie et al., 2017). Combining this information, one can identify important genes within a QTL that may be differentially expressed, thereby possibly contributing to the trait (Maschietto et al., 2017). Many QTLs associated with disease resistance appear to have genes encoding proteins involved in defence, including defensins, PR proteins and secondary metabolites (Corwin & Kliebenstein, 2017).

1.7 Secondary metabolites: phytoalexin biosynthesis

Secondary metabolites are compounds that are involved in plant processes that are not necessary for day-to-day plant survival and development. Plants produce a number of secondary metabolites in response to pathogen attack, including, but not limited to, flavonoids, phenolics and terpenoids (Meyer, Murray & Berger, 2016). Terpenoids constitute a large and structurally diverse group of secondary metabolites that are involved in direct and indirect resistance to both biotic and abiotic stress (Cheng et al., 2007). Terpenoid phytoalexins are secondary metabolites that are low molecular weight,

antimicrobial compounds that are synthesised and accumulate in plants in response to biotic and abiotic stress (VanEtten et al., 1994). Terpenoid phytoalexins accumulate in response to pests and pathogens in a number of crop plants, including grapevine, legumes and cereals, all of which produce diverse phytoalexins (Ahuja, Kissen & Bones, 2012). As well as induction by pests, pathogens and abiotic stresses, phytoalexins are also produced at basal levels in some tissues. Phytoalexins accumulate in uninfected maize plants in the scutellum and ten day old seedlings, suggesting that as well as for defence, they are expressed constitutively at certain points in development (Huffaker et al., 2011; Schmelz et al., 2011). In maize, the two classes of terpenoid phytoalexins identified thus far are the diterpenoid kauralexins and the sesquiterpenoid zealexins (Huffaker et al., 2011; Schmelz et al., 2011). Maize phytoalexins are a group of non-volatile terpenes that provide direct defence against pests and pathogens (Cheng et al., 2007; Schmelz et al., 2014). Studies focusing on maize-specific phytoalexins have emerged relatively recently, but much progress on the role and biosynthetic pathways of kauralexins and zealexins has already been made. The initial kauralexin biosynthetic model was based on diterpenoids produced in rice, a model cereal crop that has been studied for some time (Peters, 2006).

A number of diterpenoid phytoalexins, specifically momilactones, oryzalexins and phytocassanes, amongst others, are produced and accumulate to the site of pathogen infection or herbivory in rice (Peters, 2006). Diterpenoid phytoalexin synthesis occurs via a series of cyclisation reactions of the diterpenoid precursor (*E,E,E*)-geranylgeranyl diphosphate (GGPP) (Peters, 2006; Schmelz et al., 2014). GGPP is a universal diterpenoid precursor of phytoalexins, but is also a precursor for the phytohormone gibberellic acid (GA) (Harris et al., 2005). GGPP is converted to copalyl diphosphate (CPP) by a copalyl diphosphate synthase (CPS), and the downstream product is determined by the biosynthetic enzyme as well as the stereoisomeric structure of CPP (Harris et al., 2005; Schmelz et al., 2014). Terpene synthases (TPS), and specifically kaurene synthases (KS) and kaurene synthase-like (KSL) proteins convert CPP to *ent*-kaurene (Schmelz et al., 2014). KS are involved in the GA biosynthesis pathway, and KSL proteins are

involved in the phytoalexin biosynthesis pathway (Schmelz et al., 2014; Fu et al., 2016). Cytochrome P450s (CYPs) are involved in the oxidation of *ent*-kaurene to produce either GA or terpenoid phytoalexins depending on the enzymatic activity (Schmelz et al., 2014).

Six diterpenoid compounds have been found in maize thus far, and they are termed kauralexin A1, A2, A3, B1, B2 and B3 (Schmelz et al., 2011). The precursors and intermediates involved in maize kauralexin biosynthesis and the enzymes that are involved in catalysing the cyclisation reactions are related to those in rice (Schmelz et al., 2014). In maize, two CPS have been identified and while both are involved in CPP synthesis from GGPP, their downstream products differ (Harris et al., 2005). The first CPS is Anther ear 1 (*ZmAn1*) and is involved in GA biosynthesis (Bensen et al., 1995), and the second CPS is *ZmAn2* and is involved in diterpenoid kauralexin accumulation (Harris et al., 2005). *ZmAn2* is induced following fungal inoculation, while *An1* is not, suggesting that *An1* and *ZmAn2* have separate roles, although *ZmAn2* may partially compensate CPP production when *An1* is mutated (Bensen et al., 1995; Doehlemann et al., 2008; Schmelz et al., 2011). *TPS* genes that are up-regulated following fungal inoculation include *ZmTPS1*, *ZmKSL2* and *ZmKSL4* (Lanubile et al., 2014; Christie et al., 2017; Lambarey, 2017).
ZmTPS1 has been shown to have a closely related expression pattern with *ZmAn2* (Fu et al., 2016), while *ZmKSL2* and *ZmAn2* have also been shown to be co-expressed (Christie et al., 2017). As *ZmKSL4* is up-regulated following inoculation, it is likely that it is also involved in the kauralexin pathway. Although functional analysis on this gene has not yet been performed, it has been suggested that it may be involved in the production of *ent*-isokaurene from CPP (Fu et al., 2016). *Ent*-kaurene and *ent*-isokaurene are two intermediates formed from CPP, and are upstream of the kauralexin A's and kauralexin B's respectively (Fu et al., 2016). CYPs are putatively involved in the oxidation of *ent*-kaurene and *ent*-isokaurene to kauralexins, and in particular a kaurene oxidase gene (*ZmKO*) has been shown to be up-regulated following fungal inoculation and co-expressed with *ZmAn2* and *ZmKSL2* (Christie et al., 2017). Another CYP, *CYP81A1*, is also up-regulated following fungal inoculation (Lanubile et al., 2014; Christie et al., 2017;

Lambarey, 2017). Although the exact role of this CYP in this pathway is still unknown, it is likely to be involved in the oxidation of intermediates into terpenoid phytoalexins, be it kauralexins or zealexins. The maize kauralexin biosynthetic pathway is shown in Figure 1.1.

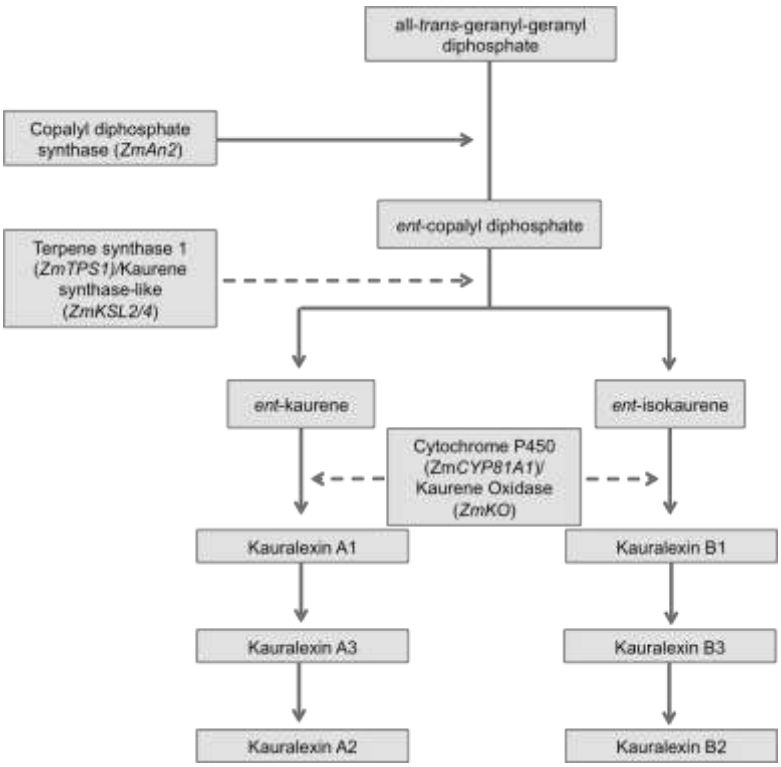

Figure 1.1 The maize kauralexin biosynthetic pathway. Dashed arrows represent enzymes with a putative role in the pathway. Figure adapted from pmn.plantcyc.org [Accessed July 2017]

Much like kauralexins, zealexin biosynthesis is the result of a series of cyclisation events. Zealexins are products formed downstream of the isoprenoid precursor farnesyl diphosphate (FPP) (Degenhardt, Köllner & Gershenzon, 2009). Terpene synthases, of which there are many, are responsible for converting FPP to a variety of volatile sesquiterpenes including, but not limited to, (*E*)-β-farnesene, α-copaene and β-bisabolene (Köllner et al., 2004). Volatile sesquiterpenes accumulate in plants following herbivory and attract predators of pests as an indirect defence mechanism (Schnee, 2002; Schnee et al., 2006; Köllner, Gershenzon & Degenhardt, 2009). For zealexin production, FPP is converted to (*S*)-β-bisabolene by terpene synthases 6 and 11 (TPS6/TPS11), which are also responsible for catalysing the conversion of (*S*)-β-bisabolene to (*S*)-β-macrocarpene (Köllner

et al., 2008). Following the production of the volatile sesquiterpene intermediates, a cytochrome P450, recently identified as CYP71Z18, is involved in the oxidation of (*S*)-β-macrocarpene to zealexin A1 (Mao et al., 2016). The full biosynthetic pathway for the other zealexin compounds, zealexin A2, A3 and B1, is not yet known. The maize zealexin biosynthetic pathway is shown in Figure 1.2.

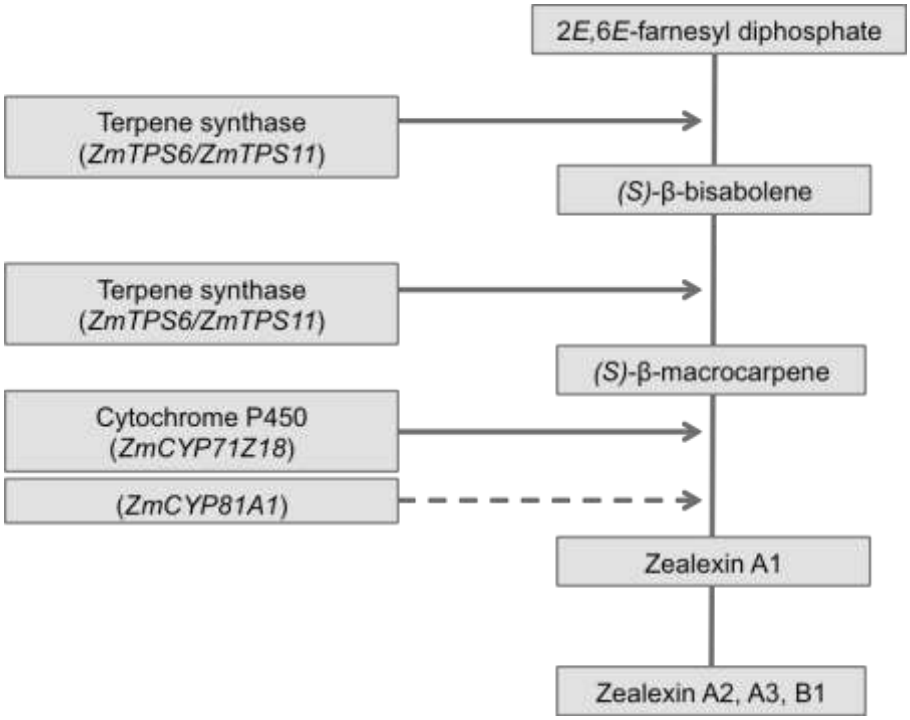

Figure 1.2 The maize zealexin biosynthetic pathway. Dashed arrows represent enzymes with a putative role in the pathway. Figure adapted from pmn.plantcyc.org [Accessed July 2017]

1.8 Phytoalexin activity

Phytoalexins act both directly and indirectly to elicit a defence response against pests and pathogens, as well as to resist abiotic stresses. Kauralexins have been shown to accumulate following infection by *Cercospora zeina* (Christie et al., 2017), *F. verticillioides* (Vaughan et al., 2015), *Rhizopus microsporus, Colletotrichum graminicola, F. graminearum,* as well as by *Ostilago nubilalis* herbivory (Schmelz et al., 2011). However, the levels of kauralexin accumulation, as well as the specific kauralexin compounds induced, differ depending on the infecting pathogen or pest (Schmelz et al., 2011). For example, *R. microsporus* infection resulted in higher kauralexin accumulation than *C. graminicola*, and kauralexins A3 and B3 were the most

highly induced kauralexins, while kauralexins A1, B1, B2 and B3 accumulated to significantly higher levels than the control following *O. nubilalis* feeding (Schmelz et al., 2011). In short- and long-term feeding and infection assays, it was found that kauralexins accumulated to higher levels the longer the biotic challenging occurred, showing that time is an important factor for kauralexin biosynthesis and accumulation (Schmelz et al., 2011). Kauralexins also accumulate in response to drought and salinity stress (Vaughan et al., 2015).

Prior to kauralexin accumulation, *ZmAn2* was highly induced by *F. graminearum* (Harris et al., 2005) and *Ustilago maydis* infection (Doehlemann et al., 2008), indicating that the gene is involved in kauralexin biosynthesis. Mutant *Zman2* plants had reduced *ZmAn2* transcript levels and displayed reduced kauralexin accumulation, resulting in increased susceptibility to drought (Vaughan et al., 2015). *Zman2* mutants also displayed reduced kauralexin accumulation and increased susceptibility to *F. verticillioides*, providing further functional analysis for the role of *ZmAn2* in kauralexin biosynthesis (Wighard, 2017). As well as the induction of biosynthetic enzymes, increased JA and ethylene levels preceded kauralexin accumulation, suggesting that these phytohormones are involved in kauralexin induction (Schmelz et al., 2011). This role was observed when maize was treated with exogenous JA and ethylene, which significantly increased kauralexin accumulation (Schmelz et al., 2011). Although kauralexin accumulation is influenced by JA and ethylene levels, it is not dependent on phytohormone signalling, and accumulation is most likely regulated by β-glucan elicitors (Schmelz et al., 2014).

Much like kauralexins, zealexin accumulation is induced by biotic and abiotic stresses and is preceded by *ZmTPS6* and *ZmTPS11* transcript accumulation, as well as JA and ethylene (Huffaker et al., 2011). Volatile compounds, including the zealexin intermediates (*S*)-β-bisabolene and (*S*)-β-macrocarpene, were emitted from *Fusarium*-infected maize, and their emission correlated with *ZmTPS6/ZmTPS11* transcript accumulation (Becker et al., 2014). Furthermore, virus-induced gene silencing (VIGS) showed that maize was more susceptible to *U. maydis* when *ZmTPS6/ZmTPS11* was

silenced, providing functional genomic evidence for the role of these genes in the defence response (van der Linde et al., 2011). *ZmCYP71Z18* was also induced following *F. graminearum* inoculation and *ZmCYP71Z18* expression increased for a longer period of time than *ZmTPS6/ZmTPS11*, probably since its role is downstream of *ZmTPS6/ZmTPS11* (Mao et al., 2016). *ZmCYP71Z18* was also shown to be involved in the oxidation of (*S*)-β-macrocarpene *in vitro* (Mao et al., 2016). Fungi that have been shown to induce zealexin accumulation include *F. graminearum, R. microsporus, Cochliobolus heterosporus, Colletotrichum sublineolum, U. maydis*, *A. flavus* (Huffaker et al., 2011) and *F. verticillioides* (Vaughan et al., 2015). In a similar response to that shown for kauralexin accumulation, *C. graminicola* did not induce zealexins following infection (Huffaker et al., 2011). Therefore, zealexin accumulation is dependent on the infecting agent, as are the specific zealexin compounds that are induced (Huffaker et al., 2011). Interestingly, both mycotoxin and mycotoxin non-producing strains of fungi induce zealexins to the same level (Huffaker et al., 2011). As well as induction by fungal infection, zealexins accumulate in response to drought and salinity stress (Vaughan et al., 2015). Studies show that generally, herbivory and abiotic stress, such as drought and salt stress, induce higher accumulation of kauralexins than zealexins, while fungal pathogens induce the opposite response (Huffaker et al., 2011; Vaughan et al., 2015).

Kauralexins and zealexins provide direct and indirect defence against pests and pathogens. Exogenous treatment of fungal cultures with kauralexins and zealexins directly reduced fungal growth (Huffaker et al., 2011; Schmelz et al., 2011; Vaughan et al., 2014). In a choice feeding assay, feeding on kauralexin-treated stems was greatly reduced compared to an untreated stem, but feeding on kauralexin-treated stems in a non-choice assay did not affect the growth or health of *O. nubilalis* (Schmelz et al., 2011). Therefore, kauralexins act as anti-feedants to pests but are not necessarily harmful.

Phytoalexin accumulation is localised to the site of infection/herbivory, although systemic signalling may influence the levels of accumulation in distant tissues (Huffaker et al., 2011; Vaughan et al., 2015). For example,

phytoalexins have been shown to accumulate in roots in response to drought stress. However, when drought stressed plants were inoculated with *F. verticillioides* in aboveground tissue, phytoalexin accumulation in the roots was lower than uninoculated drought stressed plants (Vaughan et al., 2015). Additionally, *F. verticillioides* inoculation in maize stalks induced more total phytoalexins in the stalks in watered plants than drought-stressed plants, which also accumulated in the roots (Vaughan et al., 2015). These results show that although phytoalexin accumulation is localised, the defence response may affect distant tissues.

1.9 Biological control

Another aspect of plant disease resistance is to seek aid from external sources. While chemicals have been used for years to reduce crop diseases, this is a burden on both the economy and environment (Wagacha & Muthomi, 2008). In recent years, more focus has been put on introducing biological control agents into the field. A number of microorganisms exist in the rhizosphere and interact with each other and the plant (Heydari & Pessarakli, 2010).

A variety of bacterial and fungal microorganisms have been shown to have antagonistic effects on pathogenic fungi. *Bacillus amyloliquefaciens* and *Microbacterium oleovorans* have been shown to reduce *F. verticillioides* colonisation and fumonisin content in maize (Pereira, Nesci & Etcheverry, 2007). Atoxigenic strains of *A. flavus* (Atehnkeng et al., 2008) and *F. verticillioides* (Luongo et al., 2005) have been shown to reduce mycotoxin accumulation when co-inoculated with their respective toxigenic strains compared to controls inoculated with the toxigenic strain only. One of the advantages of using atoxigenic strains of the same infecting pathogen is that they are adapted to survive in the same environment. However, in the case of *F. verticillioides*, because fumonisins are not necessary for virulence, using atoxigenic strains reduces mycotoxin accumulation but does not reduce FER incidence (Desjardins & Plattner, 2000; Wagacha & Muthomi, 2008). One of

the most common fungal biological control agents (BCA) used commercially is *Trichoderma* spp. (Benítez et al., 2004).

Trichoderma spp. used for BCAs include, but are not limited to, *T. asperellum* (Steyaert, Weld & Stewart, 2010), *T. harzianum*, *T. viride* and *T. virens* (Benítez et al., 2004). In order for antagonistic fungi to be successful, it is very important that the micro-climate in the rhizosphere and the mode of colonisation is favourable (Luongo et al., 2005). These factors are often not a problem for *Trichoderma* spp., as they are often able to survive in unfavourable conditions and have a high reproductive capacity (Benítez et al., 2004). They also have advanced and efficient methods of nutrient uptake. In cultivated, aerobic soils, iron is present in the ferric form (Fe^{3+}), which is not readily available for plant uptake (Colombo et al., 2014). However, *Trichoderma* are able to produce siderophores that chelate iron and make it more readily available for plant uptake (Benítez et al., 2004; Harman, Howell, et al., 2004). *Trichoderma* spp. have many beneficial effects on the plants whose roots they colonise. *Trichoderma* spp. can have fertilization effects on plants, and studies have shown that *T. harzianum* root colonisation can enhance root and shoot growth in tomatoes and maize (Tucci et al., 2011; Saravanakumar et al., 2017). *T. harzianum* seed treatment increased the germination and vigour index of maize in the laboratory and enhanced growth in the field, and it had the same or better effect on plant growth than a chemical fungicide (Chandra Nayaka et al., 2010). Another *Trichoderma* spp., *T. asperellum,* has been shown to enhance rice yields and grain weight (de França et al., 2015; Charoenrak & Chamswarng, 2016). Although the exact growth factors produced by *Trichoderma* spp. are not yet known, it is possible that an up-regulation of proteins involved in carbohydrate metabolism is associated with enhanced plant growth in maize (Shoresh & Harman, 2008). As well as enhancing plant growth, *Trichoderma* spp. is effective in reducing colonisation of pathogenic fungi.

Trichoderma spp. are able to directly influence bacterial and fungal pathogen growth in the rhizosphere in a number of ways (Leelavathi, Vani & Reena, 2014). *Trichoderma* spp. are extremely efficient at nutrient uptake and are

therefore able to outcompete other fungi (Vos et al., 2015). They are also able produce and secrete enzymes such as hydrolytic enzymes, antibiotics and secondary metabolites that are toxic to pathogens in the rhizosphere (Benítez et al., 2004). Sesquiterpenes are included in the secondary metabolites synthesised by *Trichoderma* spp. and they have been shown to display antibacterial and antifungal activity (Cardoza et al., 2005). *Trichoderma* spp. can also interact directly with the pathogen via mycoparasitism, a complex interaction that involves pathogen recognition, production of endochitnases toxic to the pathogen, followed by physical attachment of *Trichoderma* spp., whereby cell-wall-degrading enzymes are produced and break down the pathogen's cell walls (Benítez et al., 2004; Harman, Howell, et al., 2004). They have also been shown to indirectly reduce herbivory by attracting pest parasitoids (Coppola et al., 2017).

In vitro studies have shown that *Trichoderma* spp. inhibit growth of pathogenic fungi. Specifically, *T. harzianum* inhibited *F. verticillioides* growth by over 50%, while *T. asperellum* has been shown to inhibit *F. oxysporum* growth (Chandra Nayaka et al., 2010; El Komy et al., 2015). The latter grew over the pathogenic fungus and microscopy revealed abnormal hyphal morphology and mycelial lysis of *F. oxysporum* at the region where the fungi interacted (El Komy et al., 2015). *T. longibrachiatum, T. hamatum,* and *T. pseudokoningii* inhibited *F. verticillioides* and a bioactive fungal extract of secondary metabolites from *T. harzianum* reduced *F. graminearum* growth significantly (Sobowale et al., 2005, 2010; Saravanakumar et al., 2017). *Trichoderma* spp. also proved to be efficient in reduction of pathogenic fungi in the field.

Tomato leaves inoculated with *Botrytis cinerea* had smaller, delayed lesions when *T. harzianum* colonised the plant roots than when no colonisation occurred (Tucci et al., 2011). *T. virens* has been shown to reduce disease severity of *Rhizoctonia solani* in cotton plants (Harman, Howell, et al., 2004). In rice, the incidences of sheath blight caused by *R. solani,* and dirty panicle disease, caused by a number of fungi, were significantly reduced following *T. asperellum* treatment (Chen et al., 2015; de França et al., 2015; Charoenrak & Chamswarng, 2016). In maize, *T. harzianum* has been effective

in reducing *Colletotrichum graminicola* colonisation on maize leaves and *Pythium ultimum* in the field (Harman, Petzoldt, et al., 2004). *F. verticillioides* growth was also reduced in the field following *T. harzianum* treatment (Sobowale et al., 2007; Chandra Nayaka et al., 2010). Although *Trichoderma* spp. were effective in reducing pathogenic fungal growth in many incidences, antagonistic efficacy is determined by the *Trichoderma* isolate used as well as the host genotype (Harman, Petzoldt, et al., 2004; Chandra Nayaka et al., 2010; Tucci et al., 2011). Interestingly, although *Trichoderma* spp. colonise the roots, they are able to reduce pathogenic growth in distant tissues, such as the leaves, suggesting that they are involved in inducing a systemic defence response (Harman, Howell, et al., 2004).

When *Trichoderma* spp. initially colonises roots, the plants respond as they would to any invading pathogen – by inducing a defence response. This response is referred to as an induced systemic response (ISR), and results in the production of secondary metabolites, an up-regulation of *PR* genes and an initiation of phytohormone signalling (Tucci et al., 2011; Vos et al., 2015; Patel et al., 2017). As well as the production of their own antimicrobial terpenoids (Cardoza et al., 2005), *Trichoderma* spp. has also been shown to induce plant terpenoid production, as seen by the induction of phytoalexins in cucumbers following *T. asperellum* inoculation (Yedidia et al., 2003). *Trichoderma* spp. are resistant to many of the compounds produced by plants following defence initiation, although cell wall material deposition and the production of phenolics limits the *Trichoderma* growth to a small area of the root (Benítez et al., 2004; Vos et al., 2015). This limited colonisation 'primes' the plant for defence against further colonisation by pathogenic fungi.

The ability of *Trichoderma* spp. to directly inhibit fungal pathogens as well as induce a systemic plant response shows that they are a viable management strategy for crop defence. However, the genetic variation of *Trichoderma* spp. and the plant host means that the interaction between the two is more complex than what is known so far. The combination of *Trichoderma* spp. as a BCA as well as breeding maize for enhanced resistance could provide excellent protection for maize crops with further studies in these two fields.

1.10 Aims and objectives

The aims of this study were two-fold:

1. To determine whether phytoalexin accumulation is induced by *F. verticillioides* in diverse southern African maize lines.
2. To determine whether *T. asperellum,* isolated as an endophyte from maize seeds, affects the maize phytoalexin response and whether *T. asperellum* inhibits the growth of *F. verticillioides in vitro*.

The objectives for aim 1 were as follows:

- To obtain a selection of southern African maize lines and to grow the seedlings following *F. verticillioides* inoculation.
- To analyse the extent of disease resistance of inoculated maize lines by scoring the phenotypic disease symptoms of the plant and by quantifying fungal growth using qPCR.
- To analyse the defence response of inoculated maize lines by measuring accumulation of phytoalexins using gas chromatography mass spectrometry (GC/MS) and expression of candidate phytoalexin biosynthesis genes using RT-qPCR.

The objectives for aim 2 were as follows:

- To isolate and identify *Trichoderma* spp. growing as an endophyte in the maize line ZM401.
- To determine the phytoalexin accumulation profiles of maize containing endophytic *Trichoderma* sp. compared to that of maize inoculated with *F. verticillioides.*
- To analyse the ability of *T. asperellum* to inhibit growth of *F. verticillioides in vitro.*

CHAPTER 2

INTRODUCTION

Plants are constantly exposed to biotic and abiotic stresses, and in crop plants these stresses can greatly reduce grain yield and quality. *Fusarium verticillioides* is a hemi-biotrophic fungus that can cause Fusarium ear rot (FER) in maize, but also produces mycotoxins called fumonisins, which are harmful to human and animal health (Thiel et al., 1992; Munkvold, 2003a; Glazebrook, 2005). *F. verticillioides* infection may affect the physical development of maize, but also has an effect on the plant's defence response.

Following pathogen attack, a defence response in maize is induced, which includes phytohormone signalling, up-regulation of PR proteins and secondary metabolites such as phytoalexins (Corwin & Kliebenstein, 2017). Phytoalexins in maize, specifically kauralexins and zealexins, accumulate in response to a number of different fungal pathogens and herbivory, as well as to abiotic stress such as drought (Huffaker et al., 2011; Schmelz et al., 2011; Vaughan et al., 2015). Treatment of some fungi with kauralexins and zealexins resulted in reduced fungal growth, and phytoalexin accumulation appears to act as an anti-feedant to herbivores (Huffaker et al., 2011; Schmelz et al., 2011). Kauralexins and zealexins are derived from (*E,E,E*)-geranylgeranyl diphosphate (GGPP) and farnesyl diphosphate (FPP) respectively (Peters, 2006; Degenhardt, Köllner & Gershenzon, 2009). Their synthesis is the result of a number of cyclisation reactions from their respective precursor, catalysed by a variety of enzymes.

Kauralexins are synthesized when GGPP is converted to copalyl diphosphate (CPP) by a copalyl diphosphate synthase called Anther ear 2 *(ZmAn2)* (Harris et al., 2005). The role of *ZmAn2* in kauralexin biosynthesis was shown in *Zman2* mutants, which had reduced kauralexin accumulation as a result of knock-down *Zman2* (Vaughan et al., 2015). Terpene synthases (TPS) are involved in terpenoid synthesis. In the kauralexin biosynthetic pathway, TPS include kaurene synthase-like (KSL) proteins (Fu et al., 2016). *ZmKSL2* and *ZmTPS1* are putatively involved in the conversion of CPP to *ent*-kaurene, and *ZmKSL4*, which has been shown to be up-regulated following *F. verticillioides* inoculation, is likely involved in the pathway, and has been

suggested to be a part of the conversion of CPP to *ent*-isokaurene (Fu et al., 2016; Christie et al., 2017; Lambarey, 2017). Cytochrome P450 monooxygenases, including kaurene oxidase (KO) and a cytochrome P450 (CYP81A1), are putatively responsible for the oxidation of *ent*-kaurene to kauralexins A1, A2, A3, B1, B2 and B3 (Figure 1.1). *ZmAn2*, *ZmKSL2* and *ZmKO* are co-expressed and are associated with a *trans*-eQTL on chromosome 8 (Christie et al., 2017) that may contain genes responsible for their regulation. The co-expression of these three genes has been linked to kauralexin accumulation (Christie et al., 2017). Zealexins are synthesized from FPP, which is converted to (*S*)-β-bisabolene by TPS6/TPS11. TPS6/TPS11 are also responsible for catalysing the conversion of (*S*)-β-bisabolene to (*S*)-β-macrocarpene (Köllner et al., 2008). Following the production of the volatile sesquiterpene intermediates, a cytochrome P450, recently identified as CYP71Z18, is involved in the oxidation of (*S*)-β-macrocarpene to zealexin A1 (Mao et al., 2016). The full biosynthetic pathway for the other zealexin compounds, zealexin A2, A3 and B1, is not yet known (Figure 1.2).

The aim of this chapter was to determine whether phytoalexin accumulation is induced by *F. verticillioides* in diverse maize lines. Bioinformatics analysis of genes putatively involved in phytoalexin biosynthesis was performed and the promoter sequences of *ZmAn2, ZmKSL2* and *ZmKO* were analysed for regulatory elements corresponding to all three genes that may be responsible for their co-expression. The defence response of three maize lines, B73, CML444 and CB248 was analysed by measuring *F. verticillioides* growth and phytoalexin accumulation in the maize lines. Phenotype analysis of disease symptoms and severity in control and inoculated plants was performed in order to observe the effect that *F. verticillioides* has on the phenotype of the maize lines. DNA extracted from inoculated maize tissue was analysed using both fungal-specific and plant-specific primers in a quantitative PCR assay in order to determine the amount of *F. verticillioides* DNA present in the maize DNA (Boutigny et al., 2012; Korsman et al., 2012). Phytoalexin accumulation was measured using gas-chromatography mass-spectrometry (GC/MS) (Huffaker et al., 2011; Schmelz et al., 2011). Lastly, gene expression of *ZmAn2*, *ZmKSL2, ZmKO, ZmKSL4, ZmCYP81A1* and *ZmTPS11* was measured using RT-qPCR to provide information about the activity of the putative phytoalexin biosynthetic enzymes following *F. verticillioides* inoculation.

MATERIALS AND METHODS

2.1.1 Fungi and Maize growth conditions

Fusarium verticillioides strain MRC826 (Gelderblom et al., 1988) was grown on potato dextrose agar (PDA) at 30°C for 7-8 days until conidiospores were produced.

Maize plants were grown in the Department of Molecular and Cell Biology (MCB) at the University of Cape Town (UCT). Seeds from diverse lines were sourced from Dr. Lindy Rose (Stellenbosch University), Professor Brad Flett (Agricultural Research Council Grain Crops Institute), Dr. Bridget Crampton (University of Pretoria) and National Tested Seeds (Jean Ntuli - Harare, Zimbabwe) (Table 2.1).

Table 2.1 Maize lines used in this study

Maize line	Seed source	Seed origin
B73	Bridget Crampton (UP)	Iowa State University (USA)
CB222	Lindy Rose (SU)	ARC-GCI (South Africa)
CB248	Lindy Rose (SU)	ARC-GCI (South Africa)
CML182	Lindy Rose (SU)	CIMMYT (Zimbabwe)
CML444	Bridget Crampton (UP)	ARC-GCI (South Africa)
R119W	Lindy Rose (SU)	ARC-GCI (South Africa)
R2565Y	Lindy Rose (SU)	CIMMYT (Zimbabwe)
RO549 W	Lindy Rose (SU)	CIMMYT (Zimbabwe)
US2540W	Lindy Rose (SU)	ARC-GCI (South Africa)
VO617Y-2	Lindy Rose (SU)	CIMMYT (Zimbabwe)
ZM401	Jean Ntuli (UCT)	CIMMYT (Zimbabwe)

Seeds were surfaced sterilised in 100% ethanol for one minute, followed by 15 minutes in 50% commercial bleach. Seeds were washed with sterile water five times and left to soak for one hour. Seeds were inoculated in a 2% (volume/volume) Tween 20 solution containing $1x10^3$ conidiospores.ml^{-1} according to Oren et al. (2003). Control seeds were treated in the same way as the inoculated seeds, but *F. verticillioides* conidiospores were omitted from the 2% Tween solution. Two rows of four seeds were seeded in 6L tubs containing 600ml MS media (Highveld Biological, Johannesburg, South Africa) using sterile forceps. All work with *F. verticillioides* was performed in the ESCO Class II Biosafety cabinet (Esco,

Singapore). Maize was grown in a plant growth chamber (Percival Scientific, Iowa, United States) at 28°C on a 16 hour light/8 hour dark cycle.

Maize was grown for 5, 10 and 14 days, after which roots and shoots were harvested separately and flash frozen in liquid nitrogen. Three biological replicates were harvested for each treatment, and one biological replicate was represented by two plants with pooled tissue to reduce variation. Tissue was ground to powder form in a pestle and mortar using liquid nitrogen and the tissue was stored at -80°C until further use.

2.1.2 Phenotype analysis

Maize disease symptoms were analysed qualitatively by scoring plants according to the level of symptom development. The disease symptoms and their related scores are described in Table 2.2. The biological replicates were scored for disease symptoms and the mean disease score for each treatment was determined.

Table 2.2 Disease scores to describe symptom development in plants inoculated with *F. verticillioides*

Score	Description of symptoms	
0	no germination	
1	germination - no symptoms	
2	**mild**	leaf tips are slightly discoloured roots are slightly brown/discoloured
3	**medium**	leaf tips are brown and beginning to shrivel roots are brown and slightly stunted
4	**severe**	leaf tips are brown and leaves are shrivelled shoot growth and leaf emergence is stunted roots are very brown and growth is severely stunted

2.1.3 Fungal quantification

DNA extraction

DNA was extracted from ground maize tissue and *F. verticillioides* using the cetrimonium bromide (CTAB) method modified by Korsman et al. (2011). The NanoDrop 2000 Spectrophotometer (Thermo Scientific, Waltham, USA) was used to determine the quantity of DNA extracted and the quality of the extracted DNA was analysed using A260/280 and A260/230 ratios. DNA with A260/280 and A260/230 ratios of 1.8 and 2 respectively was of acceptable quality. A gel electrophoresis was run as an additional quality control measure (Figure S2.1).

Quantitative PCR (qPCR)

Primers for the fungal gene elongation factor 1α (*FvEF1α*) (Nicolaisen et al., 2009) and the plant genes membrane protein PB1A10.07c (*ZmMEP*) (Manoli et al., 2012) and glutathione S-transferase III (*ZmGST3*) (Korsman et al., 2012) were used to determine the quantity of fungal DNA present in the total DNA extracted from the maize (Table 2.3).

Table 2.3 Primers used to amplify fungal and plant gene products for fungal quantification

Gene name	Forward primer	Reverse primer
FvEF1α	5'-CGTTTCTGCCCTCTCCCA-3'	5'-TGCTTGACACGTGACGATGA-3'
ZmMEP	5'-TGTACTCGGCAATGCTCTTG-3'	5'-TTTGATGCTCCAGGCTTACC-3'
ZmGST3	5'-CACCACTTCTACCCGAAC-3'	5'-GTAGACGTCGAGCACCTTG-3'

Pure *F. verticillioides* DNA was diluted in 10ng.µl^{-1} uninoculated B73 maize DNA and dilutions in the following concentrations were made in order to generate a standard curve: 5ng.µl^{-1}, 3.5ng.µl^{-1}, 2.5ng.µl^{-1}, 1ng.µl^{-1}, 0.75ng.µl^{-1}, 0.5ng.µl^{-1} and 0.2ng.µl^{-1}. These dilutions were used to detect and quantify amplicons produced by the Fv*EF1α* primer pairs. In order to generate a standard curve for the plant genes, DNA extracted from uninoculated maize was pooled and dilutions in the following concentrations were made: 80ng.µl^{-1}, 50ng.µl^{-1}, 25ng.µl^{-1}, 12.5ng.µl^{-1}, 6.25ng.µl^{-1} and 3.125ng.µl^{-1}. This standard curve was used to quantify the amount of plant DNA present in the total DNA. The amplification efficiency (E), R^2 and R values – to

measure correlation efficiency and pipetting accuracy respectively – of the standard curve were used to determine the run quality.

Extracted DNA was diluted to a working concentration of 80ng.µl^{-1} for each sample. The KAPA SYBR® FAST qPCR Master Mix (2X) Kit (Kapa Biosystems, Wilmington, USA) was used to set up 10µl reactions and 80ng maize DNA was added to each reaction. A no template control (NTC) was included to detect possible contamination in the reactions. Each sample was tested in triplicate. The qPCR was carried out on the Rotor-Gene™ 6000 (Corbett Life Science, Sydney, Australia) using the following conditions for 30 cycles: 95°C for 3s followed by 60°C for 20s and finally 72°C for 1s.

Data was analysed using the Rotor-Gene™ 6000 series software, version 1.7 (Corbett Life Science, Sydney, Australia). The average DNA concentration of each sample was calculated according to the standard curve. The amount of fungal DNA (using the *FvEF1α* primers) was divided by the amount of plant DNA (using either *ZmMEP* or *ZmGST3*) in order to normalize fungal DNA quantification across the samples.

2.1.4 Gene expression

RNA extraction

RNA was extracted from ground maize tissue using the PureLink® Plant RNA Reagent (Thermo Fisher Scientific, Waltham, USA) according to the manufacturers instructions for <100mg tissue. The reagent was added to ground tissue and left at room temperature for five minutes for the tissue to lyse, after which it was centrifuged. Sodium chloride (NaCl) and chloroform were added to the clarified supernatant in order to separate the phases and isopropanol was used to precipitate the RNA. The nucleic acid yield and quality of the RNA was determined using the NanoDrop 2000 Spectrophotometer (Thermo Scientific, Waltham, USA). Samples with A260/280 ratios ~2 and A260/230 ratios ~1.8 were taken as acceptable quality.

cDNA synthesis

cDNA was synthesized from 1000ng RNA/sample using the Maxima First Strand cDNA Synthesis Kit for RT-qPCR with dsDNase (Thermo Scientific, Waltham, USA) accordind to the manufacturers instructions.

Primers

Primers were obtained from literature or designed according to the Agilent Microarray probe sequence found on the MaizeGDB (Sen et al., 2010) if applicable, or they were designed according to the B73 genome on MaizeGDB, version 3. Primers were designed to amplify a region ~100-200bp in length. The stability of heterodimers and homodimers was analysed using the OligoAnalyzer 3.1 Tool by Integrated DNA Technologies (https://eu.idtdna.com/calc/analyzer). Forward and reverse primer sequences of the genes analysed in this study, as well the origin of the primer sequences is shown in Table 2.4.

Table 2.4 Forward and reverse primer sequences that were used for RT-qPCR to analyse expression of the candidate phytoalexin biosynthetic genes and reference genes

	Gene name	Transcript ID	Forward (F) primer (5' – 3')	Reverse (R) primer (5' – 3')	Reference
Candidate genes	*ZmAn2*	GRMZM2G044481	TGTTCTTGTGAAGGCAGTTC	CAGACACGTTTGCTTGTCATG	F primer = Schmelz et al., 2011; R primer = designed from sequence on MaizeGDB
	ZmCYP81A1	GRMZM2G087875	TTTCAGCTCATCGCACGCTG	CGTCAAGAGGTGGTGGAGC	Designed from sequence on MaizeGDB
	ZmKO	GRMZM2G161472	GAAGCATCCAGGCAGTGAAC	GAGGTACACATGCAACGGGT	Christie et al., 2017
	ZmKSL2	AC214360.3_FG001	ACTCATCTCCGCTCACGAAT	ACCGGGGAGTTGATCTTCTT	Christie et al., 2017
	ZmKSL4	GRMZM2G016922	AGTTCAGCAGTGAGTCCAGC	CCGGTCTAGGGTGGTGTAGA	Moola, 2016
	ZmTPS11	GRMZM2G127087	GAAATGCGACAAAGGGCT	TCTTGAAGGCATCTCGTAGTA	Huffaker et al., 2011
	ZmtRNA	GRMZM2G140754	TCGTCTACTTCGATGATATGG	GGAGCCAGGTTCCTTGTTG	Designed from sequence on MaizeGDB
Reference genes	*ZmGST3*	GRMZM2G146246	CACCACTTCTACCCGAAC	GTAGACGTCGAGCACCTTG	Korsman et al., 2012
	ZmLUG	GRMZM2G425377	AATAGCGATCGGTGTGAAGAC	GTTAGTTCTTGAGCCCACGC	Manoli et al., 2012
	ZmMEP	GRMZM2G018103	TGTACTCGGCAATGCTCTTG	TTTGATGCTCCAGGCTTACC	Manoli et al., 2012
	ZmRPol	GRMZM2G034326	AGCCAAAACGCTAAAGTGGA	TAAGTGACGAGCAAGGCAAA	Ma et al., 2006

RT-qPCR

cDNA samples were diluted 1:5 and an equal volume of each diluted sample was pooled. Serial dilutions of the pooled samples were carried out (1, 1:2, 1:4, 1:8, 1:16, 1:32, 1:64, 1:128) in order to generate a standard curve. The standard curve was used to determine relative gene expression. E, R^2 and R values were analysed in order to ensure that the run was of acceptable quality.

The KAPA SYBR® FAST qPCR Master Mix (2X) Kit (Kapa Biosystems, Wilmington, USA) was used to set up 10µl reactions. 1µl unpooled cDNA of unknown concentration was added to each reaction. Each sample was tested in triplicate. A no template control and a no-reverse transcriptase (no-RT) control were also included.

The RT-qPCR runs were carried out on the Rotor-Gene™ 6000 (Corbett Life Science, Sydney, Australia). The samples were run using the following cycling parameters: 95°C for 3s, 60°C for 20s and 72°C for 1s. The parameters were run for 40 cycles.

Data analysis

Data was extracted from the Rotor-Gene™ 6000 series software, version 1.7 (Corbett Life Science, Sydney, Australia). Triplicate samples were only accepted if they were within 1 C_t of each other. A melt/dissociation curve was used to determine the presence of multiple amplicons.

Data was analysed using qBase+ software, version 3.0 (Biogazelle, Zwijnaarde, Belgium – www.qbaseplus.com). Reference gene stability was analysed and reference genes with an M value less than 1 and a CV value less than 0.5 were accepted. The calibrated normalized relative quantities (CNRQ) table was exported into Microsoft Excel® (Mac 2011) and the triplicate values of each sample were averaged.

2.1.5 Sequencing

PCR amplicons were cleaned up using the DNA Clean and Concentrator™-5 (Zymo Research, Irvine, USA). Samples were sequenced at the Central Analytical Facilities (CAF) at Stellenbosch University in order to confirm primer specificity to the genes of interest. The BLASTn function in Ensembl Plants (Kersey et al., 2016, http://plants.ensembl.org/Zea_mays/Tools/Blast) was used to compare the sample sequences to the reference *Zea mays* genome (version 4).

2.1.6 Phytoalexin accumulation

Approximately 100mg ground maize tissue of each sample was sent for phytoalexin analysis at the United States Department of Agriculture (USDA). Phytoalexins were extracted with 2:1 Dichloromethane($MeCl_2$):propanol for two hours and separated into organic and aqueous layers, and the organic layer was used for analysis. Phytoalexin accumulation was measured using gas-chromatography mass-spectrometry, as described by Schmelz et al. (2011) and Huffaker et al. (2011).

2.1.7 Statistical analysis and data presentation

A one-tailed t test was performed in Microsoft Excel® (Mac 2011) to determine the statistical significance of fungal growth in the inoculated samples. Data from gene expression and phytoalexin accumulation was log_{10}-transformed in order to obtain a normal distribution for statistical analysis. Microsoft Excel® (Mac 2011) was used to perform unpaired t tests (unequal variance) to test for significance between variable means of control and *F. verticillioides* inoculated samples. Correlation analysis was performed in GraphPad Prism 7 (GraphPad Software, San Diego, USA). Graphs were produced using GraphPad Prism 7 (GraphPad Software, San Diego, USA).

2.1.8 Bioinformatics

Sequences and information about the candidate genes in this study were obtained from MaizeGDB (Sen et al., 2010) and Ensembl Plants (Kersey et al., 2016, http://plants.ensembl.org) using the B73 RefGen_V3 genome annotation version. The sequences were validated using the newly released B73 RefGen_V4 genome annotation version (Jiao et al., 2017). The BLASTn tools from NCBI (Madden, 2002, https://blast.ncbi.nlm.nih.gov/Blast.cgi), MaizeGDB and Ensembl Plants were used to

validate gene sequences and their annotations across different databases. Differentially expressed gene data from Christie et al. (2017), Lanubile et al. (2014) and Lambarey (2017) were used to identify candidate genes in this study. Genes within the GY-s co-expression module on chromosome 8, between markers npi110a and bnlg669 at positions 25.4cM and 50.1cM respectively (Berger et al., 2014), were obtained from Christie et al. (2017) and differential gene expression was compared to the gene expression in the study by Lanubile et al. (2014). Genes were annotated using the MaizeGDB B73 RefGen_V3 browser (http://www.maizegdb.org). The $\log_2$ fold change (FC) for the expression data from Christie et al. (2017) was multiplied by -1 because the FC was calculated as control/*C. zeina,* while the other studies calculated FC as *F. verticillioides*/control. This was done so that up-regulation is represented as a positive FC throughout the data.

Promoter sequences 1.5kb upstream of the transcription start site (TSS) were obtained from PlantPAN 2.0 (Chow et al., 2016). Individual sequences were analysed for *cis*-acting regulatory elements using PlantCARE (Lescot et al., 2002). The sequences were also analysed in conjunction with each other using Multiple Em for Motif Elicitation (MEME) in order to identify similar motifs between sequences (Bailey & Elkan, 1994). MEME was run three times in order to ensure that the same motifs were identified each time.

RESULTS AND DISCUSSION

2.2.1 Identification of candidate phytoalexin biosynthesis genes

Previous studies have identified numerous putative phytoalexin biosynthetic genes, and a number of these have been chosen for this study. The bioinformatics process used in this study is shown in Figure 2.1.

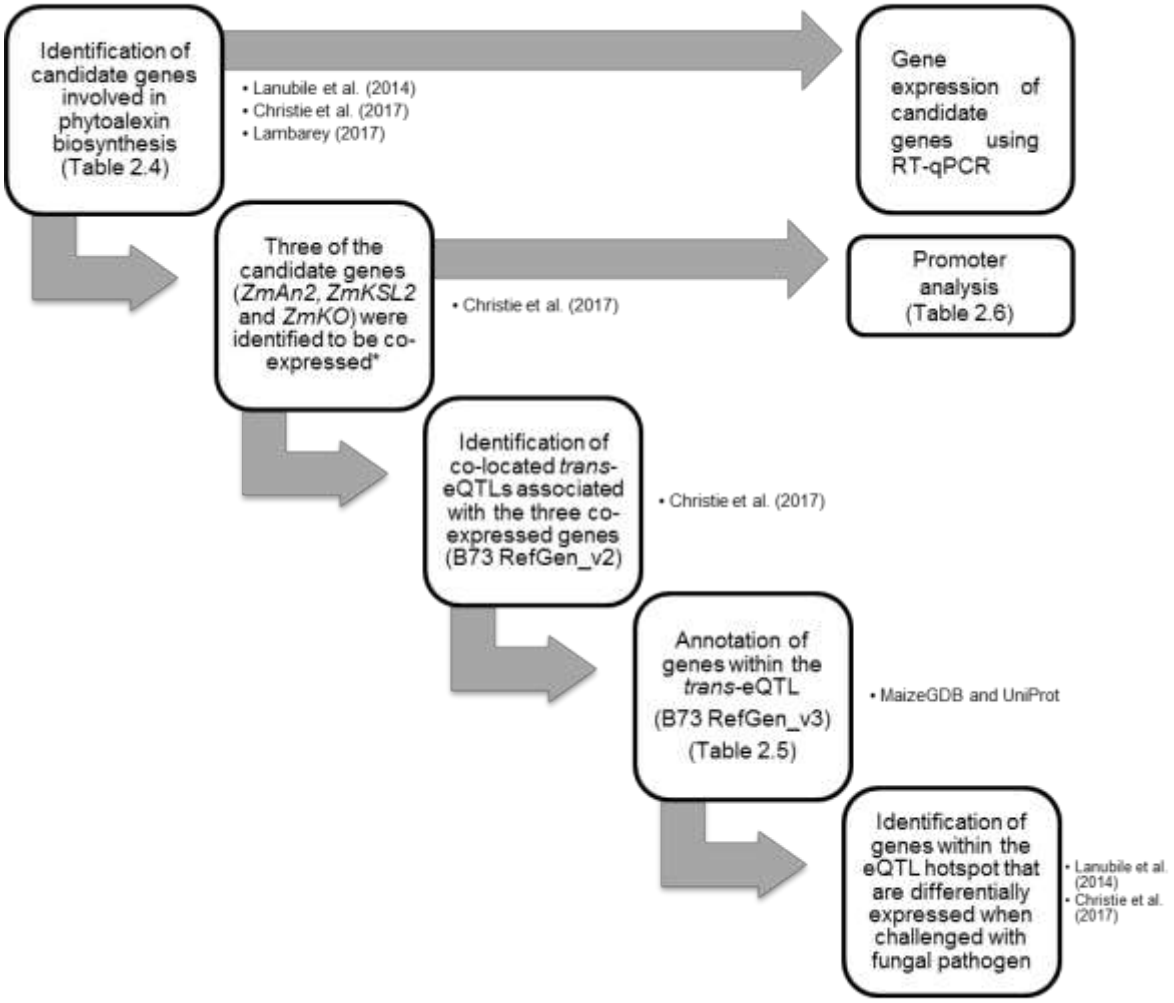

Figure 2.1 Flow chart of the bioinformatics work process used in this study. *geneIDs of *ZmAn2, ZmKSL2* and *ZmKO* are GRMZM2G044481, AC214360.3_FG001 and GRMZM2G161472 respectively

(Lanubile et al., 2014) used RNA-sequencing to measure the response of the susceptible CO354 and resistant CO441 maize lines to *F. verticillioides.* Kernels were inoculated with *F. verticillioides* using the side-needle inoculation method and transcriptional changes were measured 72 hours post inoculation (hpi). 6,951 genes were differentially expressed in response to *F. verticillioides* compared with the uninoculated control, including *ZmAn2, ZmCYP81A1, ZmKSL2, ZmKSL4* and *ZmTPS11* genes (Table 2.5). RNA-seq was also performed by Humaira Lambarey (Lambarey, 2017) on CML144 to analyse the response of this susceptible line to *F. verticillioides*. A number of genes were differentially expressed 14 days after a seed inoculation, and of the putative phytoalexin biosynthetic genes, *ZmCYP81A1* and *ZmTPS1* were significantly expressed. *ZmKSL4* was not significantly expressed, but was induced following *F. verticillioides* inoculation and the adjusted p-value fell just short of significance ($p<0.05$), thus it is included here (Table 2.5). A systems genetics study of transcriptional changes that occur in response to *Cercospora zeina* infection, the causal agent of grey leaf spot (GLS), was performed by Christie et al. (2017). In this study, a microarray was performed on a recombinant inbred line (RIL), CML444 x SC Malawi, and an RNA-sequencing study was performed on B73 maize. In the RNA-seq study, 4447 genes were differentially expressed following *C. zeina* inoculation, and genes putatively involved in phytoalexin biosynthesis that were up-regulated included *ZmAn2, ZmCYP81A1, ZmKO, ZmKSL2* and *ZmKSL4* (Table 2.5). In this study, *ZmAn2, ZmKSL2* and *ZmKO* were also found to be co-expressed (Christie et al., 2017).

Table 2.5 Differential expression of phytoalexin biosynthetic genes in three studies in which different maize lines were challenged with fungal pathogens.

			Lanubile et al. 2014				Lambarey 2017		Christie et al. 2017	
			CO354		CO441		CML144		B73	
Gene ID (B73 RefGen_V3)	Gene ID (B73 RefGen_V4)	Gene	Log_2FC(*F.vert*/ CTRL)	padj	Log_2FC(*F.vert*/ CTRL)	padj	Log_2FC	padj	log_2FC(CTRL/ *C. zeina*)[a]	padj
GRMZM2G044481	Zm00001d029648	*ZmAn2*	6,86	$3,32x10^{-18}$	7,67	$2,91x10^{-28}$	-	-	3,36	$5,45x10^{-21}$
GRMZM2G087875	Zm00001d012322	*ZmCYP81A1*	5,87	$8,20x10^{-13}$	6,27	$1,22x10^{-29}$	3,28	$4,26x10^{-3}$	2,57	$8,34x10^{-45}$
-	Zm00001d014134	*ZmCYP71Z18*[b]	-	-	-	-	-	-	-	-
GRMZM2G161472	Zm00001d046342	*ZmKO*	-	-	-	-	-	-	3,05	$3,72x10^{-19}$
AC214360.3_FG001	Zm00001d041082	*ZmKSL2*	6,34	$9,38x10^{-19}$	6,57	$32,63^{-39}$	-	-	3,16	$7,06x10^{-26}$
GRMZM2G016922	Zm00001d032858	*ZmKSL4*	7,70	$9,27x10^{-32}$	9,99[c]	$2,06x10^{-19}$	3,94	$6,83x10^{-2}$	-	-
GRMZM2G049538	Zm00001d002351	*ZmTPS1*	-	-	-	-	4,40	$4,26x10^{-3}$	0,41	$5,98x10^{-2}$
GRMZM2G127087	Zm00001d024210	*ZmTPS11*	6,85	$1,44x10^{-11}$	8,18	$7,01x10^{-61}$	-	-	2,35	$2,37x10^{-22}$

Log_2FC = log_2 fold change; Positive FC = up-regulation; negative FC = down-regulation. Adjusted p-values (padj) show significant difference when $p<0.05$; genes that are differentially expressed are in bold. - = no differential expression. [a] = log_2FC x -1, [b] = B73 RefGen_V3 not available for *ZmCYP71Z18*, differential expression of this gene not available, [c] = control was 0 fragments per kilobase million (FPKM), therefore log_2FC(INOC/CTRL) cannot be properly computed.

Putative phytoalexin biosynthetic genes, *ZmAn2, ZmKSL2, ZmKSL4, ZmKO, ZmCYP81A1* and *ZmTPS11,* were chosen as candidate genes for this study because they were significantly differentially expressed in one or more of the studies discussed following fungal inoculation (Table 2.5). *ZmAn2* (GRMZM2G044481), which is responsible for the conversion of GGPP to CPP was significantly up-regulated following *F. verticillioides* and *C. zeina* inoculation (Lanubile et al., 2014; Christie et al., 2017). *ZmKSL2* (AC214360.3_FG001) and *ZmKSL4* (GRMZM2G016922), which are putatively downstream of *ZmAn2,* are both up-regulated by *F. verticillioides* (Lanubile et al., 2014). The RNA-seq results from Lambarey (2017) returned an FDR-adjusted p-value for *ZmKSL4* expression that was just greater than 0.05, and although not significant, supports the findings from Lanubile et al. (2014) that *ZmKSL4* is significantly up-regulated following *F. verticillioides* inoculation. As well as up-regulation by *F. verticillioides, ZmKSL2* was also significantly up-regulated by *C. zeina* (Christie et al., 2017). *ZmKO* (GRMZM2G161472), which is putatively downstream of *ZmKSL2* (Figure 1.1), was only significantly up-regulated following *C. zeina* inoculation (Christie et al., 2017). Although *ZmKO* was not significantly up-regulated following *F. verticillioides* inoculation, the gene remains of interest in this study due to the finding that it is co-expressed with *ZmAn2* and *ZmKSL2* (Christie et al., 2017). *ZmCYP81A1* (GRMZM2G087875) was significantly up-regulated in all three studies when inoculated with *F. verticillioides* or *C. zeina* (Lanubile et al., 2014; Christie et al., 2017; Lambarey, 2017). *ZmCYP81A1* is putatively involved in both or either of the kauralexin and zealexin biosynthetic pathways, as CYPs are predicted to catalyse the final steps in the synthesis of both phytoalexins (Schmelz et al., 2014).

ZmTPS11 (GRMZM2G127087), which is responsible for catalysing the cyclisation of FPP to (*S*)-β-bisabolene, was also significantly expressed following inoculation with *F. verticillioides* (Lanubile et al., 2014) and *C. zeina* (Christie et al., 2017) (Table 2.5). *ZmTPS6* is also involved in this process but is not included in this study as previous research has shown that the *ZmTPS6* transcript was not up-regulated in CML444 in response to *C. zeina* inoculation (Ntuli, 2016). Downstream of *ZmTPS11*, *ZmCYP71Z18* (B73 RefGen_v4 gene ID: Zm00001d014134) has been found to be involved in the oxidation of (*S*)-β-macrocarpene to zealexin A1, and following *F. graminearum* inoculation the gene was up-regulated prior to zealexin

accumulation (Mao et al., 2016). *ZmCYP71Z18* could not be identified in the three studies due to the lack of B73 RefGen_V3 gene ID available for the gene, and therefore the differential expression could not be analysed in the context of Lanubile et al. (2014), Lambarey (2017) and Christie et al. (2017). Another interesting gene involved in the phytoalexin pathway is *ZmTPS1* (GRMZM2G049538), which has recently been shown to be involved in kauralexin biosynthesis (Fu et al., 2016). *ZmTPS1* was significantly up-regulated following *C. zeina* and *F. verticillioides* inoculation of leaves and shoots respectively (Christie et al., 2017; Lambarey, 2017), but was not differentially expressed in root tissue following *F. verticillioides* inoculation (Moola, 2016). All of the genes that were significantly expressed following *F. verticillioides* inoculation were more highly expressed in the partially resistant maize line CO441 compared to the susceptible maize CO354 line, and the significant difference between control and *F. verticillioides* inoculation was much greater in CO441 than in CO354, with the exception of *ZmKSL4* (Table 2.5, Lanubile et al., 2014). Although *ZmCYP71Z18* and *ZmTPS1* appear to have interesting roles in the phytoalexin biosynthetic pathway, they were not analysed in this study.

The genes that were differentially expressed in CO354 and CO441 in response to *F. verticillioides* appear to be more highly induced than in CML144 inoculated with *F. verticillioides* and in B73 following *C. zeina* inoculation, but this could be the result of the tissue used, and time point harvested after fungal inoculation (Table 2.5). In addition, the maize genotypes varied in each study, which would affect the defence response observed. Furthermore, experimental design varied between the different studies. Lanubile et al. (2014) investigated the defence response to *F. verticillioides* in kernels following inoculation via the side-needle method, while Christie et al. (2017) used field-inoculated plants in which *C. zeina* infected leaf tissue was harvested. Lambarey (2017) used a seed soak method to inoculate the maize and harvested the leaves of the plant. The latter experimental design is most similar to the one used in the present study.

Co-expression of phytoalexin biosynthetic genes

Christie et al. (2017) performed a microarray study on an RIL population in order to analyse the transcriptional response of the maize lines to *C. zeina* inoculation. Following the microarray, a weighted gene co-expression network analysis (WGCNA) was performed and a number of PR proteins and other defence-related genes, including three genes involved in kauralexin biosynthesis (*ZmAn2*, *ZmKSL2*, *ZmKO*), were represented in a GY-s co-expression module (Christie et al., 2017). This co-expression module was also found to be highly correlated with GLS symptom development (Christie et al., 2017). *ZmAn2*, *ZmKSL2* and *ZmKO* had overlapping *trans*-eQTL sites on chromosome 8. Nanette Christie extracted a list of 39 genes that fell between markers npi110a and bnlg669 at positions 25.4cM and 50.1cM respectively on chromosome 8, according to the Maize B73 RefGen_v2 genome annotation version (Berger et al., 2014; Christie et al., 2017). This is the overlapping region of the *trans*-eQTL associated with *ZmAn2, ZmKSL2* and *ZmKO*. Genes were annotated using MaizeGDB (Sen et al., 2010) for gene names and the UniProt Knowledgebase (UniProtKB) (The UniProt Consortium, 2017) for protein names (Table 2.6). Gene names were annotated from the best Arabidopsis and rice hits using the phytozome annotations provided on the MaizeGDB gene record page.

Identification of significantly expressed genes in *trans*-eQTL chromosomal region

A significant number of genes in the GY-s co-expression module in the RIL study, including the three kauralexin biosynthetic genes, were induced nine- to tenfold in the B73 maize line when inoculated with *C. zeina* in a field experiment (Christie et al., 2017). This suggests that the B73 line will have similar transcriptional control of the three kauralexin biosynthetic genes via an overlapping *trans*-eQTL region as proposed for the RILs. Differential expression from the B73 RNA-seq experiment was used to determine whether any genes in the *trans*-eQTL site were differentially regulated in B73 maize exposed to *C. zeina*. Ten genes from the list were differentially expressed, four of which were up-regulated (positive log_2FC) and six of which were down-regulated (negative log_2FC) (Table 2.6). In order to determine whether any of these genes were differentially expressed following *F. verticillioides* inoculation, the RNA-seq results from Lanubile et al. (2014) were used to analyse expression of the genes in the *trans*-eQTL. Out of the 39 genes on chromosome 8 between markers npi110a and bnlg669, only two were differentially expressed in both the CO354 and CO441 maize lines (Lanubile et al., 2014). GRMZM2G049781 was down-regulated (negative log_2FC) and GRMZM2G140754 was up-regulated (positive log_2FC) (Table 2.6).

Table 2.6 Differential expression of genes on chromosome 8 between markers npi110a and bnlg669 that fall within the co-locating *trans*-eQTL associated with *ZmAn2, ZmKSL2* and *ZmKO* co-expressed genes

		MaizeGDB RefGen_v3		UniProtKB annotation	Christie et al. 2017		Lanubile et al. 2014			
					B73		CO354		CO441	
geneID	Genome position	Best arabidopsis hit	Best rice hit	Protein name	log_2FC(*C. zeina* /CTRL)*	padj	Log_2FC(*F.vert* /CTRL)	padj	Log_2FC(*F.vert* /CTRL)	padj
GRMZM2G566786	10,072,049-10,076,873	tRNA synthetase class I (I, L, M and V) family protein	tRNA synthetase class I putative expressed	NULL	-0,69	$1,80x10^{-5}$	-	-	-	-
GRMZM5G858471	10,078,647..10,080,295	-	-	-	-	-	-	-	-	-
GRMZM2G140754	**10,082,252-10,085,842**	**alanine-tRNA ligases;nucleic acid binding;ligases forming aminoacyl-tRNA and related compounds;nucleotide binding;ATP binding**	**alanyl-tRNA synthetase putative expressed**	**Alanyl-tRNA synthetase**	**1,02**	**$5,99x10^{-6}$**	**1,22**	**$6,70x10^{-7}$**	**1,74**	**$3,49x10^{-2}$**
GRMZM2G140782	10,086,438-10,093,231	-	expressed protein	NULL	-0,17	$3,15x10^{-1}$	-	-	-	-
GRMZM2G094050	10,122,605-10,125,067	-	splicing factor putative expressed	Sarcoplasmic reticulum histidine-rich calcium-binding protein	-0,1	$5,71x10^{-1}$	-	-	-	-
GRMZM2G003821	10,155,509-10,156,262	-	expressed protein	-	-	-	-	-	-	-
AC186894 .3_FG002	10,187,640-10,188,110	-	-	-	-	-	-	-	-	-
GRMZM2G003861	10,284,341-10,287,345	S-adenosyl-L-methionine-dependent methyltransferases superfamily protein	methyltransferase putative expressed	Protein-lysine N-methyltransferase	-0,02	$9,03x10^{-1}$	-	-	-	-
GRMZM2G484516	10,286,237-10,287,136	-	-	-	-	-	-	-	-	-
GRMZM2G003930	10,288,196-10,291,863	RING/FYVE/PHD zinc finger superfamily protein	protein binding protein putative expressed	-	-	-	-	-	-	-
GRMZM2G374085	10,392,528-10,394,245	-	-	-	-0,16	$5,12x10^{-1}$	-	-	-	-
GRMZM2G083072	10,510,602-10,511,066	-	-	-	-	-	-	-	-	-
GRMZM2G457339	10,528,417-10,529,394	-	-	-	-	-	-	-	-	-
GRMZM2G157279	10,530,171-10,538,375	-	-	-	-	-	-	-	-	-
GRMZM2G451605	10,544,277-10,545,252	-	-	-	-	-	-	-	-	-
GRMZM2G386944	10,584,598-10,585,573	-	-	-	-	-	-	-	-	-
GRMZM2G386929	10,586,677-10,588,212	-	-	-	-	-	-	-	-	-
GRMZM2G534485	10,588,492-10,589,521	-	-	-	-	-	-	-	-	-
GRMZM2G086952	10,591,351-10,592,438	-	expressed protein	-	-	-	-	-	-	-
GRMZM2G086930	10,592,772-10,593,090	-	-	-	-	-	-	-	-	-
GRMZM2G569903	10,620,225-10,623,682	Protein of unknown function (DUF1624)	heparan-alpha-glucosaminide N-acetyltransferase putative	-	-	-	-	-	-	-

		MaizeGDB RefGen_v3		UniProtKB annotation	Christie et al. 2017		Lanubile et al. 2014			
					B73		CO354		CO441	
geneID	Genome position	Best arabidopsis hit	Best rice hit	Protein name	log_2FC(*C. zeina* /CTRL)*	padj	Log_2FC(*F.vert* /CTRL)	padj	Log_2FC(*F.vert* /CTRL)	padj
			expressed							
GRMZM2G445667	10,635,255-10,637,066	RING/U-box superfamily protein	zinc finger C3HC4 type family protein expressed	-	-	-	-	-	-	-
AC206579.3_FG001	10,639,380-10,639,862	-	AMP-binding domain containing protein expressed	-	-	-	-	-	-	-
AC212575.3_FG002	10,657,364-10,658,884	Uncharacterized protein	cyclin-related protein putative expressed	-	-	-	-	-	-	-
GRMZM2G119345	10,756,078-10,762,016	ABC-2 type transporter family protein	white-brown complex homolog protein 7 putative expressed	ABC-2 type transporter family protein	-0,75	$5,97x10^{-5}$	-	-	-	-
GRMZM2G060061	10,809,680-10,813,733	Core-2/I-branching beta-1 6-N-acetylglucosaminyltransferase family protein	xylosyltransferase putative expressed	Xylosyltransferase 1	0,38	$1,25x10^{-1}$	-	-	-	-
GRMZM2G049661	10,855,882-10,857,679	Protein with RING/U-box and TRAF-like domains	seven in absentia protein family protein expressed	-	-	-	-	-	-	-
GRMZM2G049781	10,862,573-10,865,304	Heavy metal transport/detoxification superfamily protein	heavy-metal-associated domain-containing protein putative expressed	Heavy metal transport/detoxification superfamily protein	-	-	-1,07	$7,55x10^{-5}$	-1,12	$8,45x10^{-1}$
GRMZM2G030543	10,868,102-10,868,626	-	-	-	-	-	-	-	-	-
GRMZM2G030384	10,871,147-10,877,296	transducin family protein / WD-40 repeat family protein	WD domain G-beta repeat domain containing protein expressed	Actin-interacting protein 1-2	0,16	$2,85x10^{-1}$	-	-	-	-
GRMZM2G377550	10,910,622-10,911,909	alfin-like 2	PHD finger protein putative expressed	-	-	-	-	-	-	-
GRMZM2G377520	10,910,622..10,911,909	60S acidic ribosomal protein family	60S acidic ribosomal protein putative expressed	-	-	-	-	-	-	-
GRMZM2G078360	10,926,467-10,939,556	UBC23) ubiquitin-conjugating enzyme 23	ubiquitin conjugating enzyme protein putative expressed	Ubiquitin-conjugating enzyme E2	0,21	$1,35x10^{-1}$	-	-	-	-
GRMZM2G078347	10,938,043-10,939,628	-	-	-	-	-	-	-	-	-
GRMZM2G336694	10,990,065-10,990,859	-	-	-	-	-	-	-	-	-
AC205906.3_FG004	11,086,564-11,086,929	-	-	-	-	-	-	-	-	-
GRMZM2G090114	11,105,738-11,106,253	-	-	-	-	-	-	-	-	-
GRMZM2G700383	11,133,358-11,133,690	-	-	-	-	-	-	-	-	-
GRMZM2G438998	11,250,034-11,251,240	Mannose-6-phosphate isomerase type I	mannose-6-phosphate isomerase putative expressed	-	-	-	-	-	-	-

Log_2FC = log_2 fold change; Positive FC = up-regulation; negative FC = down-regulation. * = log_2FC x -1. Adjusted p-values (padj) show significant difference when $p<0.05$; genes that are differentially expressed are in **bold.** - = gene annotations were not found

GRMZM2G140754 was the only gene that was significantly up-regulated in both studies, and is also the only gene that was up-regulated with an FC greater than 1 (Table 2.6 in **bold**). This gene codes for an alanyl tRNA synthetase (http://www.maizegdb.org/gene_center/gene?id=GRMZM2G140754 [April 2017]), a protein that is possibly involved in nucleic acid binding (Blast2GO annotation, F: nucleic acid binding) (Christie et al., 2017). This finding suggests that alanyl tRNA synthetase may be acting in *trans* to regulate the expression of the three putative kauralexin biosynthesis genes that are associated with *trans*-eQTLs at the same chromosomal site as GRMZM2G140754. Primers for this gene were designed in order to perform RT-qPCR in an attempt to validate tRNA synthetase expression in B73 following *F. verticillioides* inoculation (Table 2.4). However, despite multiple attempts to measure GRMZM2G140754 expression (Table S2.1), no results were obtained. As the tissue used and time point after fungal inoculation differs between the experiments, GRMZM2G140754 may have different expression patterns in seedlings following a seed soak inoculation. Other genes within this region that were significantly up-regulated following *F. verticillioides* and *C. zeina* inoculation may be of interest to study in future work, but fell out of the time scope of this project.

Promoter analysis

The promoter sequences 1.5kb upstream of the transcription start sites of *ZmAn2, ZmKSL2* and *ZmKO* were obtained from PlantPAN 2.0 (Chow et al., 2016). The promoter sequences were analysed using PlantCARE (Lescot et al., 2002) and a number of *cis*-acting regulatory elements (CARE) were identified in each sequence (Table 2.7). Phytohormones appear to be important in regulation of these three genes, as ABRE and CGTCA-/TGACG-motifs, involved in abscisic acid (ABA) responsiveness and methyl-jasmonate (MeJA) responsiveness respectively (Srivasta et al., 2010), were the only CAREs found in all three of the promoter sequences (Table 2.7). ABA treatment (Vaughan et al., 2015) and combined jasmonic acid/ethylene treatment (Schmelz et al., 2011) (MeJA is derived from JA) have been shown to induce kauralexin accumulation, supporting the activity of these motifs in the promoter regions. ABRE is the only motif that is present in more than one position in all of the gene sequences (Table 2.7), providing additional evidence for the role of ABA in the regulation of all three of the co-expressed genes. In addition to ABRE and CGTCA-/TGACG-motifs, *ZmKSL2* contains a GARE-motif and a TCA-

element, which are involved in the gibberellin response (Paquis et al., 2011) and salicylic acid (SA) responsiveness (Goldsbrough, Albrecht & Stratford, 1993), respectively. *ZmKO* also contains TCA-elements, as well as TGA-elements that are involved in the auxin response (Table 2.7) (Xing et al., 2011). The genes also contain motifs that are more specific to the defence response. *ZmAn2* and *ZmKO* contain W Boxes that bind to WRKY transcription factors. WRKYs are involved in wounding and pathogen response, and are elicited by fungal infection (Paquis et al., 2011). Although *ZmKSL2* does not contain a W box, regulation of this gene may occur following *ZmAn2* elicitation and changes in phytohormone signalling. The *ZmAn2* promoter sequence contains TC-rich repeats that are involved in defence and stress responses, and *ZmAn2* and *ZmKSL2* contain a MYB binding site (MBS) that is induced by drought (Abe et al., 1997) (Table 2.7).

Table 2.7 *Cis*-acting regulatory elements in the promoter sequences of *ZmAn2, ZmKSL2* and *ZmKO*

Name	Sequence	Function	*ZmAn2*	*ZmKSL2*	*ZmKO*
ABRE	TACGTG/CGTACGTGCA/CACGTG/ ACGTGGC	CARE involved in abscisic acid responsiveness	✓	✓	✓
CGTCA-motif	CGTCA	CARE involved in the MeJA-responsiveness	✓	✓	✓
GARE-motif	AAACAGA	gibberellin-responsive element	-	✓	-
MBS	CAACTG	MYB binding site involved in drought-inducibility	✓	✓	-
TC-rich repeats	ATTTTCTTCA	CARE involved in defence and stress responsiveness	✓	-	-
TCA-element	CAGAAAAGGA	CARE involved in salicylic acid-responsiveness	-	✓	✓
TGA-element	AACGAC	auxin-responsive element	-	-	✓
TGACG-motif	TGACG	CARE involved in the MeJA-responsiveness	✓	✓	✓
W Box (WRKY)	TTGACC	WRKY fungal responsive transcription factor binding site	✓	-	✓

✓ symbolises the presence of the *cis*-acting regulatory element (CARE) in the respective gene promoter regions; - symbolises that the CARE was not identified in the promoter region. Yellow blocks represent motifs that are found in more than one region of the promoter sequence.

As well as individual analysis of the promoter regions of the three kauralexin biosynthetic genes, Multiple Em for Motif Elicitation (MEME) was used to discover any enriched motifs 1.5kb upstream of the transcription start sites (TSS) (Bailey & Elkan, 1994). MEME is used to discover novel motifs enriched relative to other promoters sequences in the genome. However, the motifs discovered had an E value above 0.05 and were therefore not considered significantly enriched and were not analysed further.

2.2.2 *F. verticillioides*-dependent expression of putative maize phytoalexin genes: optimisation experiments in B73

B73 phenotype analysis

An initial experiment using B73 maize was performed in order to optimise the experimental design of this study. B73 maize is moderately resistant to *F. verticillioides* (Baldwin et al., 2014) and is the reference maize genome (Schnable et al., 2009). This experiment allowed for primer design and testing of expression of the candidate genes that were previously identified from Christie et al. (2017), Lambarey (2017) and Lanubile et al. (2014).

B73 maize seed was inoculated with *F. verticillioides* and grown in MS media. The root at shoot tissue were harvested ten days post inoculation (dpi). Both control and inoculated plants had three or four leaves, and differences in leaf numbers was the result of slightly different growth speed and emergence of the fourth leaf. All of the plants contained leaves with some brown tips, especially on the lower leaves (Figure 2.2a, Figure 2.2b). However, the inoculated leaves were more severely affected than the control. The slight browning of the tips observed on the control plants is most likely due to growth stress from the boxes in which the plants were grown, and the discolouration in the leaves of the inoculated plants is an additive effect of both the growth conditions and disease symptoms. The leaves on the control plants were open wide compared to the inoculated leaves, which appeared shrivelled. Although the leaves on the inoculated plants appear slightly shorter than those on the control plants, there does not appear to be marked differences in shoot sizes between the two treatments. The smaller appearance of the *F. verticillioides* inoculated shoots seems to be due to the shrivelling of the leaves rather than the actual length of the

leaves. The plants were scored according to Table 2.2 and the average scores of the control and inoculated shoots were 1,3 and 2,1 respectively (Figure 2.2e). There were virtually no disease symptoms on the control plants and the disease score is slightly greater than 1 due to the brown tips of the lower leaves. The inoculated shoots had mild symptoms.

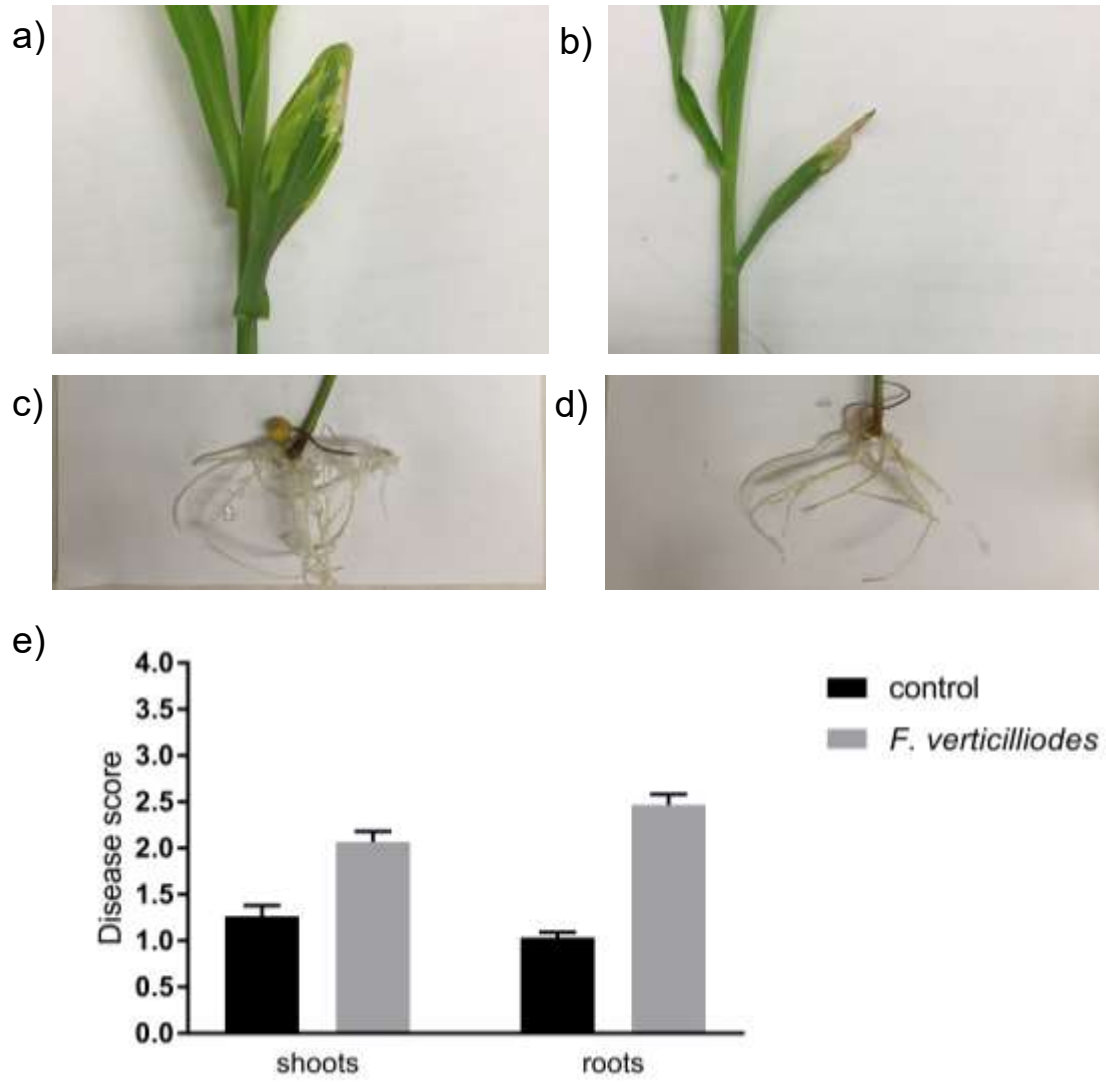

Figure 2.2 Phenotype analysis of control and inoculated B73 shoot and root tissue ten dpi. a) Control and b) *F. verticillioides* inoculated leaf 1; c) control and d) *F. verticillioides* inoculated roots, e) mean disease scores of the maize in the shoots and roots.

The roots inoculated with *F. verticillioides* were extremely stunted compared to the control, and appeared brown and discoloured in comparison to the white, long, control roots (Figure 2.2d, Figure 2.2c). The control roots also had a much more diverse root network, consisting of many seminal and lateral roots compared to the inoculated roots. The mean disease score in the control roots was 1, indicating that

the seeds germinated but the roots did not display any disease symptoms. The inoculated roots had a mean disease score of 2,5, as the roots disease symptoms were mild-to-medium (Figure 2.2e). Overall, the symptoms observed in inoculated B73 plants at ten dpi were relatively mild, with roots displaying a greater difference between control and inoculated plants.

Fungal quantification and gene expression in B73

A qPCR assay was performed to quantify the amount of *F. verticillioides* growing in the roots and shoots of B73 control and inoculated maize ten days post inoculation. Primers for an *FvEF1α F. verticillioides* gene (Nicolaisen et al., 2009) and the *ZmMEP* B73 gene (Manoli et al., 2012) were used to quantify the amount of *F. verticillioides* DNA in B73 DNA (Table 2.3). *F. verticillioides* was not detected in the control samples, but was detected in both the shoots and roots of the inoculated samples (Figure 2.3).

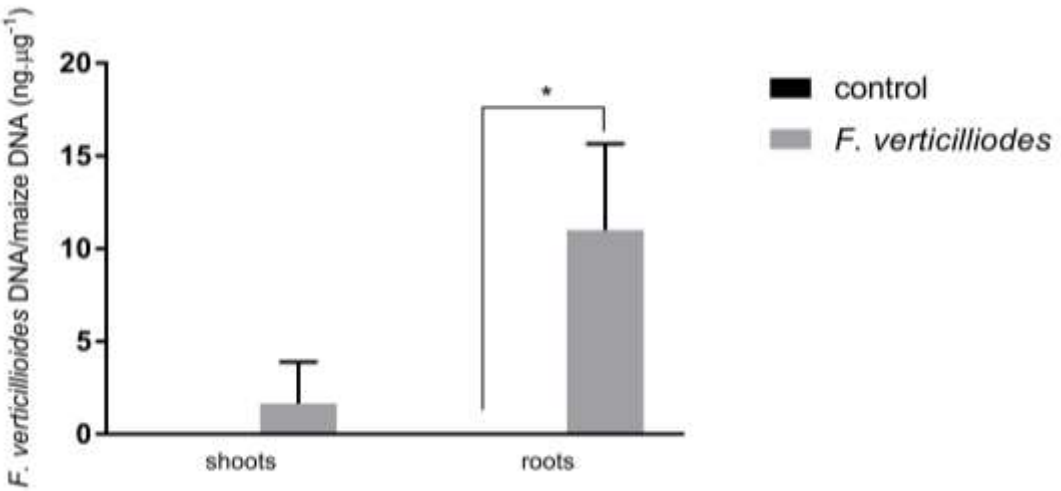

Figure 2.3 Quantitative PCR analysis to measure *F. verticillioides* in control and inoculated shoot and root tissue of B73 maize ten dpi. The amount of *F. verticillioides* growing in B73 maize (ng.µg-1) was quantified using *FvEF1α* and *ZmMEP* primers respectively. Error bars indicate standard deviation (SD). A one-tailed t test was performed to determine statistical significance between treatments. * = $p<0.05$, n=3

The amount of *F. verticillioides* in the shoots was 1.7ng.µg^{-1}, while in the roots 11ng.µg^{-1} *F. verticillioides* was detected. Although both inoculated tissues displayed an increase in fungal growth from the control treatment, there was high variation between the samples. Therefore, there was no significant difference between the

control and inoculated treatment in the shoot tissue, but growth in the roots was significantly different between the two groups. Similarly, the variation in the samples meant that although the amount of *F. verticillioides* measured in the roots was 6,5 times more than that in the shoots, there was no significant difference in growth between the two tissues.

The response of B73 maize to *F. verticillioides* inoculation was analysed by measuring candidate gene expression using RT-qPCR. *ZmMEP* and *ZmLUG* were used as reference genes. Reference gene stability is shown in Table S2.2. The standard curve and run quality of each gene is shown in Table S2.3. Relative gene expression is shown in Figure 2.4. Statistical analysis was performed on $\log_{10}$-transformed data in order to obtain a normal distribution among the data.

Relative gene expression of *ZmAn2* (Figure 2.4a)*, ZmKSL2* (Figure 2.4b)*, ZmKO* (Figure 2.4c)*, ZmKSL4* (Figure 2.4d) and *ZmTPS11* (Figure 2.4f) was significantly higher in the inoculated roots compared to the control roots. In contrast, low-to-no gene expression was observed in either treatment in the shoot tissue. Relative expression of *ZmAn2, ZmKSL2, ZmKO, ZmKSL4* and *ZmTPS11* was significantly higher in the inoculated roots than in the inoculated shoots. *ZmTPS11* expression levels in the roots were higher than any of the other genes measured (Figure 2.4f). Of the kauralexin biosynthesis genes, *ZmKSL4* and *ZmAn2* were the most highly expressed genes, followed by *ZmKSL2* and *ZmKO* (Figure 2.4a-d). *ZmKSL2* expression was observed in the control roots, but levels were significantly lower than the inoculated roots (Figure 2.4b). *ZmCYP81A1* was the only gene that was expressed more highly in the shoots than in the roots, and the difference in expression between the two inoculated tissues was significant (Figure 2.4e). However, *ZmCYP81A1* expression in the shoots did not differ between control and inoculated plants.

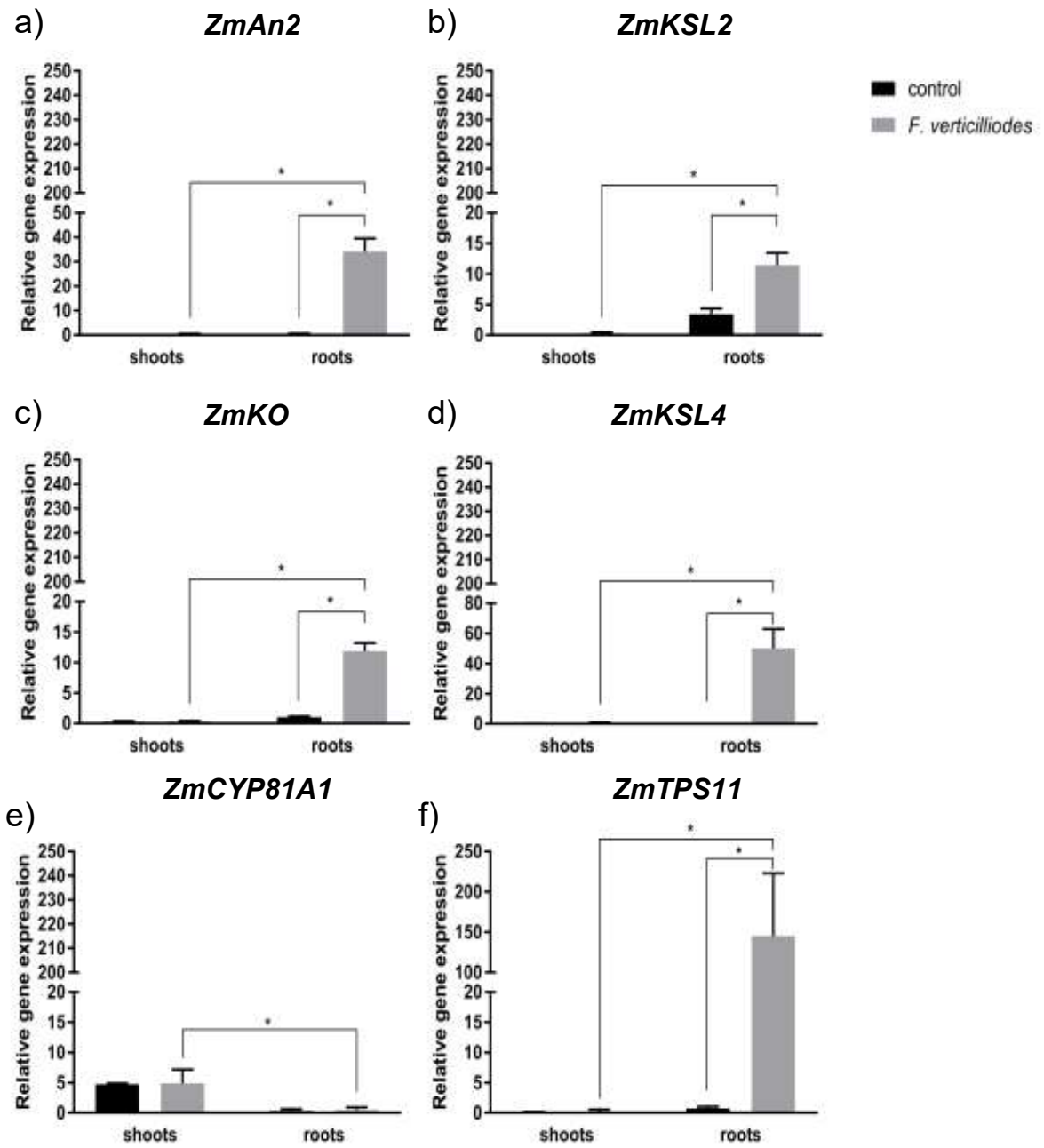

Figure 2.4 RT-qPCR analysis to measure relative gene expression in the shoot and root tissue of B73 maize in control plants and plants ten dpi. a) *ZmAn2*, b) *ZmKSL2*, c) *ZmKO,* d) *ZmKSL4,* e) *ZmCYP81A1* and f) *ZmTPS11. ZmMEP* and *ZmLUG* were used as reference genes to normalise data. Error bars indicate standard deviation (SD). An unpaired t test (unequal variance) was performed on log_{10}-transformed data to measure statistical significance. * = $p<0.05$, n=3

Summary of *F. verticillioides* growth and gene expression in B73 shoots and roots at ten days

F. verticillioides growth was observed in ten day old B73 plants following a seed soak inoculation. Phenotype analysis and fungal quantification assays led to the observation that *F. verticillioides* colonises the roots to a greater extent than the shoots. Root tissue presented a higher disease score than the shoot tissue, and the amount of *F. verticillioides* DNA detected in DNA extracted from B73 was higher in the roots than in the shoots. This result is expected due to the inoculation method used as well as the results of a previous study, which used an *F. verticillioides* GFP-expressing transgenic isolate to visualise early colonisation of *F. verticillioides* in maize (Oren et al., 2003). This study detected high levels of green fluorescent colonies in the roots, while only small amounts of green fluorescent colonies were isolated from the stem and leaves (Oren et al., 2003). Although the shoot tissue presented with mild disease symptoms following inoculation, fungal growth in this tissue was very low and no defence response (induction of phytoalexin biosynthetic genes in this case) was observed. The significant up-regulation of kauralexin biosynthesis genes (*ZmAn2, ZmKSL2, ZmKO,* and *ZmKSL4*) and the zealexin biosynthesis gene (*ZmTPS11*) following *F. verticillioides* inoculation suggests that a defence response is occurring as expected. It is surprising that *ZmCYP81A1* was not significantly expressed following *F. verticillioides* inoculation, especially as it was the only gene that was significantly up-regulated in all three studies following fungal inoculation (Table 2.5). This experiment showed that gene expression is induced following *F. verticillioides* inoculation and the response is greater in the roots than in the shoots.

2.2.3 Correlation of *F. verticillioides* growth with phytoalexin accumulation and phytoalexin biosynthetic gene expression in shoots and roots at two separate time points

a : B73 at ten and fourteen days post *F. verticillioides* inoculation

Following the optimisation of the techniques required for this study, a time course trial on the B73 maize lines was performed in order to determine whether there was an optimal time point at which to analyse the interaction between *F. verticillioides*

and maize. Maize was harvested at three time points; five, ten, and fourteen dpi. At five dpi, the maize had grown to the vegetative stage VE, which is the stage that the coleoptile emerges from beneath the soil ("Vegetative Corn Growth Stages and Scouting Tips", 2017). The size of the plant at this stage was not large enough to yield all of the tissue required for analyses, and this time point was therefore not used going forward. Therefore, only the plants harvested ten and fourteen dpi were analysed. Both of these plants were between vegetative stages V1 and V3 at these time points, which are characterised by the number of leaf collars ("Vegetative Corn Growth Stages and Scouting Tips", 2017).

B73 shoots phenotype analysis

The morphological characteristics in the ten day old B73 plants were very similar to those described in the B73 optimisation experiment. At fourteen dpi, the plants were larger in both treatments than at ten days old and space in the boxes was limited. Both treatments had ratty, yellowing/browning leaf tips, however this phenotype was more severe in the *F. verticillioides* inoculated plants than in the control (Figure 2.5a, Figure 2.5b). In the control plants, leaf 5 had already emerged, while in the inoculated plants only four leaves were seen at fourteen dpi. The ratty leaf tips in both treatments is most likely due to the effect of the limited space and nutrients in the box at that time point, as well as a general phenotype of the B73 line.

The control shoots at both time points exhibited a slight stress at the tips of the leaves, which is evident in the mean disease scores in Figure 2.6 being slightly greater than 1. This stress was more severe at fourteen dpi than at ten dpi and the scores were 1,4 and 1,1 respectively. The disease scores of the inoculated plants were higher at fourteen dpi than at ten dpi. The higher mean disease scores of both the control and inoculated plants at fourteen dpi relative to their respective treatments at ten dpi is likely due to growth effects.

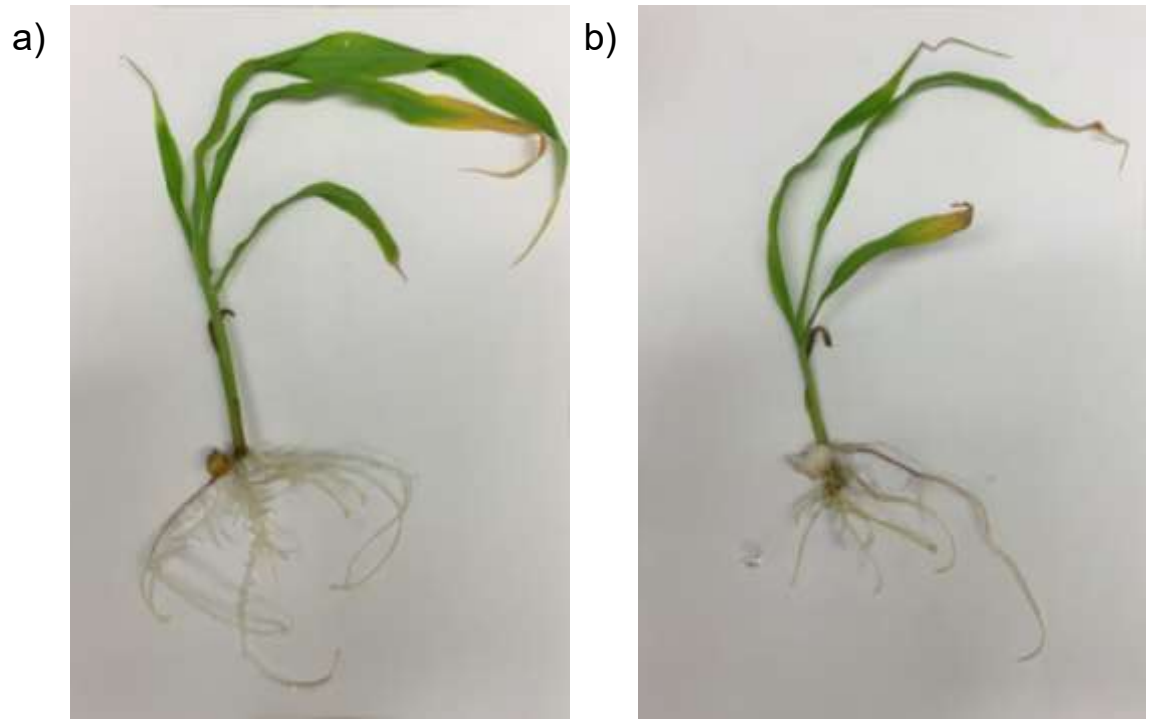

Figure 2.5 B73 maize plants in a) control and b) fourteen days post *F. verticillioides* inoculation

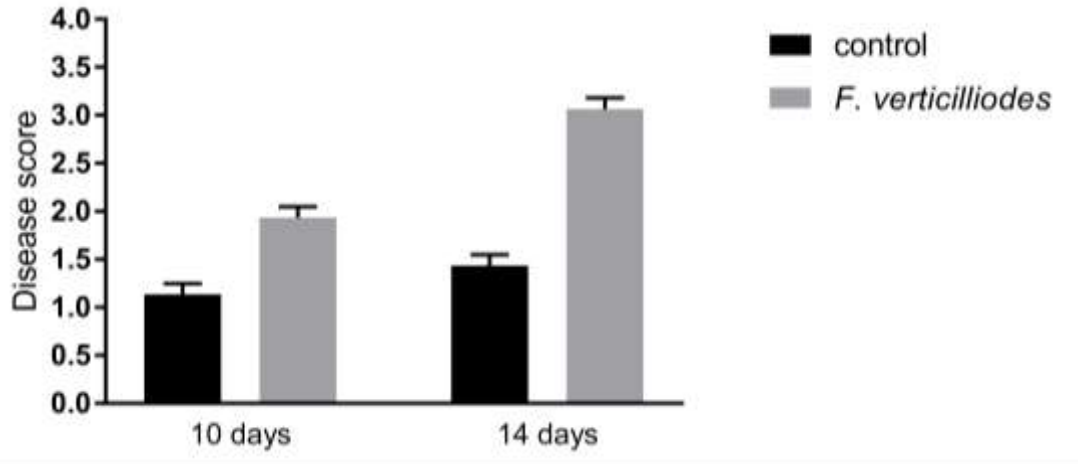

Figure 2.6 Mean disease scores of B73 maize 10 and 14 dpi in control and *F. verticillioides* inoculated shoots.

Fungal growth, phytoalexin accumulation and gene expression in B73 shoots

Fungal growth in ten and fourteen day old B73 was analysed using qPCR. *FvEF1α* primers were used to quantify fungal DNA present in the maize tissue, while *ZmMEP* primers were used to quantify the amount of plant DNA present in the total DNA extracted. Low levels of *F. verticillioides* were detected in the inoculated shoots. Growth at fourteen days was higher than at ten days and the amount of fungus at each time point was 2,27ng.μg^{-1} and 1,06 ng.μg^{-1} respectively (Figure 2.7a). Although growth in the inoculated plants was clearly higher than the controls, in which no *F. verticillioides* was detected, there was no significant difference in fungal growth between the control and inoculated plants due to variation among the samples.

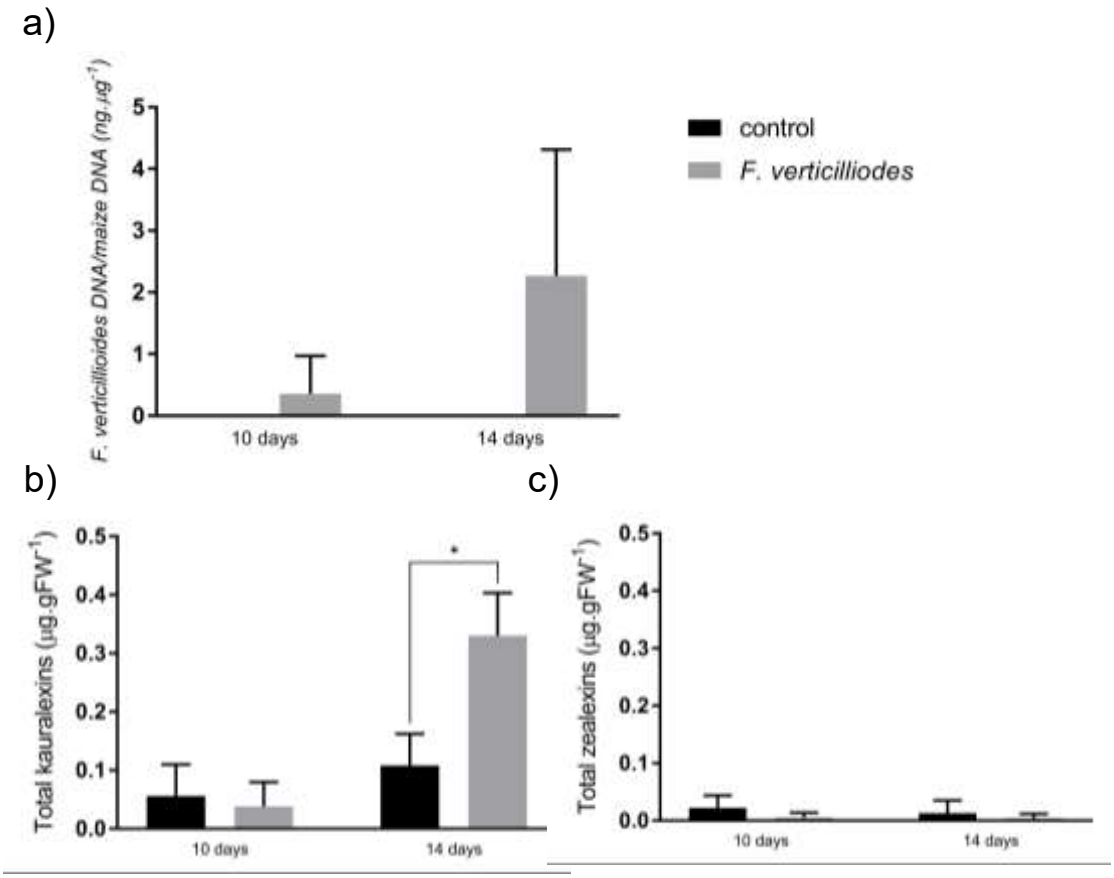

Figure 2.7 Analysis of B73 shoot tissue ten and fourteen dpi in control and *F. verticillioides* inoculated plants. a) Quantitative PCR analysis to measure *F. verticillioides* growth. The amount of *F. verticillioides* growing in B73 maize (ng.μg^{-1}) was quantified using *FvEF1α* and *ZmMEP* primers respectively. b) Total kauralexins and c) total zealexins (μg.gFW^{-1}) that accumulated in B73 maize following *F. verticillioides* inoculation were measured using gas chromatography-mass spectrometry. Error bars indicate standard deviation (SD). A one-tailed t test was performed to measure statistical significance of fungal growth. An unpaired t test (unequal variance) was performed on $\log_{10}$-transformed phytoalexin data to measure statistical significance * = $p<0.05$, n=3

Phytoalexin accumulation was measured using GC-MS and was performed at the USDA using protocols developed by Huffaker et al. (2011) and Schmelz et al. (2011). Statistical analysis was performed on log_{10}-transformed data in order to obtain a normal distribution among the data, but the untransformed data is presented on the graph. Phytoalexins accumulated to low levels in the shoots. Total kauralexins accumulated at low levels in the control treatments at both time points, and no difference in kauralexin accumulation was observed at the ten day time point (Figure 2.7b). Kauralexin accumulation increased significantly following *F. verticillioides* inoculation at fourteen days. Total zealexin levels were extremely low in the B73 shoots at both ten and fourteen days (Figure 2.7c). There was no difference in total zealexin levels between treatments and time points. The accumulation of individual kauralexins and zealexins is shown in Table S2.4.

In order to determine whether phytoalexins are induced by *F. verticillioides,* correlation analysis was performed. There is a positive correlation between *F. verticillioides* growth and kauralexin accumulation, with a correlation co-efficient of 0,94. The correlation co-efficient between *F. verticillioides* and zealexins is -0,82, and this negative correlation fits with the observation that zealexin accumulation was not induced following *F. verticillioides* inoculation.

RT-qPCR was used to measure gene expression of the phytoalexin biosynthesis genes in B73 maize harvested at the two time points. *ZmMEP* and *ZmLUG* were used as reference genes, and reference gene stability and the standard curves of all genes are shown in Tables S2.2 and S2.3 respectively. Statistical analysis was performed on log_{10}-transformed data in order to obtain a normal distribution among the data, but the untransformed data is presented on the graph. As a whole, *F. verticillioides* inoculation did not induce an up-regulation of phytoalexin biosynthesis genes in the shoots. *ZmAn2* was significantly up-regulated in the shoots at fourteen dpi (Figure 2.8a). *ZmKSL2* expression appears to increase at fourteen dpi, but there is no significant difference due to the variability of the biological samples (Figure 2.8b). This expression pattern was also observed in *ZmKO* and *ZmKSL4* (Figure 2.8c-d). Expression of *ZmAn2, ZmKSL2, ZmKO* and *ZmKSL4* did not change between the control and inoculated samples at ten dpi (Figure 2.8a-d). *ZmTPS11* expression appears higher at both ten and fourteen dpi, but once again no

significant difference in expression between control and inoculated samples is observed (Figure 2.8f). *ZmCYP81A1* expression did not change significantly between control and inoculated plants at either time point (Figure 2.8e).

Analysis of the correlations between the three kauralexin biosynthesis genes that are co-expressed according to (Christie et al., 2017) showed that there is a positive correlation between *ZmAn2* and *ZmKO* expression in the shoots, which had a correlation co-efficient of 0,87. However, *ZmAn2* and *ZmKSL2* has a lower correlation co-efficient of 0,33. *ZmKSL2* and *ZmKO* are negatively correlated. The correlation co-efficients are shown in Table 2.8. The correlations observed between *ZmAn2* and *ZmKSL2* and *ZmKSL2* and *ZmKO* are not significant, and this could be due to the low levels of fungus detected in the shoot tissue, which were not high enough to significantly induce a change in gene expression.

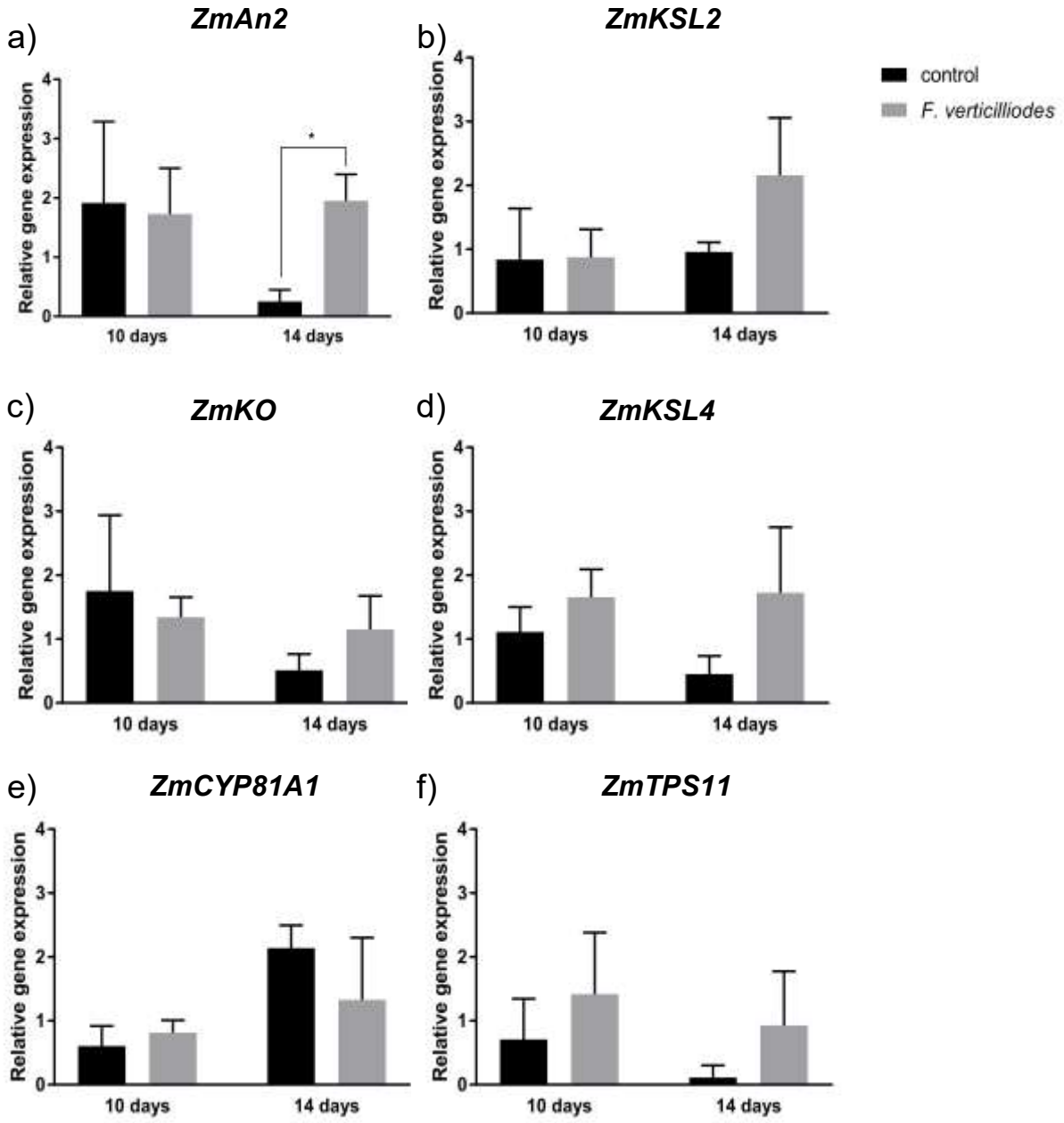

Figure 2.8 RT-qPCR analysis to measure relative gene expression in the shoot tissue of B73 maize in control plants and plants ten and fourteen dpi. a) *ZmAn2*, b) *ZmKSL2*, c) *ZmKO,* d) *ZmKSL4,* e) *ZmCYP81A1* and f) *ZmTPS11. ZmMEP* and *ZmLUG* were used as reference genes to normalise data. Error bars indicate standard deviation (SD). An unpaired t test (unequal variance) was performed on log_{10}-transformed phytoalexin data to measure statistical significance * = $p<0.05$, n=3

Table 2.8 Correlation matrix showing the correlations between *ZmAn2, ZmKSL2* and *ZmKO* expression in B73 shoots

	ZmAn2	*ZmKSL2*	*ZmKO*
ZmAn2	1		
ZmKSL2	0,33	1	
ZmKO	0,87	-0,13	1

B73 roots phenotype analysis

The root phenotypes in the B73 time point experiment were similar, for both time points, to those observed in the initial experiment. No obvious differences were observed between the control roots ten and fourteen dpi, and the inoculated roots did not appear to be significantly different between the two time points (Figure 2.2a-d, Figure 2.5a-b). The mean disease scores for the B73 control roots at both ten and fourteen dpi was 1,1, as they presented with no symptoms (Figure 2.9). The difference in disease symptoms between the inoculated plants at ten and fourteen days was very small, with scores of 2,5 and 2,8 respectively. Symptom severity was mild-to-medium in both cases, as the roots were brown and discoloured and were stunted in growth.

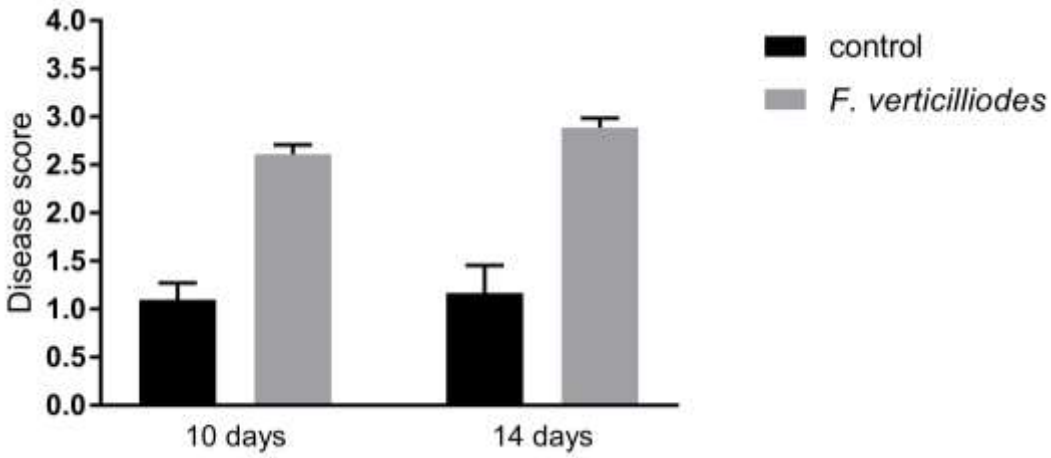

Figure 2.9 Mean disease scores of B73 maize 10 and 14 dpi in control and *F. verticillioides* inoculated roots.

Fungal growth, phytoalexin accumulation and gene expression in B73 roots

F. verticillioides DNA was not detected in the control roots at the ten and fourteen day time points following the qPCR assay. *F. verticillioides* growth was high at both ten and fourteen days following inoculation, with average growth of 6,28µg.ng^{-1} and 10,64µg.ng^{-1} respectively **(**Figure 2.10a). *F. verticillioides* growth was significantly higher in the ten day inoculated roots compared to the control roots, but no significance was observed between control and inoculated fourteen day fungal growth (Figure 2.10a). Although this is surprising due to the fact that no *F. verticillioides* DNA was detected in the fourteen day control roots and 10,64µg.ng^{-1}

was detected in the inoculated sample, the lack of significance is due to high levels of variation between biological samples, as observed by the large error bars in Figure 2.10a. There was no significant difference in *F. verticillioides* growth between the inoculated roots at the different time points.

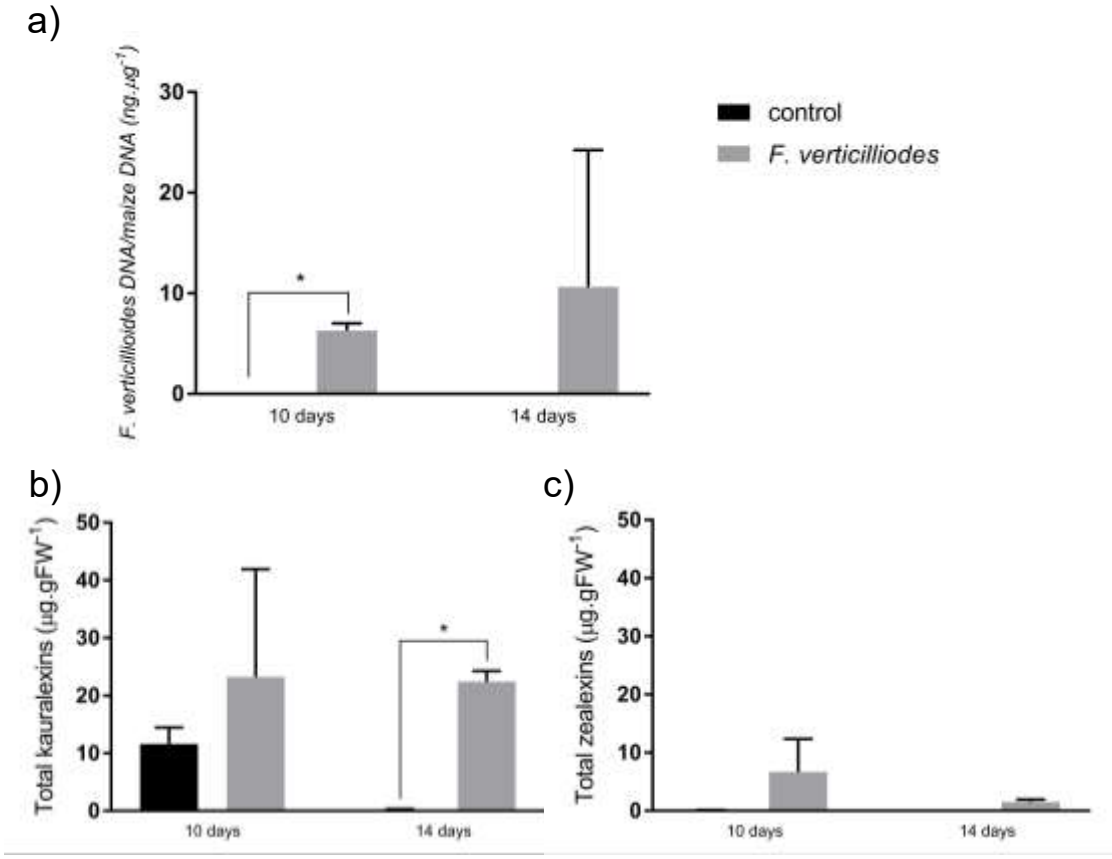

Figure 2.10 Analysis of B73 root tissue ten and fourteen dpi in control and *F. verticillioides* inoculated plants. a) Quantitative PCR analysis to measure *F. verticillioides* growth. The amount of *F. verticillioides* growing in B73 maize (ng.µg^{-1}) was quantified using *FvEF1α* and *ZmMEP* primers respectively. b) Total kauralexins and c) total zealexins (µg.gFW^{-1}) that accumulated in B73 maize following *F. verticillioides* inoculation were measured using gas chromatography-mass spectrometry. Error bars indicate standard deviation (SD). A one-tailed t test was performed to measure statistical significance of fungal growth. An unpaired t test (unequal variance) was performed on log_{10}-transformed phytoalexin data to measure statistical significance * = $p<0.05$, n=3

Statistical analysis was performed on log_{10}-transformed phytoalexin data in order to obtain a normal distribution among the data, but the untransformed data is presented on the graph. Phytoalexin accumulation in the roots was much higher relative to accumulation in the shoots. Total kauralexins were present in the ten day control roots at levels of 11,6µg.gFW^{-1} and in the inoculated roots at levels of 23,2µg.gFW^{-1}

(Figure 2.10b). Although kauralexin accumulation doubled following inoculation, there were high levels of variation among the biological samples and no significant difference was observed. Total kauralexin accumulation increased significantly following *F. verticillioides* inoculation at fourteen dpi, but kauralexins were not detected in the control roots at this time point. The presence of kauralexins in the control roots at ten days, and not at fourteen days, may be the result of developmental factors. Total kauralexin accumulation did not differ between inoculated samples of both time points (Figure 2.10b). Total zealexin accumulation was lower than total kauralexin accumulation in the roots (Figure 2.10c). Zealexins were not detected in the control roots at either time point, and they were detected in the inoculated roots at low levels of 6,7µg.gFW^{-1} and 1,5µg.gFW^{-1} at ten and fourteen days respectively. There was no significant change in total kauralexin and zealexin accumulation among the treatments and time point. The accumulation of individual phytoalexins is shown in Table S2.4.

The presence of *F. verticillioides* in root tissue resulted in the accumulation of total kauralexins, but resulted in low and not significant accumulation of total zealexins (Figure 2.10). This relationship is displayed by correlation analysis, which confirmed that *F. verticillioides* growth induces total kauralexin accumulation and is strongly, positively correlated in the root, with a co-efficient of 0,84. The low induction of total zealexins following *F. verticillioides* inoculation shows that induction of zealexins by the fungus is not as strong as kauralexins, with a positive, though not significant, correlation of 0,47.

The expression of the phytoalexin biosynthesis genes was measured in the roots using RT-qPCR. *ZmMEP* and *ZmLUG* were used as reference genes for analysis and the reference gene stability is shown in Table S2.2. The standard curves of all of genes run is shown in Table S2.3. Statistical analysis was performed on $\log_{10}$-transformed data in order to obtain a normal distribution among the data, but the untransformed data is presented on the graph. *F. verticillioides* inoculation resulted in the up-regulation of all of the candidate genes in this study in the roots (Figure 2.11). *ZmAn2* (Figure 2.11a), *ZmKSL2* (Figure 2.11b), and *ZmKSL4* (Figure 2.11d) were significantly up-regulated at both time points following inoculation compared to the control. No significant difference in gene expression between the inoculated

roots at each time point was observed for any of the genes. *ZmKO* was significantly up-regulated at fourteen dpi, but no change in expression was observed at ten dpi (Figure 2.11c). *ZmCYP81A1* expression appears to increase following inoculation with *F. verticillioides* at both time points (Figure 2.11e). However, there are high levels of variation among the biological samples and no significance was observed. *ZmTPS11* was significantly up-regulated at ten dpi, but no significant change in expression was observed at fourteen dpi, despite the appearance of increased expression following *F. verticillioides* inoculation (Figure 2.11f).

The correlations between the three co-expressed genes, *ZmAn2, ZmKSL2* and *ZmKO,* are all positively correlated with each other (Table 2.9). The correlation between *ZmAn2* and *ZmKSL2* is significant. *F. verticillioides* growth in the roots was sufficient to induce a defence response that resulted in the up-regulation of the phytoalexin biosynthesis genes, including the three co-expressed kauralexin biosynthetic genes.

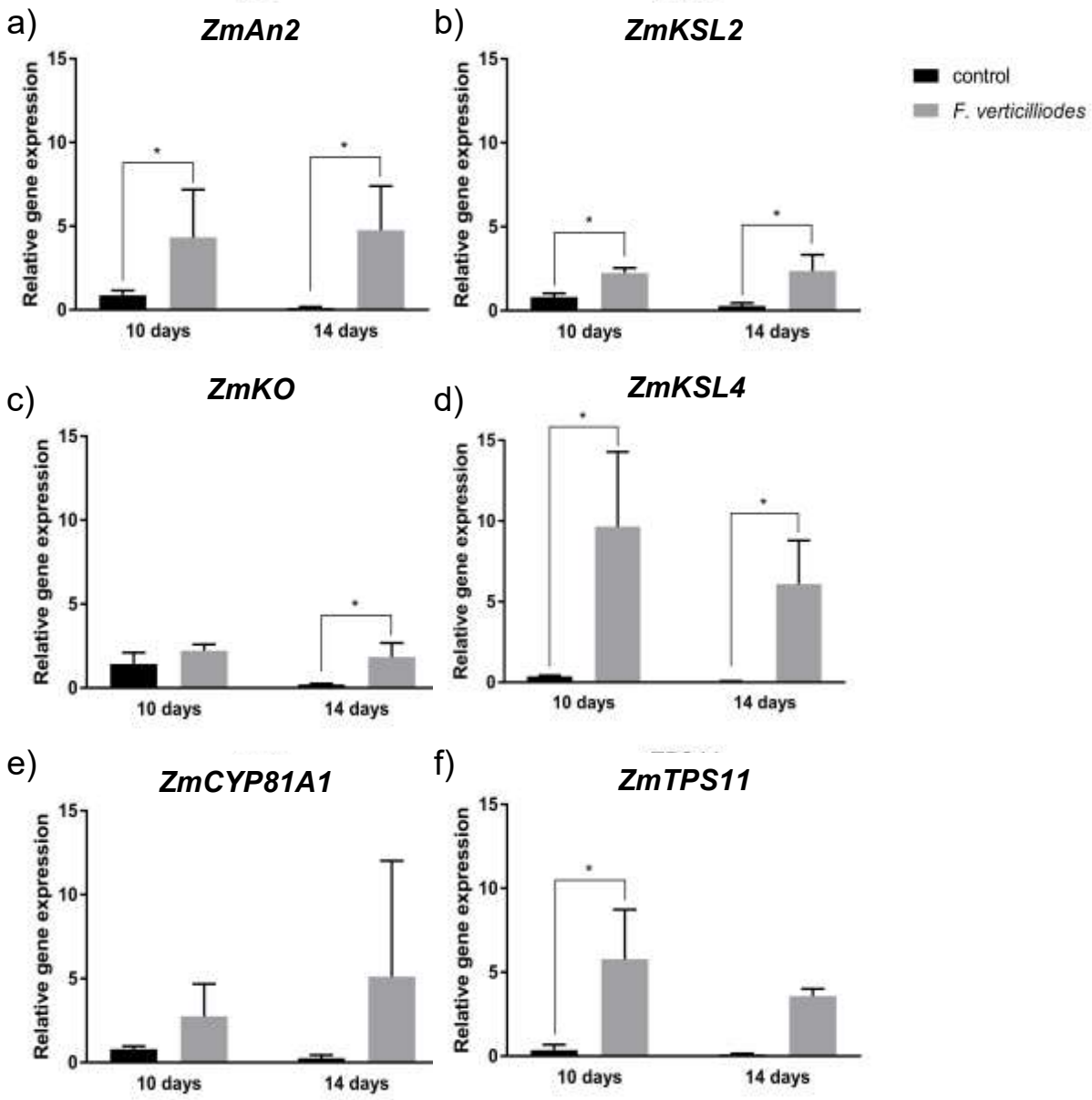

Figure 2.11 RT-qPCR analysis to measure relative gene expression in the root tissue of B73 maize in control plants and plants ten and fourteen dpi. a) *ZmAn2*, b) *ZmKSL2*, c) *ZmKO,* d) *ZmKSL4,* e) *ZmCYP81A1* and f) *ZmTPS11. ZmMEP* and *ZmLUG* were used as reference genes to normalise data. Error bars indicate standard deviation (SD). An unpaired t test (unequal variance) was performed on log_{10}-transformed phytoalexin data to measure statistical significance * = p<0.05, n=3

Table 2.9 Correlation matrix showing the correlations between *ZmAn2, ZmKSL2* and *ZmKO* expression in B73 roots

	ZmAn2	*ZmKSL2*	*ZmKO*
ZmAn2	1		
ZmKSL2	1	1	
ZmKO	0,85	0,89	1

Green shading = p<0.05

Summary of *F. verticillioides* growth, phytoalexin accumulation and gene expression in B73 shoots and roots at two time points

As previously observed, *F. verticillioides* growth was higher in the roots than in the shoots. The defence response induced in the different tissues following inoculation positively correlated to the amount of fungus detected, in that the response is stronger when more *F. verticillioides* is detected. Although *F. verticillioides* was not detected at very high levels in the shoots, disease severity scores increased following inoculation, as they did in the roots when higher levels of fungus were detected. Although the inoculated shoot tissue presented with stressed symptoms, the defence response does not correlate with the disease score. The results showed that total kauralexins accumulate to high levels in roots following *F. verticillioides*, but only to low levels in shoots. In both tissues, total kauralexin accumulation and *F. verticillioides* growth are positively correlated. Kauralexins were present in the control roots at ten days, which is possibly due to developmental factors. Kauralexins have previously been suggested to be developmentally regulated as well as induced, due to their accumulation in the scutella of untreated seedlings (Schmelz et al., 2011). Zealexins did not accumulate in the shoots but did accumulate in the roots following inoculation, albeit only to low levels that were not significant. A negative correlation between *F. verticillioides* growth and zealexin accumulation in the shoots was observed, but the correlation was positive in the root tissue. The amount of fungal growth in the shoots was not sufficient to induce differential expression of the phytoalexin biosynthesis genes as a whole, although *ZmAn2* was significantly up-regulated at fourteen dpi. Gene expression in the roots was significantly up-regulated in all genes except for *ZmCYP81A1*. The induction of the kauralexin biosynthesis genes in the roots resulted in positive correlations between the three genes that are co-expressed, with significance between *ZmAn2* and *ZmKSL2* (*ZmAn2, ZmKSL2,* and *ZmKO*). The correlations in the shoots were not significant, due to the lack of induction of these genes as a result of low *F. verticillioides* growth. Fungal growth, phytoalexin accumulation and putative phytoalexin biosynthetic gene expression were not significantly different at the two time points measured. The low induction of phytoalexin biosynthetic genes in the shoots correlates with low phytoalexin accumulation, while the induction of kauralexin biosynthetic genes correlates with

high total kauralexin accumulation in the shoots. *ZmTPS11* expression is higher in the roots at ten dpi, which is when total zealexin accumulation is at it's highest.

These results indicate that the amount of *F. verticillioides* in the shoot was not significant to induce the expression of phytoalexin biosynthesis genes, and as a result phytoalexins did not accumulate to high levels. However, when *F. verticillioides* growth is detected at higher levels, as observed in the roots, a phytoalexin response is induced.

2.2.3 Correlation of *F. verticillioides* growth with phytoalexin accumulation and phytoalexin biosynthetic gene expression in shoots and roots at two separate time points

b. CML444 at ten and fourteen days post *F. verticillioides* inoculation

CML444, a maize line obtained from the Agricultural Research Council-Grain Crops Institute (ARC-GCI), but bred by CIMMYT (Rose et al., 2017), was used in a time course experiment to determine whether any differences between genotypes at the two time points may arise, thus influencing the ultimate time point chosen for further experiments. A previous study analysing resistance of several maize lines to *F. verticillioides* showed that CML444 is partially resistant to the fungus (Small et al., 2012). CML444 was treated in the same way as B73 and harvested at the different time points. Once again, the plants harvested at five dpi were too small to yield enough tissue for all of the analyses, and this tissue was therefore abandoned. The plants harvested at ten and fourteen days were both between vegetative stages V1 and V3.

CML444 shoots phenotype analysis

The mean disease scores of the control shoots at ten and fourteen dpi once again have a slightly higher score than 1, due to the growth conditions causing stressed phenotypes (Figure 2.12). Unfortunately, as germination frequency was lower than in B73, CML444 plants could not be sacrificed for pictures. The inoculated shoots had mean disease scores of 2 and 2,3 at ten and fourteen dpi respectively, and although leaf 1 was severely symptomatic, the higher leaves were still relatively healthy with just some light brown beginning on the tips. CML444 had thicker stems and longer,

wider leaves than B73. The plants had the same leaf numbers as observed at the different time points in B73, with 3-4 leaves at ten dpi and 4-5 leaves at fourteen dpi, with slightly different rates of emergence of the last leaf among individual plants. By fourteen dpi, leaves had grown very long and were crowded within the box. *F. verticillioides* was growing on some of the inoculated plants' leaf 1, and leaf 1 of all of the inoculated plants were brown and shrivelled. The tips of the higher leaves were also beginning to brown. The control leaves were beginning to yellow at the tips. This yellowing is most likely due to a limiting of resources within the box. Therefore, the browning tips of the inoculated plants were most likely also due to the box effect, but *F. verticillioides* seems to have enhanced this phenotype.

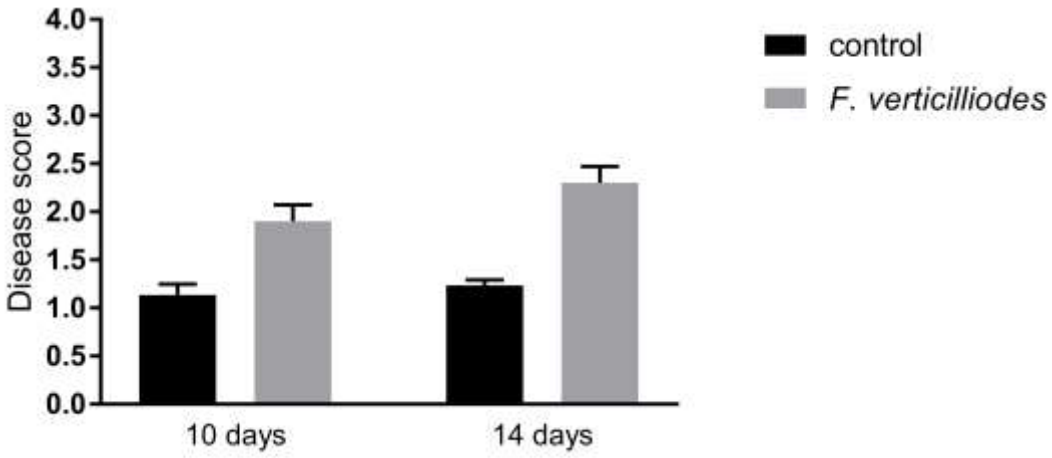

Figure 2.12 Mean disease scores of CML444 maize 10 and 14 dpi in control and *F. verticillioides* inoculated shoots.

Fungal growth, phytoalexin accumulation and gene expression in CML444 shoots

F. verticillioides growth was quantified as described previously, using qPCR. *FvEF1α* primers were used to quantify fungal DNA present in the maize tissue, while *ZmGST3* primers were used to quantify the amount of plant DNA present in the total DNA extracted. *ZmGST3* primers were used as they were found to be optimal for CML444. Fungal growth was low in the shoots at both time points. No *F. verticillioides* was detected in either the control or inoculated plants at ten dpi, while only 0,61ng.μg^{-1} *F. verticillioides* DNA was detected at fourteen days (Figure 2.13a). The amount of fungus that grew at fourteen dpi was not significantly different to the control, and there was no significant difference in fungal growth across the inoculated time points, despite the change from 0ng.μg^{-1} to 0,61ng.μg^{-1}.

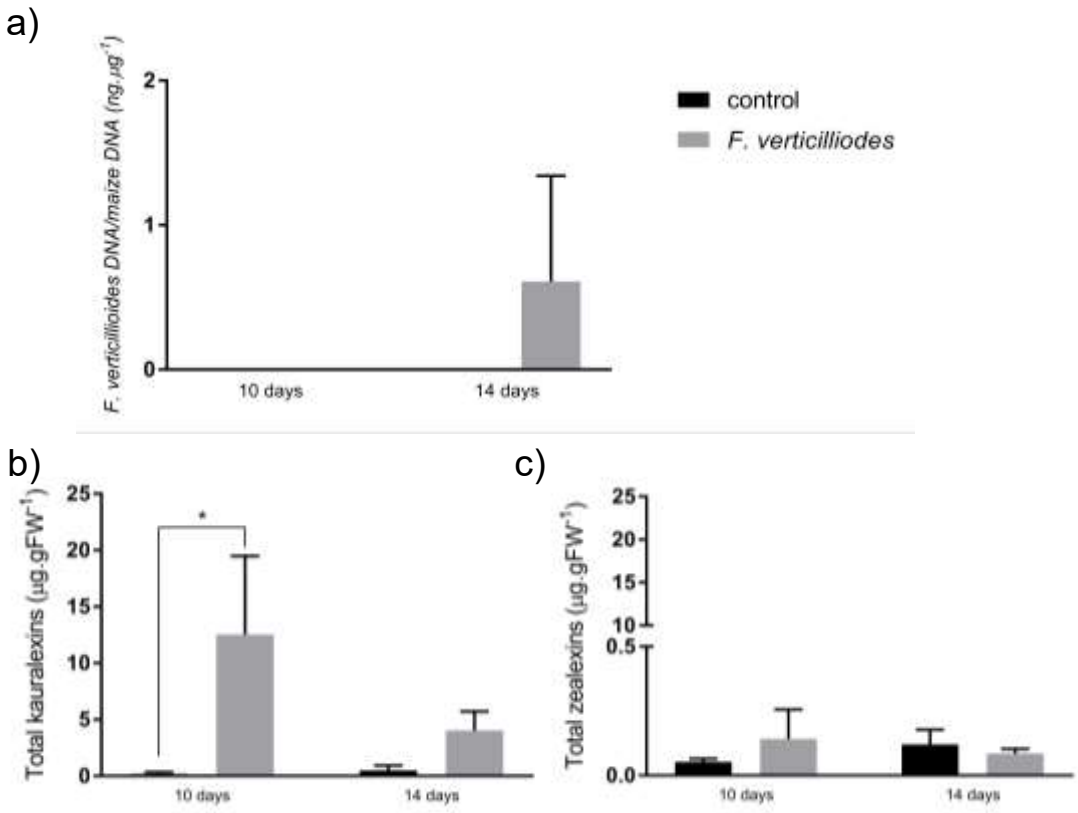

Figure 2.13 Analysis of CML444 shoot tissue ten and fourteen dpi in control and *F. verticillioides* inoculated plants. a) Quantitative PCR analysis to measure *F. verticillioides* growth. The amount of *F. verticillioides* growing in CML444 maize (ng.µg^{-1}) was quantified using *FvEF1α* and *ZmGST3* primers respectively. b) Total kauralexins and c) total zealexins (µg.gFW^{-1}) that accumulated in CML444 maize following *F. verticillioides* inoculation were measured using gas chromatography-mass spectrometry. Error bars indicate standard deviation (SD). A one-tailed t test was performed to measure statistical significance of fungal growth. An unpaired t test (unequal variance) was performed on log_{10}-transformed phytoalexin data to measure statistical significance * = $p<0.05$, n=3

Statistical analysis was performed on log_{10}-transformed phytoalexin data in order to obtain a normal distribution among the data. Phytoalexins accumulated in the shoots despite only low levels of *F. verticillioides* growth. Kauralexins accumulated significantly at ten dpi and increased following inoculation at fourteen dpi, although the increase was not significant (Figure 2.13b). Accumulation was higher at ten dpi

than at fourteen dpi, but there was no significant difference in accumulation between the two inoculated time points. *F. verticillioides* inoculation did not induce significant accumulation of zealexins at either time point (Figure 2.13b***)***. The accumulation of kauralexins despite the detection of significant amounts of *F. verticillioides* suggests that CML444 is sensitive to fungal stress and a response can be induced when *F. verticillioides* is present at low or even undetectable levels. The individual accumulation of phytoalexin compounds is shown in Table S2.4. There was no correlation observed between fungal growth and kauralexin accumulation (correlation co-efficient is -0,03), due to the fact that kauralexins accumulate despite low levels of *F. verticillioides*. There is a negative correlation between fungal growth and zealexin accumulation (-0,25).

Expression of phytoalexin biosynthesis genes were measured in the CML444 shoots using RT-qPCR. *ZmGST3* and *ZmRPol* were used as reference genes for analysis and the reference gene stability is shown in Table S2.2. The standard curves of all of genes are shown in Table S2.3. As primers for the genes were designed according to the B73 genome, the qPCR products of CML444 were sent for sequencing at the CAF. Sequencing confirmed that the primers were gene-specific in CML444 (Figure S2.2). *ZmKSL4* was not sent for sequencing as it had previously been sequenced by Naadirah Moola in the laboratory, confirming specificity of the *ZmKSL4* primers. Statistical analysis was performed on $\log_{10}$-transformed data in order to obtain a normal distribution among the data, but the untransformed data is presented on the graph. *ZmKSL2* was significantly up-regulated at ten and fourteen dpi following inoculation compared to the control, but there was no significant difference in *ZmKSL2* expression in the inoculated plants between the two time points (Figure 2.14b). *F. verticillioides* inoculation did not induce significant changes in expression of *ZmAn2, ZmKO, ZmKSL4* and *ZmTPS11* (Figure 2.14a, Figure 2.14c-f). *ZmCYP81A1* was significantly up-regulated at fourteen dpi compared to the control, and the up-regulation was also significant compared to the inoculated shoot at ten dpi (Figure 2.14e). The correlations between the co-expressed genes were variable. *ZmAn2* and *ZmKSL2* are positively correlated while *ZmAn2* and *ZmKO* are negatively correlated (close to no correlation with a co-efficient of -0,06) (Table 2.10). There was no significance in the correlations observed, which is likely due to the lack of significance of gene expression of *ZmAn2* and *ZmKO*.

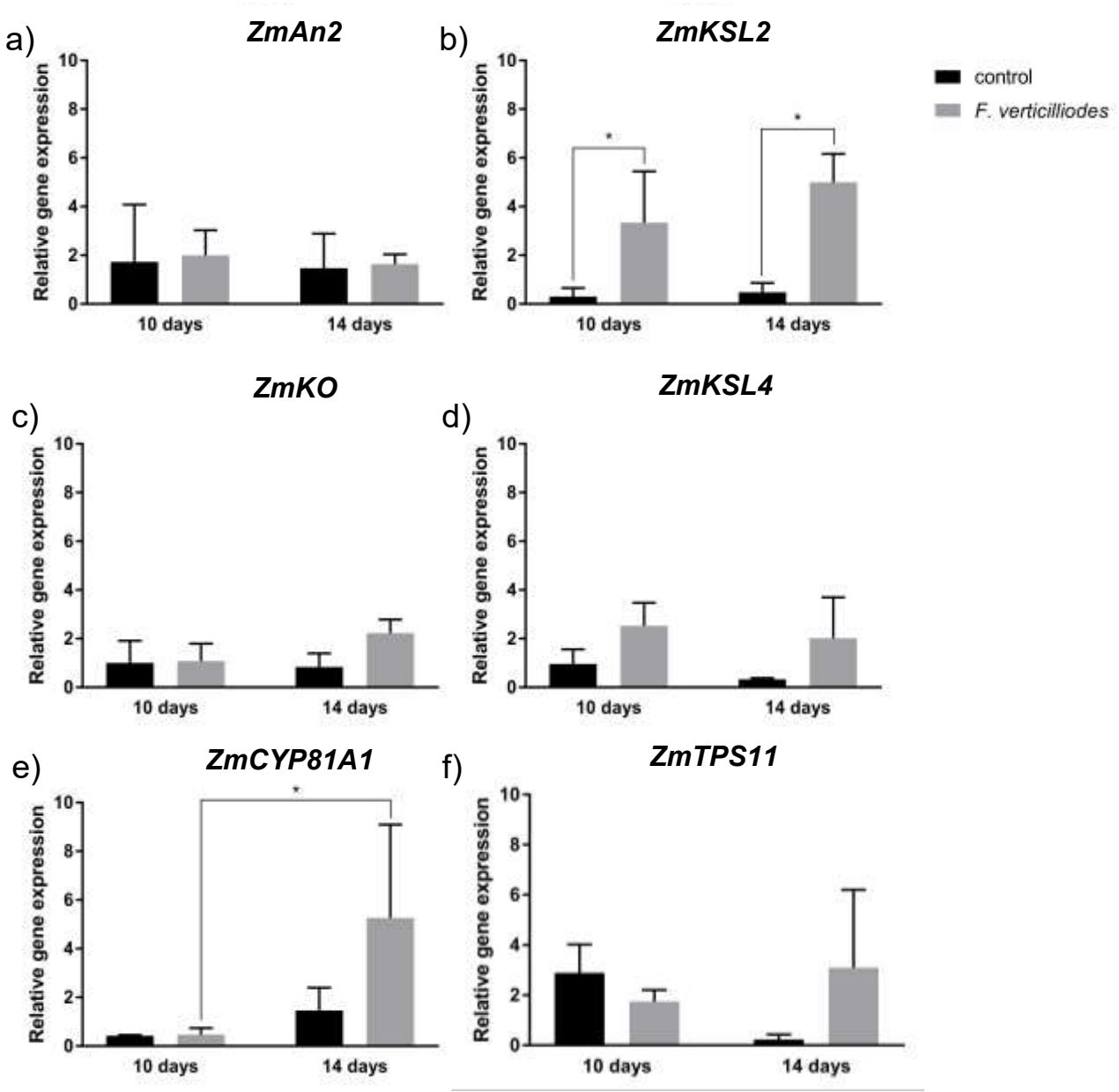

Figure 2.14 RT-qPCR analysis to measure relative gene expression in the shoot tissue of CML444 maize in control plants and plants ten and fourteen dpi. a) *ZmAn2*, b) *ZmKSL2*, c) *ZmKO,* d) *ZmKSL4,* e) *ZmCYP81A1* and f) *ZmTPS11. ZmGST3* and *ZmRPol* were used as reference genes to normalise data. Error bars indicate standard deviation (SD). An unpaired t test (unequal variance) was performed on log_{10}-transformed phytoalexin data to measure statistical significance * = $p<0.05$, n=3

Table 2.10 Correlation matrix showing the correlations between *ZmAn2, ZmKSL2* and *ZmKO* expression in CML444 shoots

	ZmAn2	*ZmKSL2*	*ZmKO*
ZmAn2	1		
ZmKSL2	0,33	1	
ZmKO	-0,06	0,85	1

CML444 roots phenotype analysis

The root network in CML444 was much larger than the B73 root network, just as the shoots were larger in CML444 than B73. Control roots were long, white and had a diverse network of lateral roots coming off of the seminal roots (Figure 2.15a). Roots of the inoculated plants were brown and stunted in growth (Figure 2.15b). However, the roots inoculated with *F. verticillioides* were still long relative to the inoculated B73 roots. Aside from slightly larger roots at ten dpi compared to fourteen dpi, there were no clear differences between the phenotypes at the two time points in both the control and inoculated plants. The disease scores in control roots were 1, as there was no obvious stress to the roots, while the scores for the inoculated plants were much higher, being over 3 for both time points (Figure 2.15c).

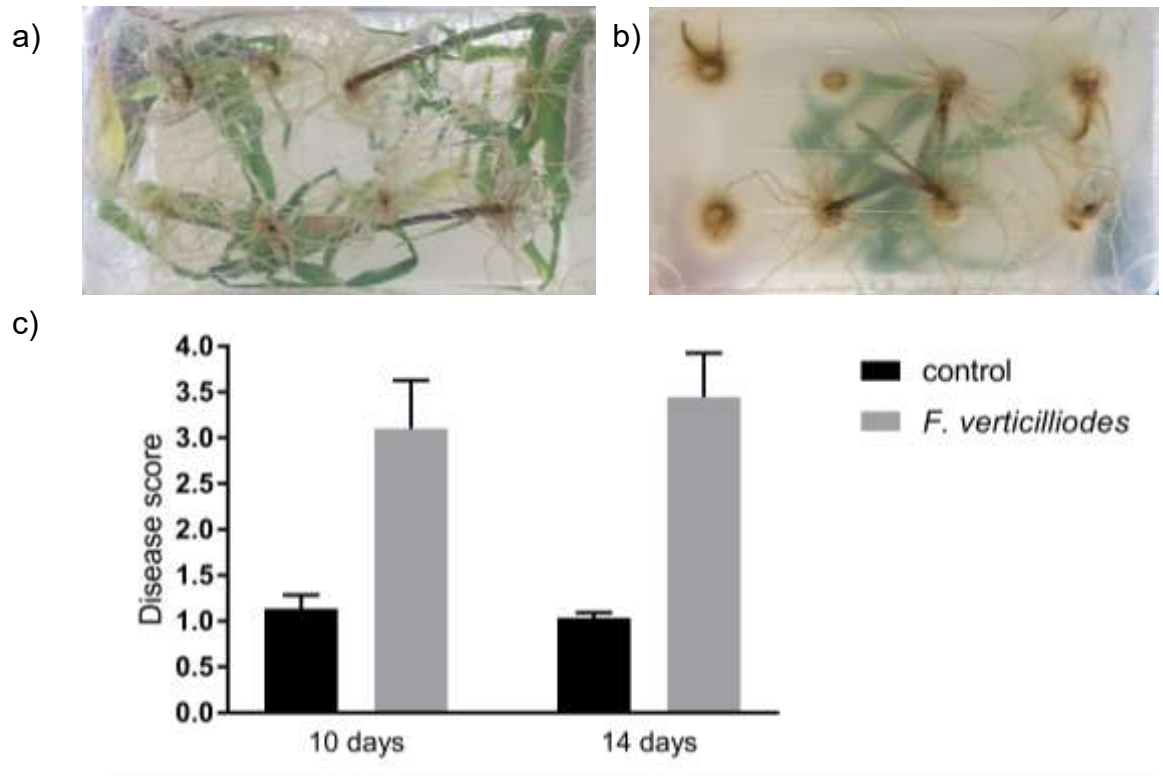

Figure 2.15 Phenotype analysis of CML444 roots ten and fourteen days after *F. verticillioides* inoculation. a) Control CML444 roots at fourteen days, b) CML444 roots fourteen dpi with *F. verticillioides,* c) mean disease scores of CML444 maize 10 and 14 dpi in control and *F. verticillioides* inoculated roots.

Fungal growth, phytoalexin accumulation and gene expression in CML444 roots

The amount of *F. verticillioides* growing in the roots of CML444 was quantified using qPCR. *ZmGST3* and *FvEF1α* primers were used for fungal quantification. Fungal growth in the roots of CML444 was very high in comparison to the shoots and in comparison to the B73 tissue. Fungal growth was highest at fourteen dpi and amounted to 55,82 ng.µg^{-1} (Figure 2.16a). Although fungal growth was detected at both inoculated time points, and not in the control, no significant difference in growth between inoculated and control plants was detected due to variation among biological samples. There was also no significant difference in fungal growth between the inoculated plants at ten and fourteen dpi.

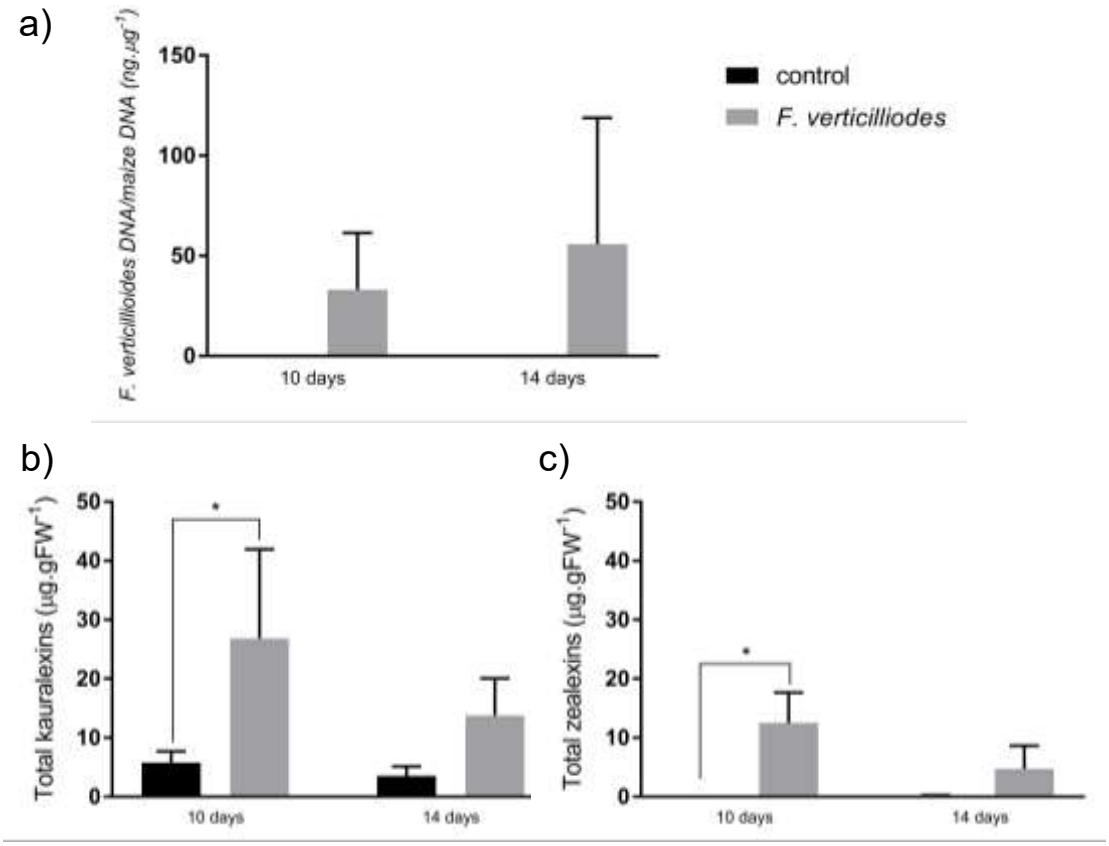

Figure 2.16 Analysis of CML444 root tissue ten and fourteen dpi in control and *F. verticillioides* inoculated plants. a) Quantitative PCR analysis to measure *F. verticillioides* growth. The amount of *F. verticillioides* growing in CML444 maize (ng.µg^{-1}) was quantified using *FvEF1α* and *ZmGST3* primers respectively. b) Total kauralexins and c) total zealexins (µg.gFW^{-1}) that accumulated in CML444 maize following *F. verticillioides* inoculation were measured using gas chromatography-mass spectrometry. Error bars indicate standard deviation (SD). A one-tailed t test was performed to measure statistical significance of fungal growth. An unpaired t test (unequal variance) was performed on log_{10}-transformed phytoalexin data to measure statistical significance * = $p<0.05$, n=3

Statistical analysis was performed on log_{10}-transformed phytoalexin data in order to obtain a normal distribution among the data, but the untransformed data is presented on the graph. Kauralexins accumulated in the roots at both ten and fourteen dpi (Figure 2.16b). Total kauralexin accumulation was significant at ten dpi in the inoculated plants compared to the control, but not at fourteen dpi. Total kauralexins were detected in low amounts in the control plants, suggesting that they may accumulate to low levels due to developmental factors. Zealexin levels increased significantly ten dpi following inoculation, and while levels also appear to increase fourteen dpi, the increase is not significant due to variation (Figure 2.16c). The accumulation of individual phytoalexin compounds is shown in Table S2.4. Both kauralexin and zealexin accumulation is induced following *F. verticillioides* inoculation, resulting in positive correlations with kauralexins and zealexins of 0,64 and 0,61 respectively.

Gene expression in the roots was measured using RT-qPCR, with *ZmGST3* and *ZmRPol* used as reference genes. The reference gene stability is shown in Table S2.2. The run quality of all of the genes is shown in Table S2.3. Statistical analysis was performed on log_{10}-transformed data in order to obtain a normal distribution among the data. Gene expression appears to increase following inoculation at all time points (Figure 2.17). However, due to variation among samples, some change in expression was not significant. *ZmAn2* gene expression increased significantly at fourteen dpi in the inoculated plants, but did not increase significantly at ten dpi (Figure 2.17a). *ZmKSL2* expression increased significantly at ten dpi when *F. verticillioides* was present, but not at fourteen dpi (Figure 2.17b). *ZmKSL4* and *ZmTPS11* expression increased significantly following *F. verticillioides* inoculation at both time points (Figure 2.17d**,** Figure 2.17f). There was no change in gene expression of *ZmKO* and *ZmTPS11* at either time point (Figure 2.17c, Figure 2.17e). There was no significant change in any of the phytoalexin biosynthetic genes measured across the inoculated plants at the two time points (Figure 2.17). The three co-expressed kauralexin biosynthesis genes all display positive correlations with each other, but the correlation between *ZmKSL2* and *ZmKO* is the only significant co-efficient (Table 2.11).

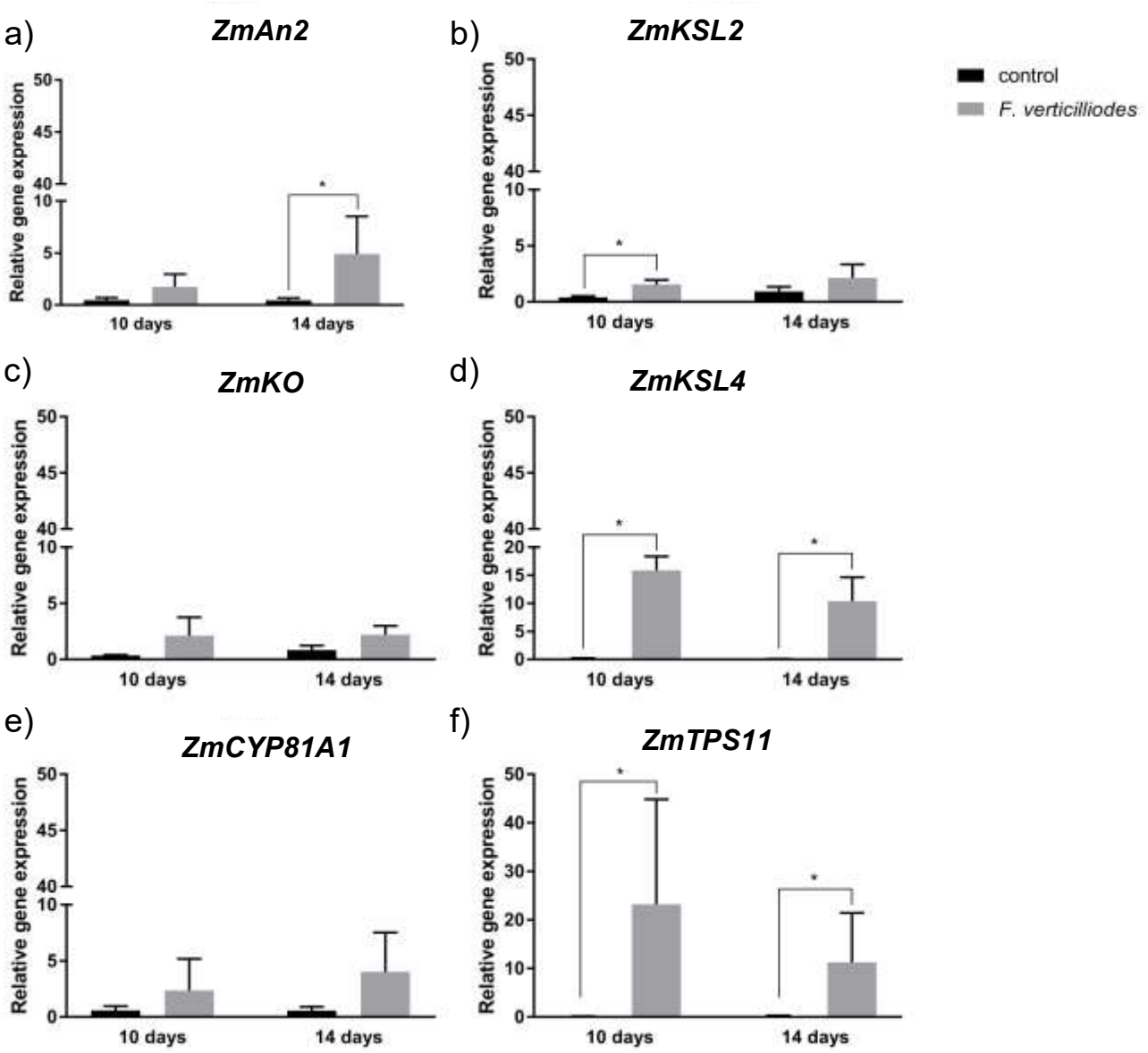

Figure 2.17 RT-qPCR analysis to measure relative gene expression in the root tissue of CML444 maize in control plants and plants ten and fourteen dpi. a) *ZmAn2*, b) *ZmKSL2*, c) *ZmKO,* d) *ZmKSL4,* e) *ZmCYP81A1* and f) *ZmTPS11. ZmGST3* and *ZmRPol* were used as reference genes to normalise data. Error bars indicate standard deviation (SD). An unpaired t test (unequal variance) was performed on log_{10}-transformed phytoalexin data to measure statistical significance * = $p<0.05$, n=3

Table 2.11 Correlation matrix showing the correlations between *ZmAn2, ZmKSL2* and *ZmKO* expression in CML444 roots

	ZmAn2	*ZmKSL2*	*ZmKO*
ZmAn2	1		
ZmKSL2	0,91	1	
ZmKO	0,79	0,96	1

Green shading = $p<0.05$

Summary of *F. verticillioides* growth, phytoalexin accumulation and gene expression in CML444 roots and shoots at two time points

The amount of *F. verticillioides* growth does not necessarily appear to correlate with disease severity in CML444. The difference in disease scores between inoculated plants at the two time points was extremely low, even though fungal quantification showed that fungal growth was higher at fourteen dpi. Although fungus was seen on leaf 1 of some of the inoculated plants, low levels of fungus were detected in the quantification assay. The low amount of fungus detected in the shoots was expected following what had been observed in the B73 maize and in previous studies (Oren et al., 2003). However, the significant accumulation kauralexins in the shoots, despite low or no *F. verticillioides* detection, was unexpected. Aside from *ZmKSL2*, the kauralexin biosynthesis genes were not significantly up-regulated, suggesting that many other genes that have not been studied here are also involved in kauralexin biosynthesis, or gene expression occurred prior to analysis and then decreased when kauralexins were produced, as observed in previous studies (Huffaker et al., 2011; Schmelz et al., 2011). Fungal growth in the roots was very high, and this could be due to the phenotype of CML444, which appears to have a more diverse network of roots and secondary roots than B73. As a result, there is an increased area for *F. verticillioides* to colonise. Phytoalexins in the roots accumulated to higher levels than in the shoots, although the accumulation was not always significant due to variation. The correlation between phytoalexin accumulation and *F. verticillioides* growth was much higher in the roots than in the shoots. *F. verticillioides* significantly induced up-regulation of all of the genes except for *ZmKO* and *ZmCYP81A1* at one or both of the time points in the roots, and the correlation between the three kauralexin co-expressed genes was also much higher in the roots than in the shoots. The results from the roots show a positive correlation between *F. verticillioides* growth and phytoalexin accumulation, as well as a positive relationship between gene expression induction and *F. verticillioides*. The correlations observed in the shoots are much weaker and not significant, supporting the fact that when small amounts of fungus are present, phytoalexin accumulation and gene expression are not induced to high levels. As observed in the B73 time course experiment, there were no obvious differences between the CML444 responses to *F. verticillioides* at either time point.

2.2.4 *F. verticillioides* growth, phytoalexin accumulation and gene expression in maize lines from the ARC-Grain Crops Institute

Due to the differing phenotypes of B73 and CML444 observed during the time course experiments, with CML444 growing much larger than B73, ten dpi was chosen as the time point for further experiments, as the phenotypes of the lines to be grown were unknown and we did not want to induce further stress on the plants due to the limited size of the box. Only one time point could be taken forward due to limited seed availability. Lines were inoculated with *F. verticillioides* using the seed soak inoculation method and the roots were harvested ten dpi. Only the roots were harvested due to the low response previously observed in the shoots. As the lines were grown in batches, inoculated B73 plants were grown in each batch with the other lines to observe any changes in response from one genotype across the experiments. Unfortunately the seeds of the lines that were due to be studied had a low germination frequency and many were contaminated with endophytes (Table S2.5). The only line that had a high enough germination frequency to conduct full analyses was CB248. This line is partially resistant to *F. verticillioides* (Rose et al., 2017).

CB248 roots phenotype analysis

The roots of CB248 control plants were short, thin and white. There was not a very large network of roots coming off of the seminal roots, as observed in the other lines. A bacterial-like endophyte was growing from two out of the three control plants and as a result the roots of these plants did not look as healthy as the clean plant. The inoculated plants had brown, discoloured roots but they did not appear more stunted than the control. Plants in both treatments did not look particularly healthy. In both cases disease scores were above 3 and individual plants showed medium to severe symptoms in both treatments (Figure 2.18). The disease score of B73 in this batch was less severe, with a score of 2.8 (Figure S2.3a).

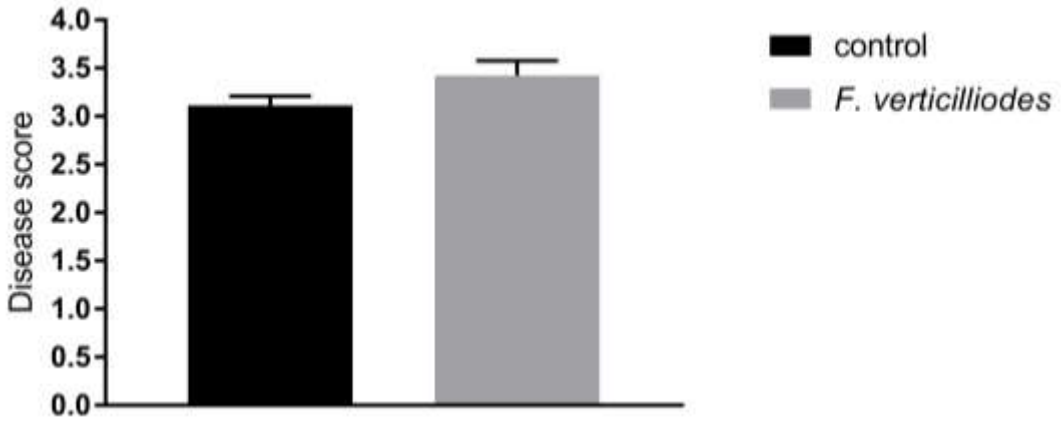

Figure 2.18 Mean disease scores of CB248 maize 10 dpi in control and *F. verticillioides* inoculated roots

Fungal growth, phytoalexin accumulation and gene expression in CB248 roots

F. verticillioides growth in the CB248 roots was measured using qPCR. *FvEF1α* and *ZmMEP* primers were used to measure *F. verticillioides* and CB248 DNA respectively. Fungal growth in B73 roots that were grown at the same time as CB248 was also measured to compare the response of one genotype across all experiment batches. This was to compare the inoculation process to previous experiments. *F. verticillioides* growth was significantly higher in B73 than in CB248 (Figure S2.3b), and the high level of *F. verticillioides* detected in B73 compared to previous experiments suggests that conditions were optimal for inoculation and fungal growth. At ten dpi, *F. verticillioides* had grown to 5,91ng.μg^{-1} in CB248 and this growth was significantly more than the control (Figure 2.19a).

Statistical analysis was performed on log_{10}-transformed phytoalexin data in order to obtain a normal distribution among the data, but the untransformed data is presented on the graph. Total kauralexin accumulation in the CB248 roots increased following *F. verticillioides* inoculation, but the increase was not significant (Figure 2.19b). Kauralexin accumulation in the control plants suggests that they are present in low amounts due to developmental factors, or they could be present due to a bacterial-like endophyte observed on the seed. Total zealexins accumulated to significant levels after *F. verticillioides* inoculation compared to the control, which had very little basal levels of total kauralexins (Figure 2.19b). Total kauralexin accumulation was

higher than total zealexin accumulation following inoculation. The accumulation of individual phytoalexin compounds is shown in Table S2.4.

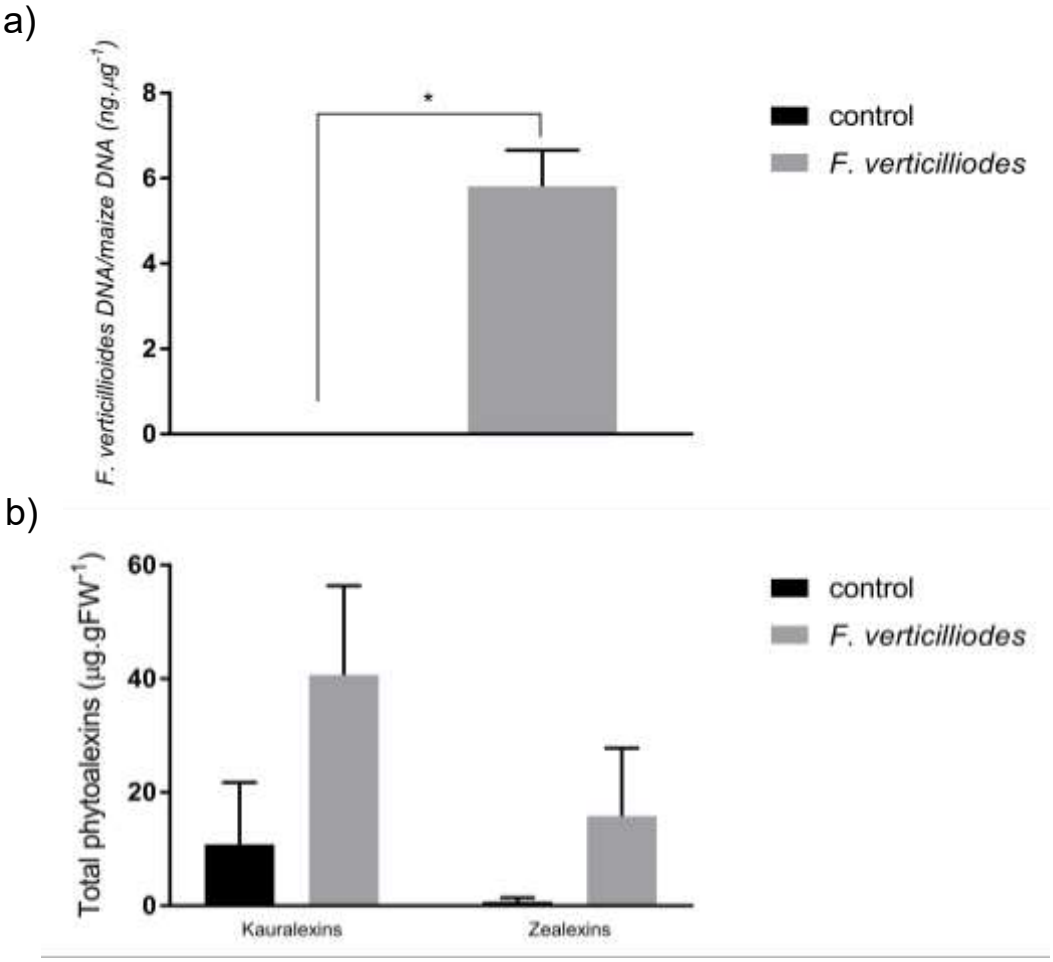

Figure 2.19 Analysis of CB248 root tissue ten dpi in control and *F. verticillioides* inoculated plants. a) Quantitative PCR analysis to measure *F. verticillioides* growth. The amount of *F. verticillioides* growing in CB248 maize (ng.µg^{-1}) was quantified using *FvEF1α* and *ZmMEP* primers respectively. b) Total kauralexins and total zealexins (µg.gFW^{-1}) that accumulated in CB248 maize following *F. verticillioides* inoculation were measured using gas chromatography-mass spectrometry. Error bars indicate standard deviation (SD). A one-tailed t test was performed to measure statistical significance of fungal growth. An unpaired t test (unequal variance) was performed on log_{10}-transformed phytoalexin data to measure statistical significance * = $p<0.05$, n=3

Gene expression in CB248 roots was measured using RT-qPCR. *ZmMEP* and *ZmLUG* were used as reference genes. Reference gene stability is shown in Table S2.2 and standard curve quality in Table S2.3. Statistical analysis was performed on log_{10}-transformed data in order to obtain a normal distribution among the data.

ZmAn2 was significantly up-regulated in response to *F. verticillioides* (Figure 2.20a), as was *ZmKSL4* (Figure 2.20d). *ZmKSL2* (Figure 2.20b), *ZmKO* (Figure 2.20c) and *ZmCYP81A1* (Figure 2.20e) did not display a change in expression between the two treatments. *ZmTPS11* expression appears to increase to the highest levels of all of the candidate genes following inoculation, but the variation in the samples results in no significant change seen (Figure 2.20f).

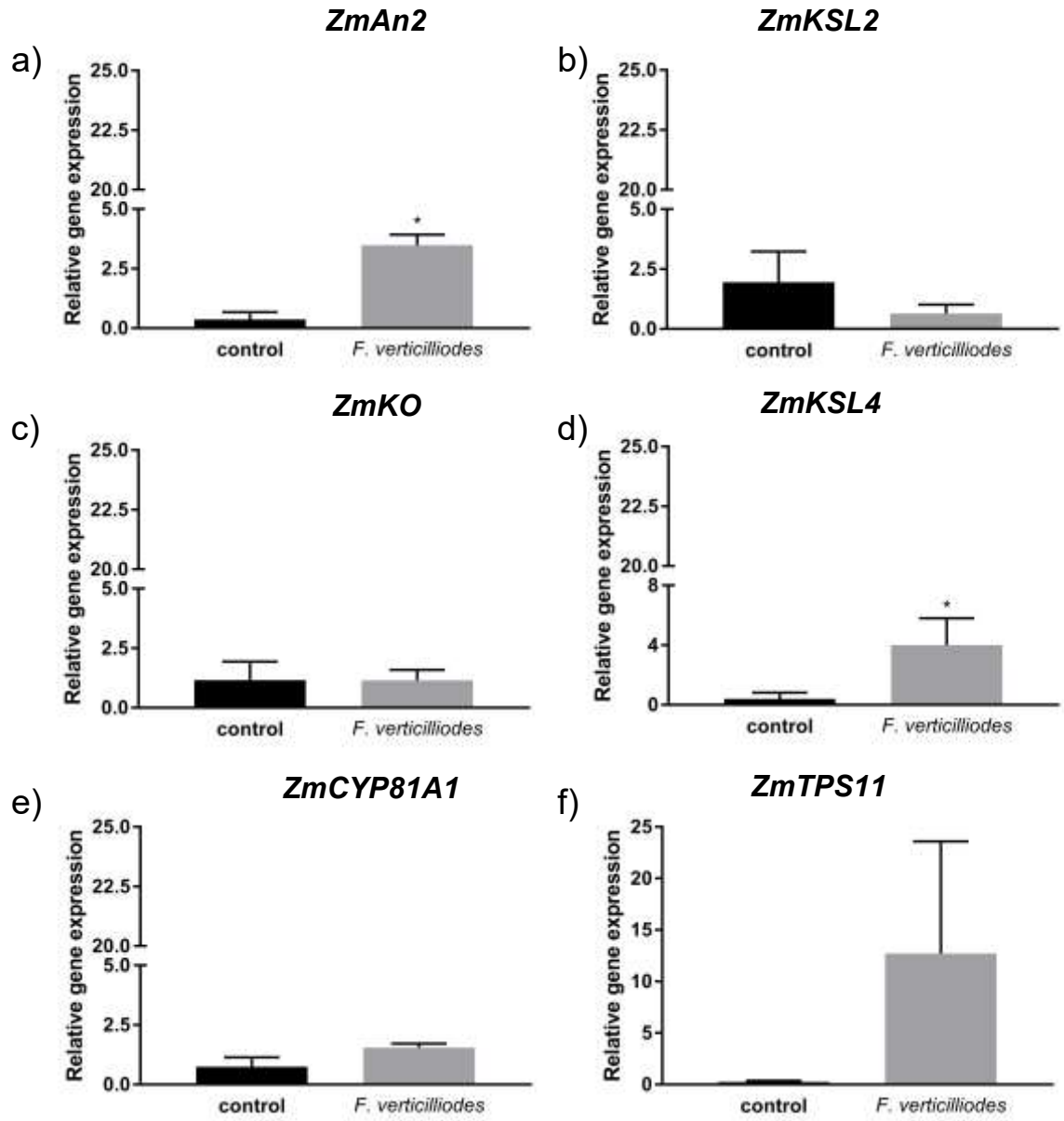

Figure 2.20 RT-qPCR analysis to measure relative gene expression in the root tissue of CB248 maize in control plants and plants dpi. a) *ZmAn2*, b) *ZmKSL2*, c) *ZmKO,* d) *ZmKSL4,* e) *ZmCYP81A1* and f) *ZmTPS11*.*ZmMEP* and *ZmLUG* were used as reference genes to normalise data. Error bars indicate standard deviation (SD). An unpaired t test (unequal variance) was performed on log_{10}-transformed phytoalexin data to measure statistical significance * = $p<0.05$, n=3

Summary of *F. verticillioides* growth, phytoalexin accumulation and gene expression in CB248 roots at ten days

The disease scores of both control and inoculated roots were high in CB248. However, the phenotype observed does not necessarily correlate with the defence response that was observed. Although both the control and inoculated roots appeared stressed, *F. verticillioides* inoculation resulted in increased phytoalexin accumulation, which was significant for zealexins but not for kauralexins. The accumulation of low levels of kauralexins in the control roots may be the result of developmental factors as well as the endophyte present on two of the biological samples. Fungal growth was significant in the inoculated roots, and the amount of *F. verticillioides* present was sufficient to induce significant zealexin accumulation. Although *ZmTPS11* expression was not significant due to variation, it was highly expressed following inoculation and has a positive relationship with zealexin accumulation. *ZmAn2* and *ZmKSL4* were significantly expressed following inoculation, and the increase (though not significant) in kauralexins following *F. verticillioides* inoculation fits this pattern. There was no change in gene expression of the other candidate genes, and this observation could be due to the accumulation of kauralexins in both treatments. The defence response of CB248 following *F. verticillioides* inoculation was variable, and the lack of significance is possibly due to the endophyte present in the control samples, which may affect these results. Therefore analysis on this line should be repeated using a clean control.

2.2.5 Discussion of *F. verticillioides* growth, phytoalexin accumulation and gene expression in B73, CML444 and CB248

Phenotype analysis throughout all of the maize lines revealed that inoculation with *F. verticillioides* causes the plants to become stressed. The shoots of B73 and CML444 were analysed and became stressed following *F. verticillioides* inoculation, as the leaf tips turned brown and the inoculated leaves were beginning to shrivel. Control leaves also appeared slightly stressed, and so environmental factors may have caused the stress to some degree. However, the shoot disease scores were higher in the inoculated plants than the control plants, suggesting that fungal growth has an additive effect on the environmental stress. Roots of B73, CML444 and CB248 were analysed and scored following *F. verticillioides* inoculation and were stunted in growth and became brown and discoloured. Control roots appeared long

and healthy in B73 and CML444, although CB248 control roots were stunted and discoloured due to the presence of a bacterial-like endophyte. The disease scores did not necessarily correlate with the plant defence response, particularly in the shoot tissue, and this may be due to the subjective manner in which disease scoring was performed.

F. verticillioides growth was higher in the roots than in the shoots in all of the plants. This is likely due to the seed soak inoculation method used in this study. Previous studies have shown, using an *F. verticillioides* GFP-expressing transgenic isolate and fluorescence microscopy, that this method results in early colonisation of *F. verticillioides* in root tissue, while only trace amounts of green-fluorescing colonies were detected in shoot tissue (Oren et al., 2003). Furthermore, studies that used seedling inoculations found that *F. verticillioides* remained primarily in belowground tissue, as observed in the present study (Murillo-Williams & Munkvold, 2008). In the time point experiments on B73 and CML444, average *F. verticillioides* growth was higher at fourteen days than at ten days. However, there was no significant difference between fungal growth at the two time points. Interestingly, CB248 presented with some of the most severe symptoms in the roots, but had the lowest fungal growth compared to the B73 and CML444 roots analysed. It appeared that CB248 had a smaller phenotype than B73 and CML444. However, due to the presence of the bacterial-like endophyte in the control, it is unknown how a 'healthy' CB248 plant should look. Therefore, the phenotypes were scored relative to what had been observed in the previous lines. If CB248 is indeed smaller than B73 and CML444, this comparison may have skewed the disease score to be more severe than they actually were. This may provide a reason for the apparent severe disease symptoms despite less fungal growth. A smaller root structure in CB248 would provide physically less space for *F. verticillioides* to grow and may be the reason that fungal growth was so low in CB248. In contrast, CML444 had the highest levels of *F. verticillioides* growth, and the root structure of this line appeared larger and more diverse than B73 and CB248, providing a larger surface area for *F. verticillioides* to colonise. However, the reason for the reduced fungal growth in CB248 may also be the induction of plant defences.

As well as having the least *F. verticillioides* growth, CB248 roots showed the highest accumulation of total kauralexin and zealexin levels respectively. CML444 roots had the second highest accumulation of total kauralexins and zealexins. However, the highest amount of *F. verticillioides* growth was measured in the CML444 roots. B73 had medium levels of total kauralexin and zealexin accumulation, and also had medium levels of *F. verticillioides* growth. The roots of B73, CML444 and CB248 all had low levels of total kauralexins present in the control roots at 10 days, which supports evidence from previous findings that kauralexins accumulate in uninfected plants early in development (Schmelz et al., 2011). Total kauralexins accumulated to higher levels than total zealexins in the roots of all of the lines analysed. The importance of kauralexin accumulation in response to *F. verticillioides* has been shown in two studies that performed *F. verticillioides* inoculations on *Zman2* mutants and observed increased fungal growth and susceptibility compared to *ZmAn2* plants (Vaughan et al., 2015; Wighard, 2017). Total zealexin accumulation was low in the shoots of B73 and CML444, and while total kauralexins did not accumulate in B73, they did accumulate to significant levels in the CML444 shoots at ten dpi (Table 2.12), despite detection of *F. verticillioides*. Previous studies have shown that phytoalexins accumulate locally to the area of infection (Huffaker et al., 2011), which provides a reason for the low phytoalexin accumulation in the shoots when very low levels of *F. verticillioides* were detected. *F. verticillioides* growth was significantly reduced when a zealexin mix or kauralexin B3, both in 0.5% ethanol, were added to the fungus exogenously at levels ranging from 50-100µg.ml^{-1} or 25µg.ml^{-1} respectively (Vaughan et al., 2014). The highest levels of total zealexin accumulation were in CB248 and were 15µg.gFW^{-1}. These levels are below those that are physiologically relevant for *F. verticillioides* growth reduction (Vaughan et al., 2014). The highest accumulation of total kauralexins was also in CB248 and the average levels of total kauralexin accumulation were 40µg.gFW^{-1}. Kauralexin B3 accumulation in this study (Table S2.4) was lower than the levels sufficient to reduce *F. verticillioides* growth in Vaughan et al. (2014). Due to the growth of *F. verticillioides* regardless of phytoalexin accumulation, especially in CML444, it appears that phytoalexins did not accumulate to levels that were sufficient to reduce fungal growth.

Gene expression in the first B73 experiment at ten days was significantly higher in the roots than in the shoots in all of the candidate genes. As was observed with total phytoalexin accumulation, in general, the putative phytoalexin biosynthetic genes were not significantly induced in the shoots following *F. verticillioides* inoculation. The genes that were significantly up-regulated in the shoots were *ZmAn2* in B73 and *ZmKSL2* in CML444. The significant up-regulation of *ZmKSL2* correlates with the relatively high levels of total kauralexins in the CML444 shoots, but the up-regulation of *ZmAn2* in B73 does not correlate with an induction of total kauralexin accumulation. In general, gene expression in the roots was significantly up-regulated following *F. verticillioides* (Table 2.12). Expression of *ZmAn2, ZmKSL2, ZmKO, ZmKSL4,* and *ZmTPS11* was significantly up-regulated in B73 roots following fungal inoculation, and in CML444 *ZmAn2, ZmKSL2, ZmKSL4,* and *ZmTPS11* were significantly up-regulated at one or both of the time points measured (Table 2.12). In CB248, only *ZmAn2* and *ZmKSL4* were up-regulated following inoculation (Table 2.12). *ZmCYP81A1* was not significantly up-regulated in any of the root tissue. However, expression in the shoots was significantly higher than in the shoots in B73. *ZmCYP81A1* was significantly induced in response to *F. verticillioides* and *C. zeina* in the studies by Lanubile et al. (2014), Lambarey (2017) and Christie et al. (2017). Therefore, it is possible that *ZmCYP81A1* is not expressed to high levels in the roots compared to the shoots, which is the tissue that was analysed by Lambarey (2017) and Christie et al. (2017). Some phytoalexin biosynthetic genes have been shown to increase prior to phytoalexin accumulation and then decrease (Huffaker et al., 2011; Schmelz et al., 2011). Aside from variation in biological samples, this could provide a reason for the apparent lack of significant expression in some of the samples. It is possible that expression occurred prior to phytoalexin accumulation, and had reduced at the harvesting time.

In summary, *F. verticillioides* growth in the roots was sufficient to induce total phytoalexin accumulation in the roots, but growth in the shoots was not sufficient to induce high levels of total phytoalexins. Total kauralexin accumulation in the roots was not significant compared to the control except in B73 at fourteen dpi and CML444 at ten dpi (Table 2.12). Total zealexin accumulation was also significantly different to the control in CML444 at ten dpi. Phytoalexin accumulation was highest in CB248 roots and fungal growth

was lowest in this line. Although phytoalexins accumulated in B73, CML444 and CB248 roots, it appears that they did not accumulate to levels that were sufficient to inhibit *F. verticillioides* growth and provide resistance. These results show that *F. verticillioides* inoculation induces a phytoalexin response in roots. Putative phytoalexin biosynthetic genes were up-regulated following *F. verticillioides* inoculation. *ZmAn2* and *ZmKSL4* were significantly up-regulated in all of the maize lines (Table 2.12).

Table 2.12 A comparison of *F. verticillioides* growth, phytoalexin accumulation and gene expression among the root tissue of B73, CML444 and CB248 maize

	B73	B73 10dpi	B73 14dpi	CML444 10dpi	CML444 14dpi	CB248
***F. verticillioides* growth**	+	+	-	-	-	+
Total kauralexin accumulation	-	-	+	+	-	-
***ZmAn2* expression**	+	+	+	-	+	+
***ZmKSL2* expression**	+	+	+	+	-	-
***ZmKO* expression**	+	-	+	-	-	-
***ZmKSL4* expression**	+	+	+	+	+	+
Total zealexin accumulation	-	-	-	+	-	-
***ZmTPS11* expression**	+	+	-	+	+	-

+ indicates significant differences between the control and *F. verticillioides* roots

- indicates no significant difference

CHAPTER 3

INTRODUCTION

As well as using the plants own ability to induce defence responses following pathogen infection or abiotic stress, the use of biological control agents (BCA) is also an effective method to reduce disease incidences. The use of chemicals such as pesticides and fungicides have become increasingly unpopular due to economic and health issues surrounding them, so more focus has been put into biocontrol in recent years (Wagacha & Muthomi, 2008). The microorganisms living in the rhizosphere, which is the zone of soil surrounding plant roots (Bais et al., 2006), interact with each other and their host plant, changing many aspects of the rhizosphere environment (Heydari & Pessarakli, 2010).

One of the ways that some microorganisms interact beneficially with plants is to have antagonistic effects on pathogenic microbes. *Trichoderma* spp. are a fungal species that are particularly adept at reducing pathogenic colonisation and are one of the most commercially used BCAs (Benítez et al., 2004). The species that are most used include *T. asperellum* (Steyaert, Weld & Stewart, 2010), *T. harzianum, T. virens* and *T. viride* (Benítez et al., 2004). *Trichoderma* spp. enhance plant growth through a variety of mechanisms (Benítez et al., 2004). *Trichoderma* spp. have a high reproductive capacity and have advanced methods for nutrient uptake, enabling them to survive in many different conditions (Benítez et al., 2004; Harman, Howell, et al., 2004). They are also beneficial to plants whose roots they colonise, as they have been shown to have fertilisation effects on plants (Tucci et al., 2011; Saravanakumar et al., 2017) and increase grain yields (de França et al., 2015; Charoenrak & Chamswarng, 2016). Furthermore, *Trichoderma* spp. can have antagonistic effects on other fungal pathogens.

Trichoderma spp. have been shown to reduce fungal pathogen colonisation of roots by also colonising plant roots and producing secondary metabolites that are toxic to pathogens (Benítez et al., 2004). They can out-compete other

fungi by their advanced nutrient uptake (Vos et al., 2015) have been shown to interact directly with other fungal pathogens via mycoparasitism (Benítez et al., 2004; Harman, Howell, et al., 2004).

Many studies have shown that different *Trichoderma* spp. reduce disease development and growth of fungal pathogens in various plants. For example, *T. harzianum* reduced lesion area in tomato leaves inoculated with *Botrytis cinerea* (Tucci et al., 2011) and *T. asperellum* reduced *Rhizoctonia solani* and dirty panicle disease in rice (Chen et al., 2015; de França et al., 2015; Charoenrak & Chamswarng, 2016). The ability of root-colonising *Trichoderma* spp. to reduce disease incidences in distant tissue suggests that the plant is 'primed' for defence following *Trichoderma* spp. colonisation (Harman, Howell, et al., 2004). Studies have shown that inoculation by *Trichoderma* spp. induces an up-regulation of *PR* genes (Tucci et al., 2011) and an initiation of phytohormone signalling (Vos et al., 2015), as well as increased reactive oxygen species (ROS) production and lignifications (Patel et al., 2017). *T. asperellum* has also been shown to induce phytoalexin accumulation in cucumbers (Yedidia et al., 2003).

In this chapter, a *Trichoderma* endophyte growing in the ZM401 maize line was isolated and identified as *T. asperellum*. The aim of this chapter is to determine whether *T. asperellum* induces phytoalexin accumulation and to see how this compares to phytoalexin accumulation following *F. verticillioides* inoculation. The second aim is to determine whether *T. asperellum* inhibits *F. verticillioides* growth in *in vitro* competition assays as there is, to our knowledge, limited information on the specific interaction between these two fungi.

MATERIALS AND METHODS

3.1.1 Fungi and Maize growth conditions

Fusarium verticillioides was grown as described in chapter 2 section 2.1.1. *Trichoderma asperellum,* growing as an endophyte in the ZM401 maize line, was isolated and grown on potato dextrose agar (PDA) at 30°C for 4-5 days. 50% glycerol stocks of *T. asperellum* were made and stored at -80°C.

The maize line ZM401 was obtained from National Tested Seeds (Harare, Zimbabwe) and was inoculated with *F. verticillioides* and grown in the same conditions as described in chapter 2 section 2.1.1.

3.1.2 Phenotype analysis

Following *F. verticillioides* inoculation, the disease scores for the ZM401 line was analysed and scored according to Table 2.2 in chapter 2 section 2.1.2.

3.1.3 Fungal quantification

DNA extractions and quantitative PCR for fungal quantification were performed as described in chapter 2 section 2.1.3.

3.1.4 Gene expression

Gene expression was analysed as described in chapter 2 section 2.1.4.

3.1.5 Phytoalexin accumulation

Phytoalexin accumulation was analysed as described in chapter 2 section 2.1.6.

3.1.6 *Trichoderma* asperellum isolation

Conidia were obtained from the MS media and plated onto PDA plates. Four days after plating, *T. asperellum* had spread over the entire 9cm PDA plate. A single spore dilution was made from the plate and approximately 50 spores were added to a new PDA plate and grown at 30°C for three days, as *T. asperellum* formed a lawn across the plate when grown for longer. Single colonies were sub-cultured and

grown for an additional four days on fresh PDA. DNA was extracted from the fungus thereafter, according to the method described in chapter 2 section 2.1.3.

3.1.7 PCR

DNA was amplified using KAPATaq Ready Mix DNA Polymerase (KAPA Biosystems, Boston, United States). Primers for the ITS1 and ITS4 region were obtained from (White et al., 1990) and primers designed according to the *T. asperellum* anchor region (Druzhinina et al., 2005) were designed by Michael Wu, an honours student in the lab. *ZmCYP81A1* primers, used as a positive control, are described in Table 2.4, chapter 2. The primer sequences are shown in Table 3.1 and the cycling parameters are shown in Table 3.2.

Table 3.1 Primers used to for *Trichoderma* identification

Gene name	Primer sequence (5' - 3')	Product size (bp)	Reference
ITS1	TCCGTAGGTGAACCTGCGG	~710	White et al. (1990)
ITS4	TCCTCCGCTTATTGATATGC		White et al. (1990)
T. asperellum F	AACTCTTTCTGTAGTCCCCTCG	~200	Michael Wu
T. asperellum R	GCAATGTGCGTTCAAAGATTCGA		Michael Wu

Table 3.2 PCR cycling parameters for the *ITS1/4* primers, *T. asperellum* primers and *ZmCYP81A1* primers

	Step	Denaturation	Denaturation	Annealing	Elongation	Elongation
	Cycles	**1**	**30**			**1**
ITS1/4	Temperature (°C)	94	95	53	72	72
	Time (min)	3:00	0:30	0:30	1:00	10:00
T. asperellum	Temperature (°C)	95	95	60	72	72
	Time (min)	2:00	0:30	0:30	0:45	3:00
ZmCYP81A1	Temperature (°C)	94	94	62	72	72
	Time (min)	5:00	0:30	0:30	0:30	10:00

3.1.8 Sequencing

Sequencing analysis was conducted at the Central Analytical Facility (CAF) at Stellenbosch University (SU), after a PCR amplicon clean-up as described in chapter 2 section 2.1.5.

3.1.9 *In vitro* competition assays

The antagonistic effect of *T. asperellum* against *F. verticillioides* was measured using the dual culture technique described by (El Komy et al., 2015). Controls containing only *T. asperellum* discs or only *F. verticillioides* discs were used. Dual cultures were analysed, where *T. asperellum* and *F. verticillioides* discs were either added at the same time or *T. asperellum* discs were added 2 days after *F. verticillioides* discs. Fungal discs were obtained from 8 day old *F. verticillioides* cultures and 4 day old *T. asperellum* cultures and were 1cm in diameter. Four replicates of each treatment were incubated at 30°C for 7 days. Radial growth (cm) of *F. verticillioides* was measured from the edge of the original disc using ImageJ 1.50i software (Schneider, Rasband & Eliceiri, 2012). Percent inhibition was calculated as described by (El Komy et al., 2015)) using the formula: I = (C-T/C)x100, where I is percent inhibition, C is the radius of the control *F. verticillioides* growth (cm) and T is radius of *F. verticillioides* growth (cm) in dual culture with *T. asperellum*.

3.1.10 Statistical analysis and data presentation

Statistical analysis and graph production for the data obtained from fungal quantification, gene expression and phytoalexin accumulation was performed as described in chapter 2 section 2.1.7. Statistical analysis on the fungal growth in the *in vitro* competition assay was performed using an unpaired t test on Microsoft Excel® (Mac 2011).

3.1.11 Bioinformatics

Sequences were assembled using DNAMAN version 9.122 (Lynnon Biosoft) and were analysed using NCBI BLASTn (Madden, 2002, https://blast.ncbi.nlm.nih.gov/Blast.cgi) in order to identify the fungal species

RESULTS AND DISCUSSION

The ZM401 maize line is a CIMMYT open pollinated variety (OPV) originating from Zimbabwe that exhibits drought tolerance and partial resistance to grey leaf spot (GLS), maize streak virus (MSV), common rust and leaf blight ("Varieties", 2015). Although there is limited evidence of ZM401 inoculation with *F. verticillioides*, it is likely that the line is partially resistant to this fungus based on it's broad spectrum disease resistance. ZM401 seeds were inoculated with *F. verticillioides* using the seed soak inoculation method and control and *F. verticillioides* inoculated roots were harvested ten days post inoculation (dpi).

3.2.1 Isolation and identification of *Trichoderma asperellum*

Despite seed sterilisation prior to growing seeds on MS media, control ZM401 plants contained an endophyte that contaminated the control plants. The growth pattern of the endophyte on the media was characteristic of the biocontrol genus *Trichoderma,* as green conidia spread in concentric rings (Figure 3.1) (Steyaert, Weld & Stewart, 2010). Therefore, the *Trichoderma*-like endophyte was isolated in order to determine the species and strain. The fungus was grown on PDA, after which a single spore dilution was performed in order to obtain a single isolate for DNA extraction.

Figure 3.1 *Trichoderma*-like endophyte growing in concentric rings from ZM401 seed

The *ITS1* and *ITS4* primers (White et al., 1990) were used to amplify the internal transcribed spacer region of the DNA. The ITS region is highly polymorphic and is used as the universal barcode to identify fungal species (Schoch et al., 2012). *ITS1* serves as the forward primer and binds to the conserved region of 18S rDNA, while *ITS4* serves as the reverse primer and binds to 28S (Figure 3.2) (White et al., 1990).

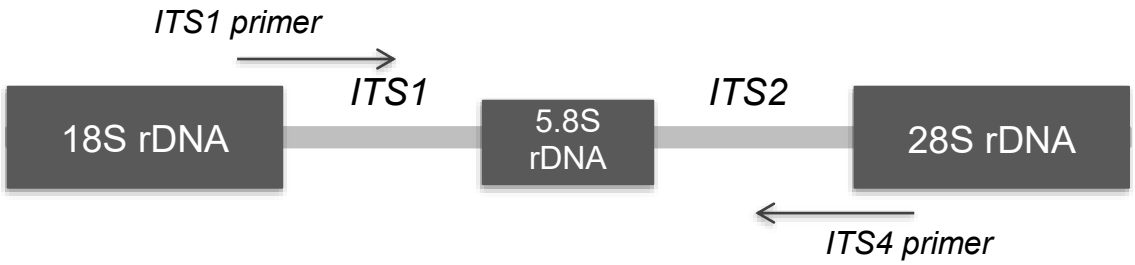

Figure 3.2 Ribosomal DNA (rDNA) and the internal transcribed spacer regions amplified by *ITS1* and *ITS4* primers. Adapted from White et al. 1990.

The sequence of the amplified product was obtained following Sanger capillary sequencing. A sequence assembly of the *ITS1* and *ITS4* sequences was performed on DNAMAN version 9.122 (Lynnon Biosoft) in order to obtain a consensus sequence (figure S3.1). NCBI BLASTn (Madden, 2002, https://blast.ncbi.nlm.nih.gov/Blast.cgi) was used to identify the sequence. The top BLASTn hits corresponded to *T. asperellum*, although the specific strain could not be identified as the sequence homology among different *T. asperellum* strains is very high. The top 100 hits from the consensus sequence were aligned to various *T. asperellum* isolates, all of which had the same score (1020), E value (0.00) and percent identity (100%). A list of *T. asperellum* strains that are published in the literature are in Table S3.1, although there are many more unpublished strains that have not been published as yet. The consensus sequence aligned to the *ITS1*, 5.8S and *ITS2* sequences in the ITS region (Figure 3.2) and the alignment to the hit at the top of the list, *T. asperellum* strain Rah4, which is the most recently submitted strain, although not yet published, is shown in Figure S3.1. The *ITS1* and *ITS4* sequences were also analysed individually on BLASTn and the identity of *T. asperellum* was confirmed from these results. However, the high sequence homology in this region means that further sequencing of other genomic regions within the *T. asperellum* DNA is required to identify the strain.

A PCR using *T. asperellum*-specific primers designed from *T. asperellum* anchors, which are reference oligonucleotides for each species (Druzhinina et al., 2005), was performed as an extra measure to ensure that the *Trichoderma* sp. present in ZM401 was indeed *T. asperellum*, as well as to confirm that *T. asperellum* was only present in the ZM401 control root tissue. In order to ensure primer specificity to *T. asperellum*, the PCR was performed on *T. asperellum* DNA (Figure S3.2a) and the product was sent for sequencing. The sequencing results confirmed that the primers were for *T. asperellum* and the top hit aligned to *T. asperellum* isolate E-465 (NCBI BLASTn, Figure S3.3**)**. This demonstrates once again that further investigation into the strain is required. The PCR was then performed on the root tissue of all of the maize lines analysed. The size of the PCR product was ~200bp and was only detected in the ZM401 control roots (Figure 3.3). In order to test that the DNA was amplifiable, a PCR using *ZmCYP81A1* primers was used as a positive control (Figure S3.2b).

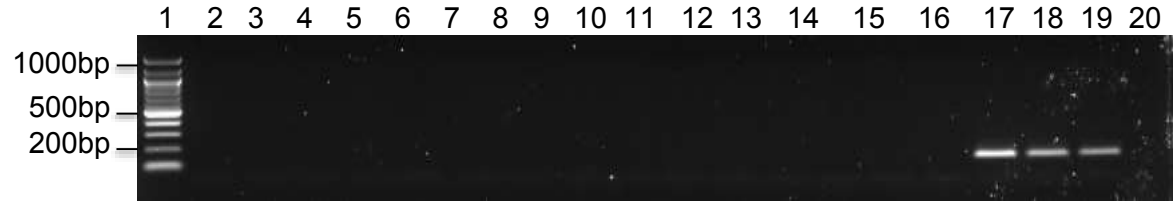

Figure 3.3 Gel electrophoresis of *T. asperellum* PCR product amplified from control root DNA. Lane 1: 100bp ladder (New England Biolabs, Ipswich, United States), lanes 2-4: B73 ten dpi, lanes 5-7: B73 fourteen dpi; lanes 8-10: CML444 ten dpi, lanes 11-13: CML444 fourteen dpi, lanes 14-16: CB248; lanes 17-19: ZM401, 20: no template control

3.2.2 *F. verticillioides* growth, phytoalexin accumulation and gene expression in the ZM401 maize line

As *T. asperellum* has previously been shown to be an effective BCA against *R. solani* in rice (de França et al., 2015; Charoenrak & Chamswarng, 2016) and has been shown to induce phytoalexin accumulation in cucumbers (Yedidia et al., 2003), the ZM401 maize inoculated with *F. verticillioides* and the untreated control (containing the *T. asperellum* endophyte) were analysed for phytoalexin accumulation despite contamination of the control.

Phenotype analysis

Although the control sample is not a traditional control, it is referred to as control in this study as no external treatment was performed on it. Phenotype was analysed as described in chapter 2. However, like CB248, only the roots were analysed as this was where a higher response was observed in B73 and CML444, and it was only measured at ten dpi as there was no significant difference in phytoalexin accumulation between the two time points in B73 and CML444. ZM401 had large leaves and a long, diverse root network with many lateral roots coming off the seminal roots, even in the inoculated plants. Some of the control roots appeared stressed by *T. asperellum* and were mildly discoloured and stunted. Other control roots had longer roots and were not discoloured, and as a result the mean disease score of the control plants was just over 1.5 (Figure 3.4), showing that the symptoms caused by *T. asperellum* as a whole were mild. The roots inoculated with *F. verticillioides* had some stunting and discolouring, but the symptoms as a whole were moderate, with a mean disease score of approximately 2.5 (Figure 3.4). Inoculated B73 plants were grown in conjunction with ZM401 as a control to ensure that infection had taken place. The B73 roots that were grown in conjunction with this experiment expressed more severe symptoms with a mean disease score of 3.2 (Figure S2.3a).

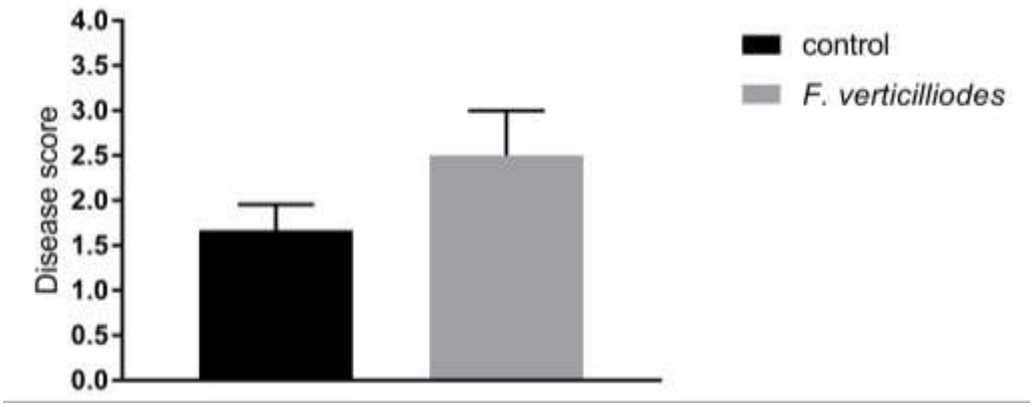

Figure 3.4 Mean disease scores of control and inoculated ZM401 root tissue ten dpi.

Fungal growth, phytoalexin accumulation and gene expression in ZM401 roots

F. verticillioides growth was quantified using qPCR. *FvEF1α* primers were used to quantify *F. verticillioides* fungal DNA present in the maize tissue, while *ZmMEP* primers were used to quantify the amount of plant DNA present in the total DNA extracted (Table 2.3). There was no *F. verticillioides* detected in the control ZM401 roots, but an average of 14,8ng.µg^{-1} of *F. verticillioides* DNA was detected in the inoculated shoots (Figure 3.5a). *F. verticillioides* growth in B73 was high, with an average of 73ng.µg^{-1} *F. verticillioides* DNA detected in the B73 roots (Figure S2.3b). The mean *F. verticillioides* growth was higher in this study than fungal growth on B73 in chapter 2, suggesting that the growth conditions were optimal for *F. verticillioides* growth in this batch of experiments. Fungal growth in the inoculated ZM401 roots was significantly higher than the control roots (Figure 3.5a).

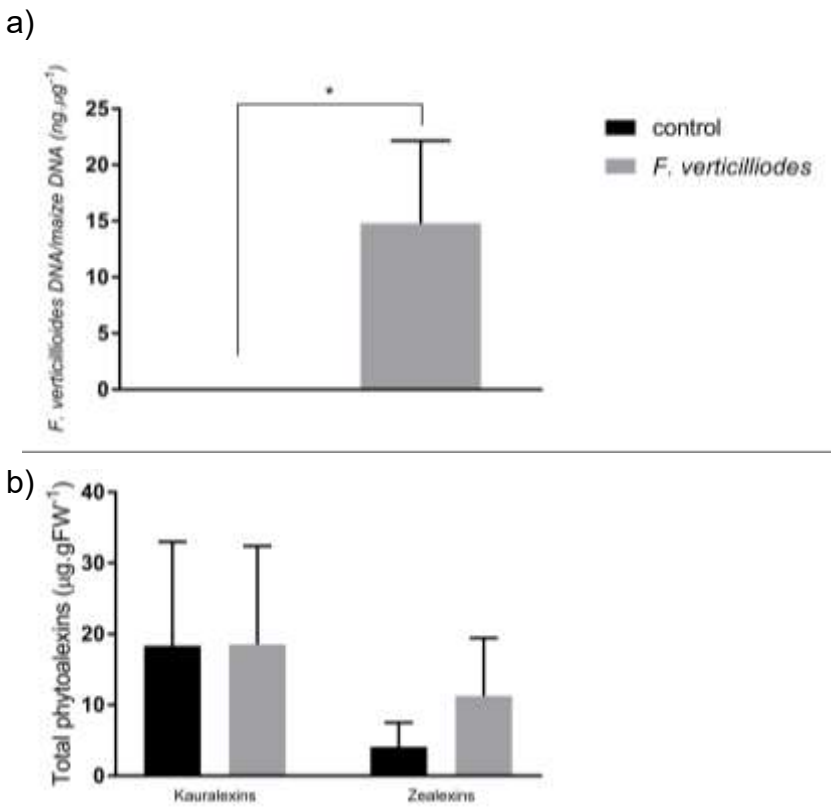

Figure 3.5 Analysis of ZM401 root tissue ten dpi in control and *F. verticillioides* inoculated plants. a) Quantitative PCR analysis to measure *F. verticillioides* growth. The amount of *F. verticillioides* growing in ZM401 (ng.µg^{-1}) was quantified using *FvEF1α* and *ZmMEP* primers respectively. b) Total kauralexins and total zealexins (µg.gFW^{-1}) that accumulated in ZM401 maize following *F. verticillioides* inoculation were measured using gas chromatography-mass spectrometry. Error bars indicate standard deviation (SD). A one-tailed t test was performed to measure statistical significance of fungal growth. An unpaired t test (unequal variance) was performed on log_{10}-transformed phytoalexin data to measure statistical significance * = $p<0.05$, n=3

Statistical analysis was performed on log_{10}-transformed phytoalexin data in order to obtain a normal distribution among the data, but the untransformed data is presented on the graph. There was no difference in total kauralexin accumulation, with average levels measured at 18,36µg.gFW^{-1} and 18,55 µg.gFW^{-1} in the control and inoculated plants respectively (Figure 3.5b). Total zealexin accumulation was lower than kauralexin accumulation, and although the mean total zealexin accumulation is higher in the inoculated than control sample, there is no statistical significance in zealexin accumulation between the two treatments (Figure 3.5b). It is likely that the control would have low levels of total phytoalexin accumulation due to their proposed role in development (Huffaker et al., 2011; Schmelz et al., 2011), but the levels that they accumulate to in ZM401 are likely due to the additive effect of *T. asperellum.* The accumulation of individual phytoalexin compounds is shown in Table S2.4.

Gene expression in the roots was measured using RT-qPCR, with *ZmLUG* used as a reference gene. The reference gene stability is not shown as only one reference gene was used for this line. Despite attempts to amplify *ZmMEP, ZmGST3* and *ZmRpol* to use as a second reference gene, *ZmLUG* was the only reference gene that had stable expression in all of the samples. The run quality of all of the genes is shown in Table S2.3. Statistical analysis was performed on log_{10}-transformed data in order to obtain a normal distribution among the data. There was no change in gene expression between control and inoculated roots in any of the genes studied (Figure 3.6). The only gene that shows any sign of increase following inoculation is *ZmKSL4*, although the variation in expression results in no significant difference (Figure 3.6d).

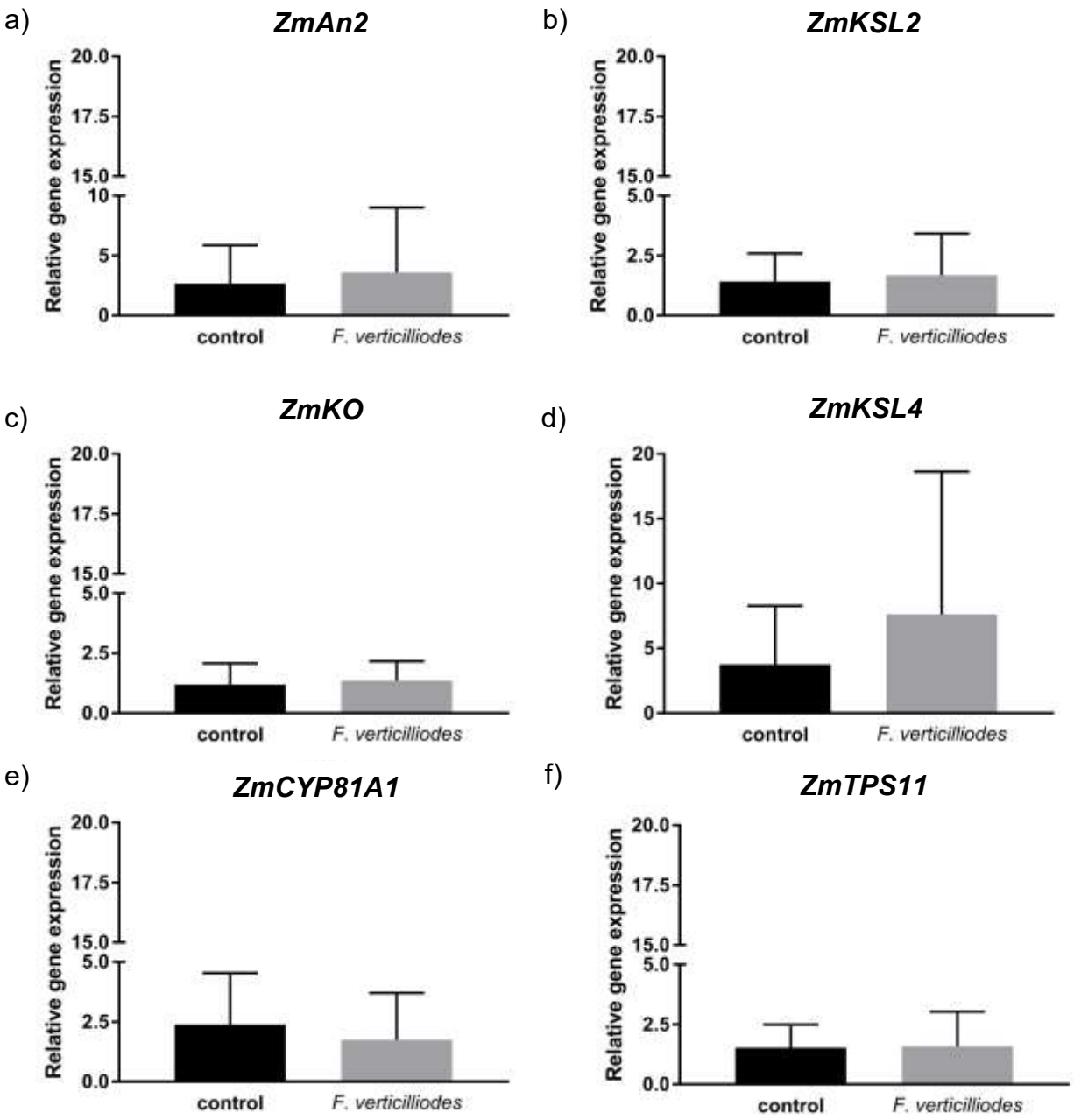

Figure 3.6 RT-qPCR analysis to measure relative gene expression in the root tissue of ZM401 maize in control plants and plants ten dpi. a) *ZmAn2*, b) *ZmKSL2*, c) *ZmKO,* d) *ZmKSL4,* e) *ZmCYP81A1* and f) *ZmTPS11. ZmLUG was* used as a reference gene to normalise data. Error bars indicate standard deviation (SD).

Summary of *F. verticillioides* growth, phytoalexin accumulation and gene expression in ZM401 roots

F. verticillioides growth in the inoculated ZM401 roots is positively correlated to the accumulation of total kauralexins and total zealexins. The control plants were contaminated with *T. asperellum* and showed high levels of total phytoalexin accumulation compared to the controls in chapter 2, especially accumulation of kauralexins. The experiments in chapter 2 and previous studies have shown that phytoalexins accumulate in uninfected roots during development (Huffaker et al., 2011; Schmelz et al., 2011). Therefore, it is likely that phytoalexins would accumulate in uninfected plants to a certain level. However, it is unknown to what extent *F. verticillioides* and *T. asperellum* induced phytoalexin accumulation, and if this accumulation is significant relative to that in a true, uninfected control. The relative gene expression did not change between the two treatments, but this result makes sense since phytoalexins accumulate in both treatments. Although this experiment should be repeated in order compare the phytoalexin accumulation and gene expression response in the infected tissue to an uninfected control, the levels to which total phytoalexins accumulate, in both the 'control' containing *T. asperellum* and the *F. verticillioides* inoculated roots, are higher than those seen in the control roots analysed in chapter 2. Furthermore, studies have shown that some *Trichoderma* spp. do induce a defence response in plants, such as increased reactive oxygen species (ROS) and lignifications in pea plants (Patel et al., 2017) and the up-regulation of *PR* genes in tomatoes (Tucci et al., 2011). *T. asperellum* has also been shown to induce phytoalexin biosynthesis in cucumbers (Yedidia et al., 2003). Therefore, from these results we can hypothesise that both *T. asperellum* and *F. verticillioides* are able to induce phytoalexin accumulation in maize.

3.2.3 *In vitro* competition assays between *F. verticillioides* and *T. asperellum*

A competition experiment between *F. verticillioides* and *T. asperellum* was set up using the dual culture technique described by El Komy et al. (2015). *F. verticillioides* discs were plated on PDA, and *T. asperellum* discs were plated either on the same day or two days after. Control plates containing only *F. verticillioides* or only *T. asperellum* were also set up. *T. asperellum* had formed a lawn across the PDA plate four days after plating, while the *F. verticillioides* growth was much slower.

Radial growth of *F. verticillioides* was measured for each treatment and the lengths of the four radii were averaged seven days after *F. verticillioides* was plated (Table 3.3). *F. verticillioides* inhibition by *T. asperellum* was measured using the percent inhibition formula described by (El Komy et al., 2015). *T. asperellum* significantly reduced *F. verticillioides* growth at both time points.

Table 3.3 Raw readings of *F. verticillioides* radial growth (cm) in control and dual culture assays

	Reading 1 (cm)	Reading 2 (cm)	Reading 3 (cm)	Reading 4 (cm)	**Average (cm)**	**Inhibition (%)**	**p value**
control	2,81	3,20	2,85	2,81	2,91	-	-
Dual culture (simultaneous plating)	1,41	1,41	1,50	1,28	1,40	52,03	$8,09x10^{-5}$
Dual culture (staggered plating)	2,07	2,17	1,93	1,97	2,03	30,20	$5,62x10^{-4}$

Percent inhibition of *F. verticillioides* by *T. asperellum* when the two were plated at the same time was 52%, while percent inhibition of *F. verticillioides* when *T. asperellum* was plated two days later was 30% (Table 3.3). An example of each treatment is shown in Figure 3.7. *F. verticillioides* growth is significantly inhibited by *T. asperellum*

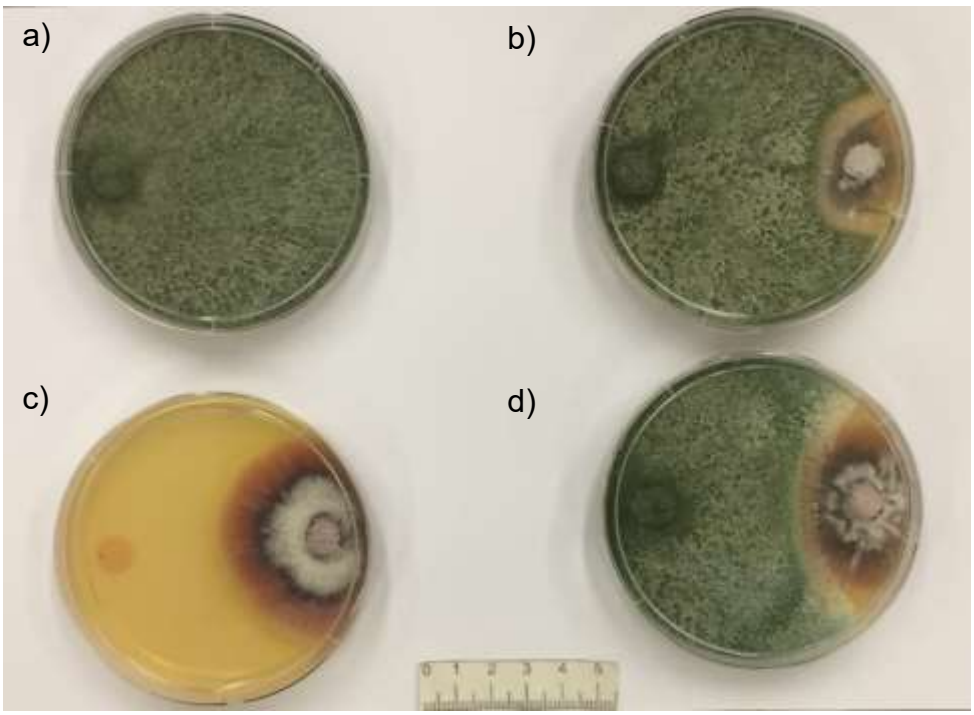

Figure 3.7 *In vitro* competition experiments between *F. verticillioides* and *T. asperellum* on PDA for seven days. a) *T. asperellum* control, b) *T. asperellum* and *F. verticillioides* plated on the same day, c) *F. verticillioides* control, d) *F. verticillioides* plated two days before *T. asperellum.*

As *T. asperellum* grows faster than *F. verticillioides*, it appeared that the initial inhibition observed between the two fungi was the result of *T. asperellum* outcompeting *F. verticillioides*. However, as time progressed and *T. asperellum* grew across the plate, it began to grow over *F. verticillioides*, interacting directly with the fungus (Figure 3.8), suggesting that *T. asperellum* may mycoparisitise *F. verticillioides*. Further microscopy studies should be performed in order to determine whether *T. asperellum* affects the morphology of *F. verticillioides* following interaction between the two.

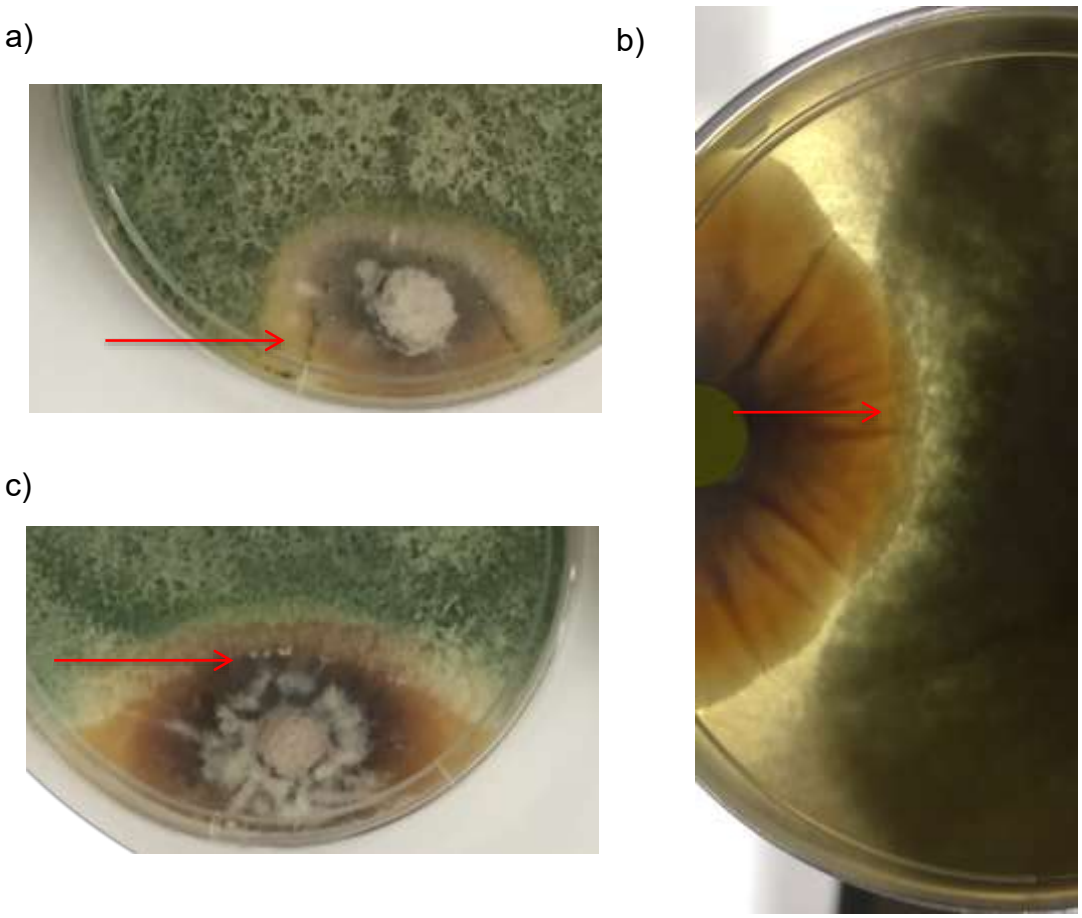

Figure 3.8 *T. asperellum* interacts directly with *F. verticillioides*. a) *T. asperellum* and *F. verticillioides* growth after plating on the same day, b) and c) *T. asperellum* and *F. verticillioides* growth when *T. asperellum* was plated two days after *F. verticillioides*. Pictures were taken seven days after plating *F. verticillioides.* Arrows indicate how *T. asperellum* grows over *F. verticillioides*.

3.2.4 Discussion of *F. verticillioides* growth, phytoalexin accumulation and gene expression in ZM401 roots and *T. asperellum* identification and *in vitro* competition

In this chapter, the defence response of ZM401 maize growing with endophytic *T. asperellum* was compared to maize inoculated with *F. verticillioides* that had no detectable *T. asperellum*. Both treatments had relatively mild disease symptoms, although the roots inoculated with *F. verticillioides* had slightly more severe symptoms than those containing *T. asperellum*. Phytoalexins accumulated to the same levels in both plants, and there was no difference in induction of phytoalexin biosynthetic gene expression. Phytoalexin accumulation, and particularly kauralexin accumulation, in the 'control' sample that contained *T. asperellum* displayed high levels of kauralexin accumulation compared to the kauralexin accumulation displayed in the control roots of the B73, CML444 and CB248 in chapter 2. ZM401 control roots accumulated total kauralexins to average levels of ~18µg.gFW^{-1} (Figure 3.5b), while the average levels of total kauralexin accumulation in B73 (Figure 2.10b) and CB248 roots (Figure 2.19b) were ~12µg.gFW^{-1}, and only ~5µg.gFW^{-1} in CML444 (Figure 2.16b). As the lower phytoalexin accumulation in the control roots in B73, CML444 and CB248 is attributed to developmental regulation, as shown by Huffaker et al. (2011) and Schmelz et al. (2011), it is likely that ZM401 would also display low levels of phytoalexin accumulation in uninfected tissue. However, as no true, endophyte-free ZM401 control was available, it is not clear as to the extent that *T. asperellum* and *F. verticillioides* induces phytoalexin accumulation in ZM401. CB248 displayed lower levels of phytoalexin accumulation in the control, despite the presence of a bacterial-like endophyte, suggesting that *T. asperellum* is able to induce phytoalexin accumulation while the bacterial-like endophyte in CB248 is not. Therefore, we hypothesise that the levels to which phytoalexins accumulated in ZM401 is the result of induction from *T. asperellum* and *F. verticillioides* infection respectively. Furthermore, previous studies have shown that *T. asperellum* induces phytoalexin biosynthesis in cucumbers (Yedidia et al., 2003) and it is possible that *T. asperellum* can also induce phytoalexin accumulation in maize. In future work falling outside the time scope of this project, this experiment should be repeated with an uninfected, true control in order to determine the extent of this induction. After *T. asperellum* was identified, primers specific to *T. asperellum* were obtained and a PCR was performed on the control and inoculated roots of all of the lines used in this study. ZM401 control roots were the only line that contained *T. asperellum*, which

further supports the hypothesis that phytoalexin accumulation in the root control of B73, CML444 and CB248 was the result of developmental regulation, while the higher levels of phytoalexins observed in ZM401 would have likely been due to developmental factors as well as the additive effect of *T. asperellum* colonisation.

T. asperellum inhibited *F. verticillioides* growth by 52% and 30% when plated on the same day or two days after *F. verticillioides* respectively, and growth in both dual culture assays was significantly less than the control. As *T. asperellum* grows faster than *F. verticillioides*, *T. asperellum* inhibits *F. verticillioides* by outcompeting it. However, seven days after plating *F. verticillioides* and five or seven days after plating *T. asperellum*, *T. asperellum* had begun to grow over *F. verticillioides*, suggesting that *T. asperellum* may have mycoparisitic effects on *F. verticillioides* when they interact. Microscopic analysis of the interaction between *T. asperellum* and *F. oxysporum* resulted in abnormal hyphal morphology and mycelial lysis of *F. oxysporum* (El Komy et al., 2015). The overgrowth seen in this experiment suggests that *T. asperellum* would have the same effect on *F. verticillioides*. Further microscopy studies are necessary to confirm this.

An endophyte growing in the ZM401 control plants was isolated and identified as *T. asperellum*. Phytoalexin accumulation in ZM401 control maize containing *T. asperellum* and *F. verticillioides* was the same ten dpi, suggesting that *T. asperellum* induces phytoalexin accumulation in maize. *In vitro* competition assays between *F. verticillioides* and *T. asperellum* showed that *T. asperellum* significantly inhibits *F. verticillioides,* firstly by outcompeting *F. verticillioides* and secondly by interacting directly with it and growing over it.

CHAPTER 4

CONCLUSIONS

In this study, maize lines were inoculated with *Fusarium verticillioides* using a seed soak method in order to determine the effect of inoculation on the maize defence response. More specifically, the B73 maize line and southern African maize lines CML444, CB248 and ZM401 were evaluated for phytoalexin accumulation using gas-chromatography mass-spectrometry. As phytoalexins have been shown to directly inhibit *F. verticillioides* growth (Vaughan et al., 2015), a comparison *of* phytoalexin accumulation in the southern African maize lines may indicate the induction of defence responses in these lines. As well as phytoalexin accumulation, the expression of putative phytoalexin biosynthetic genes *ZmAn2, ZmKSL2, ZmKO, ZmKSL4, ZmCYP81A1* and *ZmTPS11* were measured using RT-qPCR as an additional indication of the response that *F. verticillioides* induces in maize.

4.1.1 *F. verticillioides* growth and disease symptoms in B73, CML444 and CB248

F. verticillioides growth was higher in the roots than in the shoots of all of the maize lines where both tissues were analysed (Figure 2.3, Figure 2.7a, Figure 2.10a, Figure 2.13a, Figure 2.16a). This is likely due to the method of inoculation used, as a previous study also showed that *F. verticillioides* grows in the roots following seed soak inoculation, while only trace amounts of fungus were detected in the shoots (Oren et al., 2003). The plant phenotype following *F. verticillioides* inoculation was scored for disease symptoms, and all of the inoculated lines displayed more stressed symptoms than the control lines. The inoculated roots were discoloured and stunted (Table 2.2, Figure 2.2, Figure 2.9, Figure 2.15, Figure 2.18), while the shoots had browning and shrivelled leaves (Table 2.2, Figure 2.2, Figure 2.6, Figure 2.12)**.** The control leaves also appeared slightly stressed, and in the time point experiments the stress was greater at fourteen days post inoculation (dpi) than at ten dpi, likely due to the limited space inside the boxes that they were grown in. However, their symptoms were expressed to a lesser extent than the inoculated plants. Therefore, it appears that *F. verticillioides* has an additive effect on the stress symptoms seen in the shoot tissue. While high mean disease scores measured in the roots (Figure 2.2e, Figure 2.9, Figure 2.15c, Figure 2.18) correlate to higher levels of mean fungal growth (Figure 2.3, Figure 2.10a, Figure 2.16a, Figure 2.19), mean disease scores (Figure 2.2e, Figure 2.6, Figure 2.12) were high in the shoots despite only low mean levels of

F. verticillioides detected (Figure 2.3, Figure 2.7a, Figure 2.13a). This may be a result of decreased nutrient uptake from roots colonised by *F. verticillioides* and blockage of the xylem and phloem, reducing nutrient transport to above-ground tissue. This was shown in a study on soybeans that displayed leaf symptoms of sudden death syndrome, even though colonisation of *F. virguliforme* was only detected in the roots and not in the leaves (Navi & Yang, 2008). The scoring method used in this study was developed to evaluate *F. verticillioides*-induced stress on the seedlings. However, the mean disease scores of the shoots were high despite low levels of *F. verticillioides* detected in B73 and CML444 shoots. Therefore, this suggests that the stress symptoms observed were caused by secondary effects not directly linked to *F. verticillioides* growth in the tissue.

4.1.2 Phytoalexin accumulates in B73, CML444 and CB248 following *F. verticillioides* inoculation

Phytoalexin accumulation was induced in response to *F. verticillioides* inoculation in all of the maize lines, and total kauralexin accumulation was higher than total zealexin accumulation. This is interesting as previous studies have shown that zealexins accumulate to higher levels in response to fungal pathogens (Huffaker et al., 2011), while kauralexins accumulate to higher levels in response to herbivory and drought (Vaughan et al., 2015) although reduced kauralexin accumulation has been shown to increase susceptibility to *F. verticillioides* (Vaughan et al., 2015; Wighard, 2017). Induction of total kauralexin and total zealexin accumulation was higher in the roots (Figure 2.10b-c, Figure 2.16b-c) than in the shoots (Figure 2.7b-c, Figure 2.13b-c). As *F. verticillioides* colonisation in the roots was higher than in the shoots, these results support previous evidence that phytoalexin accumulation is localised to the site of infection (Huffaker et al., 2011; Schmelz et al., 2011). Interestingly, CB248 had the highest total kauralexin and total zealexin accumulation, although there was variation among the samples and it was the line with the lowest fungal growth (Figure 2.19). The control roots displayed some kauralexin accumulation at mean levels of ~12µg.gFW^{-1} in B73 (Figure 2.10b) and CB248 (Figure 2.19b) and ~5µg.gFW^{-1} in CML444 (Figure 2.16b) at ten dpi, with lower levels at fourteen dpi. This may be due to the implication that kauralexins are constitutively produced during early seedling development, presumably to protect the developing seedling from soil-borne diseases (Schmelz et al., 2011). Although zealexins have also been shown to accumulate in uninfected seedlings (Huffaker et al., 2011), they were not detected in the control plants of B73, CML444 or CB248.

Although both root and shoot tissues appeared stressed, total kauralexin and zealexin accumulation in the B73 shoot tissue (Figure 2.7b-c) was not as high as in the root tissue (Figure 2.10b-c). However, CML444 had surprisingly high accumulation of total kauralexins in the shoots at ten dpi (Figure 2.13b), even though *F. verticillioides* was not detected in the tissue (Figure 2.13a). There is limited evidence for systemic accumulation of phytoalexins, but Vaughan et al. (2015) observed that below-ground drought stress and above-ground biotic stress influences the potential of the respective tissue to accumulate phytoalexins. Although the experimental design of this study is different, with *F. verticillioides* growing predominantly in the root, and it does suggest that there may be some form of signalling between below- and above-ground tissues that influence phytoalexin accumulation in the respective tissues. This signalling may be the result of increased phytohormone production. Treatment of stems with jasmonic acid and ethylene (JA/E) have been shown to increase total kauralexin accumulation (Schmelz et al., 2011) and ABA treatment of the roots induced kauralexin accumulation (Vaughan et al., 2015). Therefore, increased signalling by JA/E (Huffaker et al., 2011; Schmelz et al., 2011), and ABA (Vaughan et al., 2015) may be responsible for the increase in kauralexin accumulation observed in the roots. The promoter analysis that shows that the promoter regions of *ZmAn2*, *ZmKSL2* and *ZmKO* support this hypothesis (Table 2.7). The result shown in CML444 may be due to efficient root to shoot phytohormone signalling of this maize line. Although *F. verticillioides* induced phytoalexin accumulation in the CML444 roots, it was not to levels sufficient to inhibit fungal growth.

4.1.3 Candidate genes are up-regulated in B73, CML444 and CB248 following *F. verticillioides* inoculation

As a whole, candidate phytoalexin biosynthetic gene expression was positively correlated with fungal growth and phytoalexin accumulation. That is, when higher levels of *F. verticillioides* were detected, phytoalexins accumulated and phytoalexin biosynthetic gene expression was increased. Following this trend, gene expression was more differentially expressed in root tissue than in shoot tissue (Figure 2.4, Figure 2.8, Figure 2.11, Figure 2.14, Figure 2.17, Table 2.12). The exception to this was *ZmCYP81A1*, which was more highly expressed in the shoots than in the roots, although there were no significant differences in expression between control and inoculated plants in any of the maize lines (Figure 2.4e). This is interesting as *ZmCYP81A1* was significantly up-regulated in the ears (Lanubile et al., 2014) and leaves of maize inoculated with *F. verticillioides* (Lambarey, 2017) and in the leaves of maize inoculated with *Cercospora*

zeina (Christie et al., 2017). Although it is not surprising that *ZmCYP81A1* was expressed in the shoots rather than the roots based on the tissue analysed in the previous studies, it is unexpected that no significant change in expression in the shoots was observed between treatments. *ZmAn2* was significantly up-regulated following *F. verticillioides* inoculation in all of the maize lines' roots (Figure 2.4a, Figure 2.11a, Figure 2.20a), except CML444 at ten dpi (Figure 2.17a). *ZmKSL2* was significantly up-regulated at all time points in the B73 roots (Figure 2.11b) and in the CML444 roots at ten dpi (Figure 2.17b). *ZmKO* was only significantly up-regulated in B73 roots in the B73 optimisation experiment (Figure 2.4c) and B73 roots at fourteen dpi (Figure 2.11c). *ZmAn2, ZmKSL2* and *ZmKO* are co-expressed (Christie et al., 2017) and had positive correlations in B73 (Table 2.9) and CML444 (Table 2.11) root tissue where *F. verticillioides* induced higher expression of these genes (Figure 2.11, Figure 2.17). However, the correlations were much weaker and not significant in the shoot tissue (Table 2.8, Table 2.10), in which the only significantly up-regulated genes were *ZmAn2* in B73 shoots at fourteen dpi (Figure 2.8a), and *ZmKO* in CML444 shoots at both time points (Figure 2.14c). Analysis of the promoter regions of these three genes identified motifs that are common between the three genes and may be responsible for their co-regulation. Motifs related to phytohormone signalling, including abscisic acid (ABA) and methyl-jasmonate (MeJA) were present in all of the promoter regions (Table 2.7). Kauralexins have been shown to accumulate following treatment with ABA (Vaughan et al., 2015) and jasmonic acid and ethylene (JA/E) (Schmelz et al., 2011) and JA/E are up-regulated in response to fungal elicitation prior to phytoalexin accumulation (Huffaker et al., 2011; Schmelz et al., 2011). This suggests a mechanism by which *ZmAn2, ZmKSL2* and *ZmKO* are co-expressed. *ZmKSL4* was up-regulated in the inoculated root tissue of B73, CML444 and CB248 (Table 2.12). *ZmKSL4* expression was significantly up-regulated following *F. verticillioides* inoculation in the study by Lanubile et al (2014), and *ZmKSL4* was differentially up-regulated in leaves following *F. verticillioides* inoculation compared to the control in the study by Lambarey (2017), with the adjusted p-value just shy of 0.05. Therefore, it appears that *F. verticillioides* induces *ZmKSL4* expression strongly in both shoots and roots. *ZmTPS11* expression increased significantly following *F. verticillioides* inoculation in the B73 roots ten dpi (Figure 2.11f), and in the CML444 roots at both time points (Figure 2.17f). The reason for the lack of significant expression in some of the tissues is likely due to the variation among the biological samples. However, timing is also important for phytoalexin accumulation and it has been shown that *ZmAn2* and *ZmTPS11* increase prior to phytoalexin accumulation (Huffaker et al., 2011; Schmelz et al., 2011). High total kauralexin accumulation in the root tissue of

these maize lines following *F. verticillioides* inoculation correlates with significant up-regulation of *ZmAn2*, supporting previous evidence for the role of *ZmAn2* as a biosynthetic gene in the kauralexin pathway (Harris et al., 2005; Schmelz et al., 2011; Vaughan et al., 2015). *ZmKSL2* and *ZmKO* were significantly up-regulated in some, but not all, of the root tissue, although their co-expression with *ZmAn2* suggests that they are involved in kauralexin biosynthesis (Christie et al., 2017). *ZmKSL4*, whose role in the kauralexin biosynthetic pathway has not been confirmed as yet, was also positively correlated to total kauralexin accumulation and was significantly up-regulated in the roots of all lines, providing strong evidence for it's role in kauralexin biosynthesis. Furthermore, *ZmAn2* and *ZmKSL4* were the only two genes significantly up-regulated following *F. verticillioides* inoculation in CB248 (Figure 2.20a, Figure 2.20d), which had the highest mean total kauralexin accumulation (Figure 2.19b). The role of *ZmKSL4* in the kauralexin biosynthetic pathway should be investigated further as it was consistently significantly up-regulated (Table 2.12).

4.1.4 *Trichoderma asperellum* growing as an endophyte in ZM401 appears to induce phytoalexin accumulation

A *Trichoderma*-like endophyte growing in the control ZM401 plants was isolated and the ITS barcoding region was amplified from DNA and sequenced. The consensus sequence of the forward *ITS1* primer and the reverse *ITS4* primer was analysed on NCBI BLASTn (Madden, 2002, https://blast.ncbi.nlm.nih.gov/Blast.cgi) and the isolate was identified as *T. asperellum*. Further studies are required to identify the strain of *T. asperellum*.

ZM401 roots inoculated with *F. verticillioides* accumulated total kauralexins and total zealexins to levels of ~18µg.gFW^{-1} and 12µg.gFW^{-1} respectively when *F. verticillioides* was detected at average levels of ~15ng.µg^{-1} (Figure 3.5). However, the control roots, in which no *F. verticillioides* was detected, but containing *T. asperellum,* also accumulated total kauralexins to levels of ~18µg.gFW^{-1} and total zealexins to levels of ~5µg.gFW^{-1}. Although total zealexins increased following *F. verticillioides* inoculation, there is no significant difference between control and treated samples. Phytoalexin biosynthetic genes were expressed at the same level in both treatments (Figure 3.6), which makes corresponds to the similar levels of phytoalexin accumulation. Although the basal levels of phytoalexins in uninfected ZM401 is unknown, it is likely that total kauralexins will accumulate to some extent in uninfected roots due to their accumulation in developing seedling (Schmelz et al., 2011) and as seen in the other maize lines. However, when the total kauralexin accumulation patterns of B73, CML444 and CB248 control roots are

compared to ZM401 containing *T. asperellum*, it seems likely that *T. asperellum* induced accumulation of total kauralexins and total zealexins beyond the levels previously seen in uninfected maize. Furthermore, previous studies have shown that *Trichoderma* spp. are able to induce defence responses in host plants (Tucci et al., 2011; Vos et al., 2015; Patel et al., 2017), and a study has shown that *T. asperellum* induces phytoalexin accumulation in cucumber (Yedidia et al., 2003). Therefore, it is likely that they are also able to induce phytoalexin accumulation in maize. In order to determine the true extent to which phytoalexins accumulate in ZM401 in response to both *F. verticillioides* and *T. asperellum*, this experiment must be repeated with an uninfected control.

4.1.5 *T. asperellum* inhibits *F. verticillioides in vitro*

T. asperellum has been shown to be an effective biocontrol agent (BCA). It has been shown to effectively reduce sheath blight and dirty panicle disease in rice while enhancing grain yield and weight (Chen et al., 2015; de França et al., 2015; Charoenrak & Chamswarng, 2016). *In vitro* studies have also shown that *T. asperellum* inhibits *F. oxysporum* growth (Chandra Nayaka et al., 2010; El Komy et al., 2015). Following competition experiments between *T. asperellum* and *F. verticillioides*, it was observed that *T. asperellum* significantly inhibits *F. verticillioides* growth by 52% when both fungi are plated at the same time, while *F. verticillioides* was inhibited by 30% when it was plated two days prior to *T. asperellum* (Table 3.3). Initial inhibition of *F. verticillioides* is likely due to *T. asperellum* outcompeting *F. verticillioides*, but *T. asperellum* interacted directly with *F. verticillioides* and by seven days overgrowth was observed (Figure 3.8). As previous studies have shown that *T. asperellum* mycoparisitises *F. oxysporum* (El Komy et al., 2015), it likely changes the morphological structure of *F. verticillioides* too. Microscopic investigation into this is necessary to understand how *T. asperellum* interacts with *F. verticillioides*.

4.2 Future work

Although this study provided preliminary results showing that phytoalexins accumulate in response to *F. verticillioides* inoculation, there is still much work to be done. It would be beneficial to perform this study on a larger scale in a field trial in order to evaluate phytoalexin accumulation in cob tissue inoculated with *F. verticillioides*. This is of particular interest, as *F. verticillioides* is most known as the causal agent of Fusarium ear rot (FER). The study could also be extended to a wider range of southern African maize lines, including the lines analysed in this study, those that did not germinate (Table S2.4) as well

other lines that were not considered for this study. The use of susceptible and partially resistant lines would provide evidence for the extent to which phytoalexins contribute to *F. verticillioides* resistance in southern African maize lines. Fumonisin accumulation in dried cob tissue could also be measured, and the correlations between phytoalexin accumulation, *F. verticillioides* growth, and fumonisin accumulation could be determined. While it has been shown that mycotoxin producing fungi do not significantly induce phytoalexin accumulation compared to mycotoxin-nonproducing fungi (Huffaker et al., 2011), it would be interesting to see whether maize lines that accumulate higher levels of phytoalexins have reduced fumonisin levels. In terms of phytoalexin biosynthetic genes, gene expression analysis could be extended to other candidate genes that were not looked at in this study, including *ZmTPS1* for the kauralexin pathway, and *ZmTPS6* and *ZmCYP71Z18* for the zealexin pathway.

In order to obtain a better understanding of the phytoalexin biosynthetic pathways, functional analysis could be performed on some of the biosynthetic enzymes that have been identified thus far. A knockdown *Zman2* mutant displayed reduced kauralexin accumulation and increased susceptibility to *F. verticillioides* (Vaughan et al., 2015; Wighard, 2017). However, functional analysis on other genes in the kauralexin pathway is limited. It would be of particular interest to look more closely at the co-expression of *ZmAn2, ZmKSL2* and *ZmKO*. This could be done by cloning the promoter regions of these genes and performing analyses on them. It would also be of interest to study the role of *ZmKLS4*, which is highly up-regulated in this study and is suggested to be involved in the conversion of *ent*-copalyl diphosphate (CPP) to *ent*-isokaurene, the intermediate upstream of kauralexin B1, B2, and B3 (Fu et al., 2016). Therefore, *ksl4* knockdown experiments using *Ac/Ds* (Vollbrecht et al., 2010) or the CRISPR/Cas system (Liang et al., 2014) would be useful in determining whether kauralexin accumulation decreases in the absence of the ZmKSL4 protein. Virus-induced gene silencing (VIGS) of *ZmTPS11* has been shown to increase susceptibility to *Ustilago maydis* (van der Linde et al., 2011), although zealexin accumulation was not measured. Therefore, generating *tps11* knockdown mutants to measure zealexin accumulation would provide more concrete evidence to the already thoroughly studied role of *ZmTPS11*.

More specifically to the results of this study, it is necessary to perform the analyses on ZM401 again with a true, uninfected control to determine whether *F. verticillioides* is able to induce significant phytoalexin accumulation compared to the control. Inoculation of

ZM401 with *T. asperellum* could also be performed in order to determine whether *T. asperellum* does indeed induce phytoalexin accumulation, and whether this phytoalexin accumulation is significantly more than the control. The efficacy of *T. asperellum* as a BCA against *F. verticillioides* could also be analysed by performing competition experiments between the two fungi in maize and measuring *F. verticillioides* growth when treated with *T. asperellum* compared to no *T. asperellum* treatment. Finally, microscopic analysis of the dual culture competition assays between *T. asperellum* growth and *F. verticillioides* could be performed in order to see whether mycoparasitism occurs and whether *T. asperellum* changes the morphology of *F. verticillioides*.

The prevalence of *F. verticillioides* in maize in southern Africa is of great concern, particularly due to fumonisin B_1 accumulation in *F. verticillioides*-infected maize that is harmful to both livestock and human health. It is therefore important to find ways to reduce *F. verticillioides* long-term, and one of the best ways to do this is to breed for resistance. In this study, it was found that phytoalexins accumulate as a defence response following *F. verticillioides* inoculation, but did not accumulate to levels sufficient for reduced *F. verticillioides* growth. However, as previous studies have shown that phytoalexins are able to significantly reduce the growth of a number of pathogens and herbivory (Huffaker et al., 2011; Schmelz et al., 2011; Vaughan et al., 2015), they are still important candidates to enhance *F. verticillioides* resistance. Therefore, enhanced phytoalexin accumulation could be bred into maize in order to provide sufficient levels for resistance to *F. verticillioides*. Furthermore, the use of biocontrol agents such as *T. asperellum* could be used in combination with maize breeding to provide optimal resistance to fungal pathogens.

REFERENCE LIST

Abe, H., Yamaguchi-Shinozaki, K., Urao, T., Iwasaki, T., Hosokawa, D. & Shinozaki, K. 1997. Role of *Arabidopsis* MYC and MYB homologs in drought-and abscisic acid-regulated gene expression. *The Plant Cell*. 9(10):1859–1868.

Agrios, G.N. 1997. *Plant Pathology*. 4th ed. United States of America: Academic Press.

Ahuja, I., Kissen, R. & Bones, A.M. 2012. Phytoalexins in defense against pathogens. *Trends in Plant Science*. 17(2):73–90. DOI: 10.1016/j.tplants.2011.11.002.

Alvarado-Marchena, L. & Rivera-Méndez, W. 2016. Molecular Identification of *Trichoderma* spp. in Garlic and Onion Fields and *In Vitro* Antagonism Trials on *Sclerotium cepivorum*. *Revista Brasileira de Ciência do Solo*. 40(0). DOI: 10.1590/18069657rbcs20150454.

Atehnkeng, J., Ojiambo, P.S., Ikotun, T., Sikora, R.A., Cotty, P.J. & Bandyopadhyay, R. 2008. Evaluation of atoxigenic isolates of *Aspergillus flavus* as potential biocontrol agents for aflatoxin in maize. *Food Additives & Contaminants: Part A*. 25(10):1264–1271. DOI: 10.1080/02652030802112635.

Bailey, T.L. & Elkan, C. 1994. Fitting a mixture model by expectation maximization to discover motifs in biopolymers. In *Proceedings of the Second International Conference on Intelligent Systems for Molecular Biology*. Menlo Park, California: AAAI Press. 28–36.

Bais, H.P., Weir, T.L., Perry, L.G., Gilroy, S. & Vivanco, J.M. 2006. The role of root exudates in rhizosphere interactions with plants and other organisms. *Annu. Rev. Plant Biol.* 57:233–266.

Baldwin, T.T., Zitomer, N.C., Mitchell, T.R., Zimeri, A.-M., Bacon, C.W., Riley, R.T. & Glenn, A.E. 2014. Maize Seedling Blight Induced by *Fusarium verticillioides*: Accumulation of Fumonisin B_1 in Leaves without Colonization of the Leaves. *Journal of Agricultural and Food Chemistry*. 62(9):2118–2125. DOI: 10.1021/jf5001106.

Balint-Kurti, P.J. & Johal, G.S. 2009. Maize Disease Resistance. In *Handbook of Maize: Its Biology*. J.L. Bennetzen & S.C. Hake, Eds. New York, NY: Springer New York. 229–250. DOI: 10.1007/978-0-387-79418-1_12.

Becker, E.-M., Herrfurth, C., Irmisch, S., Köllner, T.G., Feussner, I., Karlovsky, P. & Splivallo, R. 2014. Infection of Corn Ears by *Fusarium* spp. Induces the Emission of Volatile Sesquiterpenes. *Journal of Agricultural and Food Chemistry*. 62(22):5226–5236. DOI: 10.1021/jf500560f.

Benítez, T., Rincón, A.M., Limón, M.C. & Codón, A.C. 2004. Biocontrol mechanisms of *Trichoderma* strains. *International microbiology*. 7(4):249–260.

Bensen, R.J., Johal, G.S., Crane, V.C., Tossberg, J.T., Schnable, P.S., Meeley, R.B. & Briggs, S.P. 1995. Cloning and characterization of the maize *An1* gene. *The Plant Cell*. 7(1):75–84.

Berger, D.K., Carstens, M., Korsman, J.N., Middleton, F., Kloppers, F.J., Tongoona, P. & Myburg, A.A. 2014. Mapping QTL conferring resistance in maize to gray leaf spot disease caused by *Cercospora zeina*. *BMC genetics*. 15(1):60.

Binder, E.M. 2007. Managing the risk of mycotoxins in modern feed production. *Animal Feed Science and Technology*. 133(1–2):149–166. DOI: 10.1016/j.anifeedsci.2006.08.008.

Boutigny, A.-L., Beukes, I., Small, I., Zühlke, S., Spiteller, M., Van Rensburg, B.J., Flett, B. & Viljoen, A. 2012. Quantitative detection of *Fusarium* pathogens and their mycotoxins in South African maize. *Plant Pathology*. 61(3):522–531. DOI: 10.1111/j.1365-3059.2011.02544.x.

Bowers, E., Hellmich, R. & Munkvold, G. 2014. Comparison of Fumonisin Contamination Using HPLC and ELISA Methods in *Bt* and Near-Isogenic Maize Hybrids Infested with European Corn Borer or

Western Bean Cutworm. *Journal of Agricultural and Food Chemistry*. 62(27):6463–6472. DOI: 10.1021/jf5011897.

Bush, B.J., Carson, M.L., Cubeta, M.A., Hagler, W.M. & Payne, G.A. 2004. Infection and fumonisin production by *Fusarium verticillioides* in developing maize kernels. *Phytopathology*. 94(1):88–93.

Cardoza, R.-E., Hermosa, M.R., Vizcaino, J.A., Sanz, L., Monte, E. & Gutierrez, S. 2005. Secondary metabolites produced by *Trichoderma* and their importance in the biocontrol process. *Microorganisms for industrial enzymes and biocontrol*. 207.

Chakraborty, S. & Newton, A.C. 2011. Climate change, plant diseases and food security: an overview: Climate change and food security. *Plant Pathology*. 60(1):2–14. DOI: 10.1111/j.1365-3059.2010.02411.x.

Chandra Nayaka, S., Niranjana, S.R., Uday Shankar, A.C., Niranjan Raj, S., Reddy, M.S., Prakash, H.S. & Mortensen, C.N. 2010. Seed biopriming with novel strain of *Trichoderma harzianum* for the control of toxigenic *Fusarium verticillioides* and fumonisins in maize. *Archives Of Phytopathology And Plant Protection*. 43(3):264–282. DOI: 10.1080/03235400701803879.

Charoenrak, P. & Chamswarng, C. 2016. Efficacies of wettable pellet and fresh culture of *Trichoderma asperellum* biocontrol products in growth promoting and reducing dirty panicles of rice. *Agriculture and Natural Resources*. 50(4):243–249. DOI: 10.1016/j.anres.2016.04.001.

Chen, L.-H., Zhang, J., Shao, X.-H., Wang, S.-S., Miao, Q.-S., Mao, X.-Y., Zhai, Y.-M. & She, D.-L. 2015. Development and evaluation of *Trichoderma asperellum* preparation for control of sheath blight of rice (*Oryza sativa* L.). *Biocontrol Science and Technology*. 25(3):316–328. DOI: 10.1080/09583157.2014.977225.

Cheng, A.-X., Lou, Y.-G., Mao, Y.-B., Lu, S., Wang, L.-J. & Chen, X.-Y. 2007. Plant terpenoids: biosynthesis and ecological functions. *Journal of Integrative Plant Biology*. 49(2):179–186.

Chow, C.-N., Zheng, H.-Q., Wu, N.-Y., Chien, C.-H., Huang, H.-D., Lee, T.-Y., Chiang-Hsieh, Y.-F., Hou, P.-F., et al. 2016. PlantPAN 2.0: an update of plant promoter analysis navigator for reconstructing transcriptional regulatory networks in plants. *Nucleic Acids Research*. 44(D1):D1154–D1160. DOI: 10.1093/nar/gkv1035.

Christie, N., Myburg, A.A., Joubert, F., Murray, S.L., Carstens, M., Lin, Y.-C., Meyer, J., Crampton, B.G., et al. 2017. Systems genetics reveals a transcriptional network associated with susceptibility in the maize-grey leaf spot pathosystem. *The Plant Journal*. 89(4):746–763. DOI: 10.1111/tpj.13419.

Colombo, C., Palumbo, G., He, J.-Z., Pinton, R. & Cesco, S. 2014. Review on iron availability in soil: interaction of Fe minerals, plants, and microbes. *Journal of Soils and Sediments*. 14(3):538–548. DOI: 10.1007/s11368-013-0814-z.

Coppola, M., Cascone, P., Chiusano, M.L., Colantuono, C., Lorito, M., Pennacchio, F., Rao, R., Woo, S.L., et al. 2017. *Trichoderma harzianum* enhances tomato indirect defense against aphids: *Trichoderma* helps tomatoes attacked by aphids. *Insect Science*. (July, 10). DOI: 10.1111/1744-7917.12475.

Corwin, J.A. & Kliebenstein, D.J. 2017. Quantitative Resistance: More Than Just Perception of a Pathogen. *The Plant Cell*. 29(4):655–665. DOI: 10.1105/tpc.16.00915.

Council for Agricultural Science and Technology Ed. 2003. *Mycotoxins: risks in plant, animal, and human systems*. (Task force report no. 139). Ames, Iowa: Council for Agricultural Science and Technology.

Dangl, J.L. & Jones, J.D. 2001. Plant pathogens and integrated defence responses to infection. *Nature*. 411(6839):826–833.

Degenhardt, J., Köllner, T.G. & Gershenzon, J. 2009. Monoterpene and sesquiterpene synthases and the origin of terpene skeletal diversity in plants. *Phytochemistry*. 70(15–16):1621–1637. DOI: 10.1016/j.phytochem.2009.07.030.

Denancé, N., Sánchez-Vallet, A., Goffner, D. & Molina, A. 2013. Disease resistance or growth: the role of plant hormones in balancing immune responses and fitness costs. *Frontiers in Plant Science*. 4. DOI: 10.3389/fpls.2013.00155.

Desjardins, A.E. & Plattner, R.D. 2000. Fumonisin B_1-Nonproducing Strains of *Fusarium verticillioides* Cause Maize (*Zea mays*) Ear Infection and Ear Rot. *Journal of Agricultural and Food Chemistry*. 48(11):5773–5780. DOI: 10.1021/jf000619k.

Ding, J.-Q., Wang, X.-M., Chander, S., Yan, J.-B. & Li, J.-S. 2008. QTL mapping of resistance to Fusarium ear rot using a RIL population in maize. *Molecular Breeding*. 22(3):395–403. DOI: 10.1007/s11032-008-9184-4.

Doehlemann, G., Wahl, R., Horst, R.J., Voll, L.M., Usadel, B., Poree, F., Stitt, M., Pons-Kühnemann, J., et al. 2008. Reprogramming a maize plant: transcriptional and metabolic changes induced by the fungal biotroph *Ustilago maydis*. *The Plant Journal*. 56(2):181–195. DOI: 10.1111/j.1365-313X.2008.03590.x.

Druzhinina, I.S., Kopchinskiy, A.G., Komoń, M., Bissett, J., Szakacs, G. & Kubicek, C.P. 2005. An oligonucleotide barcode for species identification in *Trichoderma* and *Hypocrea*. *Fungal Genetics and Biology*. 42(10):813–828. DOI: 10.1016/j.fgb.2005.06.007.

Dutton, M.F. 2009. The African Fusarium/maize disease. *Mycotoxin Research*. 25(1):29–39. DOI: 10.1007/s12550-008-0005-8.

El Komy, M.H., Saleh, A.A., Eranthodi, A. & Molan, Y.Y. 2015. Characterization of Novel *Trichoderma asperellum* Isolates to Select Effective Biocontrol Agents Against Tomato Fusarium Wilt. *The Plant Pathology Journal*. 31(1):50–60. DOI: 10.5423/PPJ.OA.09.2014.0087.

Fandohan, P., Hell, K., Marasas, W.F.O. & Wingfield, M.J. 2003. Infection of maize by *Fusarium* species and contamination with fumonisin in Africa. *African Journal of Biotechnology*. 2(12):570–579.

Food and Agriculture Organization of the United Nations. 2017. *Crops*. Available: http://www.fao.org/faostat/en/#data/QC [2017, June 26].

de França, S.K.S., Cardoso, A.F., Lustosa, D.C., Ramos, E.M.L.S., de Filippi, M.C.C. & da Silva, G.B. 2015. Biocontrol of sheath blight by *Trichoderma asperellum* in tropical lowland rice. *Agronomy for Sustainable Development*. 35(1):317–324. DOI: 10.1007/s13593-014-0244-3.

Fu, J., Ren, F., Lu, X., Mao, H., Xu, M., Degenhardt, J., Peters, R.J. & Wang, Q. 2016. A Tandem Array of *ent* -Kaurene Synthases in Maize with Roles in Gibberellin and More Specialized Metabolism. *Plant Physiology*. 170(2):742–751. DOI: 10.1104/pp.15.01727.

Gelderblom, W.C., Jaskiewicz, K., Marasas, W.F., Thiel, P.G., Horak, R.M., Vleggaar, R. & Kriek, N.P. 1988. Fumonisins–novel mycotoxins with cancer-promoting activity produced by *Fusarium moniliforme*. *Applied and environmental microbiology*. 54(7):1806–1811.

Geraldine, A.M., Lopes, F.A.C., Carvalho, D.D.C., Barbosa, E.T., Rodrigues, A.R., Brandão, R.S., Ulhoa, C.J. & Lobo Junior, M. 2013. Cell wall-degrading enzymes and parasitism of sclerotia are key factors on field biocontrol of white mold by *Trichoderma* spp. *Biological Control*. 67(3):308–316. DOI: 10.1016/j.biocontrol.2013.09.013.

Glazebrook, J. 2005. Contrasting Mechanisms of Defense Against Biotrophic and Necrotrophic Pathogens. *Annual Review of Phytopathology*. 43(1):205–227. DOI: 10.1146/annurev.phyto.43.040204.135923.

Goldsbrough, A.P., Albrecht, H. & Stratford, R. 1993. Salicylic acid-inducible binding of a tobacco nuclear protein to a 10 bp sequence which is highly conserved among stress-inducible genes. *The Plant Journal*. 3(4):563–571.

Hansen, B.G., Halkier, B.A. & Kliebenstein, D.J. 2008. Identifying the molecular basis of QTLs: eQTLs add a new dimension. *Trends in Plant Science*. 13(2):72–77. DOI: 10.1016/j.tplants.2007.11.008.

Harman, G.E., Howell, C.R., Viterbo, A., Chet, I. & Lorito, M. 2004. *Trichoderma* species — opportunistic, avirulent plant symbionts. *Nature Reviews Microbiology*. 2(1):43–56. DOI: 10.1038/nrmicro797.

Harman, G.E., Petzoldt, R., Comis, A. & Chen, J. 2004. Interactions between *Trichoderma harzianum* strain T22 and maize inbred line Mo17 and effects of these interactions on diseases caused by *Pythium ultimum* and *Colletotrichum graminicola*. *Phytopathology*. 94(2):147–153.

Harris, L.J., Saparno, A., Johnston, A., Prisic, S., Xu, M., Allard, S., Kathiresan, A., Ouellet, T., et al. 2005. The Maize *An2* Gene is Induced by *Fusarium* Attack and Encodes an ent-Copalyl Diphosphate Synthase. *Plant Molecular Biology*. 59(6):881–894. DOI: 10.1007/s11103-005-1674-8.

Harrison, L.R., Colvin, B.M., Greene, J.T., Newman, L.E. & Cole Jr, J.R. 1990. Pulmonary edema and hydrothorax in swine produced by fumonisin B1, a toxic metabolite of *Fusarium moniliforme*. *Journal of Veterinary Diagnostic Investigation*. 2(3):217–221.

Heydari, A. & Pessarakli, M. 2010. A Review on Biological Control of Fungal Plant Pathogens Using Microbial Antagonists. *Journal of Biological Sciences*. 10(4):273–290.

Huffaker, A., Kaplan, F., Vaughan, M.M., Dafoe, N.J., Ni, X., Rocca, J.R., Alborn, H.T., Teal, P.E.A., et al. 2011. Novel Acidic Sesquiterpenoids Constitute a Dominant Class of Pathogen-Induced Phytoalexins in Maize. *Plant Physiology*. 156(4):2082–2097. DOI: 10.1104/pp.111.179457.

Hyde, K.D. & Soytong, K. 2008. The fungal endophyte dilemma. *Fungal diversity*. 33:163–173.

Jiao, Y., Peluso, P., Shi, J., Liang, T., Stitzer, M.C., Wang, B., Campbell, M.S., Stein, J.C., et al. 2017. Improved maize reference genome with single-molecule technologies. *Nature*. (June,12). DOI: 10.1038/nature22971.

Joint FAO WHO Expert Committee on Food Additives Ed. 2012. *Safety evaluation of certain food additives and contaminants: prepared by the seventy-fourth meeting of the Joint FAO/WHO Expert Committee on Food Additives (JECFA) ; [Rome, Italy, on 14-23 June 2011]*. (WHO food additives series no. 65). Geneva: World Health Organization.

Jones, J.D.G. & Dangl, J.L. 2006. The plant immune system. *Nature*. 444(7117):323–329. DOI: 10.1038/nature05286.

Karasov, T.L., Chae, E., Herman, J.J. & Bergelson, J. 2017. Mechanisms to Mitigate the Trade-Off between Growth and Defense. *The Plant Cell*. 29(4):666–680. DOI: 10.1105/tpc.16.00931.

Kersey, P.J., Allen, J.E., Armean, I., Boddu, S., Bolt, B.J., Carvalho-Silva, D., Christensen, M., Davis, P., et al. 2016. Ensembl Genomes 2016: more genomes, more complexity. *Nucleic Acids Research*. 44(D1):D574–D580. DOI: 10.1093/nar/gkv1209.

Kimura, S., Waszczak, C., Hunter, K. & Wrzaczek, M. 2017. Bound by Fate: The Role of Reactive Oxygen Species in Receptor-Like Kinase Signaling. *The Plant Cell*. 29(4):638–654. DOI: 10.1105/tpc.16.00947.

Köllner, T.G., Schnee, C., Gershenzon, J. & Degenhardt, J. 2004. The sesquiterpene hydrocarbons of maize (*Zea mays*) form five groups with distinct developmental and organ-specific distributions. *Phytochemistry*. 65(13):1895–1902. DOI: 10.1016/j.phytochem.2004.05.021.

Köllner, T.G., Schnee, C., Li, S., Svatoš, A., Schneider, B., Gershenzon, J. & Degenhardt, J. 2008. Protonation of a Neutral (*S*)-β-Bisabolene Intermediate Is Involved in (*S*)-β-Macrocarpene Formation

by the Maize Sesquiterpene Synthases TPS6 and TPS11. *Journal of Biological Chemistry*. 283(30):20779–20788. DOI: 10.1074/jbc.M802682200.

Köllner, T.G., Gershenzon, J. & Degenhardt, J. 2009. Molecular and biochemical evolution of maize terpene synthase 10, an enzyme of indirect defense. *Phytochemistry*. 70(9):1139–1145. DOI: 10.1016/j.phytochem.2009.06.011.

Korsman, J., Meisel, B., Kloppers, F.J., Crampton, B.G. & Berger, D.K. 2012. Quantitative phenotyping of grey leaf spot disease in maize using real-time PCR. *European Journal of Plant Pathology*. 133(2):461–471. DOI: 10.1007/s10658-011-9920-1.

Lambarey, H. 2017. An investigation of *Fusarium verticillioides* infection in maize using physiological and molecular approaches. Master of Science thesis. University of Cape Town.

Lanubile, A., Ferrarini, A., Maschietto, V., Delledonne, M., Marocco, A. & Bellin, D. 2014. Functional genomic analysis of constitutive and inducible defense responses to *Fusarium verticillioides* infection in maize genotypes with contrasting ear rot resistance. *BMC genomics*. 15(1):1.

Leelavathi, M.S., Vani, L. & Reena, P. 2014. Antimicrobial activity of *Trichoderma harzianum* against bacteria and fungi. *Int. J. Curr. Microbiol. Appl. Sci*. 3:96–103.

Lescot, M., Dehais, P., Moreau, P., De Moor, B., Rouze, P. & Rombauts, S. 2002. PlantCARE: a database of plant *cis*-acting regulatory elements and a portal to tools for *in silico* analysis of promoter sequences. *Nucleic Acids Research, Database issue*. 30(1):325–327.

Levasseur-Garcia, C., Bailly, S., Kleiber, D. & Bailly, J.-D. 2015. Assessing Risk of Fumonisin Contamination in Maize Using Near-Infrared Spectroscopy. *Journal of Chemistry*. 2015:1–10. DOI: 10.1155/2015/485864.

Liang, Z., Zhang, K., Chen, K. & Gao, C. 2014. Targeted Mutagenesis in *Zea mays* Using TALENs and the CRISPR/Cas System. *Journal of Genetics and Genomics*. 41(2):63–68. DOI: 10.1016/j.jgg.2013.12.001.

van der Linde, K., Kastner, C., Kumlehn, J., Kahmann, R. & Doehlemann, G. 2011. Systemic virus-induced gene silencing allows functional characterization of maize genes during biotrophic interaction with *Ustilago maydis*. *New Phytologist*. 189(2):471–483. DOI: 10.1111/j.1469-8137.2010.03474.x.

Logrieco, A., Mule, G., Moretti, A. & Bottalico, A. 2002. Toxigenic *Fusarium* species and mycotoxins associated with maize ear rot in Europe. *European Journal of Plant Pathology*. 108:597–609. DOI: 10.1023/A:1020679029993.

Luongo, L., Galli, M., Corazza, L., Meekes, E., Haas, L.D., Van Der Plas, C.L. & Köhl, J. 2005. Potential of fungal antagonists for biocontrol of *Fusarium* spp. in wheat and maize through competition in crop debris. *Biocontrol Science and Technology*. 15(3):229–242. DOI: 10.1080/09583150400016852.

Madden, T. 2002. The BLAST Sequence Analysis Tool. In *The NCBI Handbook [Internet]*. 2nd ed. J. McEntyre & J. Ostell, Eds. Bethesda, MD: National Center for Biotechnology Information (US). Chapter 16.

MAIZE. 2016. *Why MAIZE*. Available: http://maize.org/why-maize/ [2017, June 26].

Manoli, A., Sturaro, A., Trevisan, S., Quaggiotti, S. & Nonis, A. 2012. Evaluation of candidate reference genes for qPCR in maize. *Journal of Plant Physiology*. 169(8):807–815. DOI: 10.1016/j.jplph.2012.01.019.

Mao, H., Liu, J., Ren, F., Peters, R.J. & Wang, Q. 2016. Characterization of CYP71Z18 indicates a role in maize zealexin biosynthesis. *Phytochemistry*. 121:4–10. DOI: 10.1016/j.phytochem.2015.10.003.

Marasas, W.F., Riley, R.T., Hendricks, K.A., Stevens, V.L., Sadler, T.W., Gelineau-van Waes, J., Missmer, S.A., Cabrera, J., et al. 2004. Fumonisins disrupt sphingolipid metabolism, folate transport, and neural tube development in embryo culture and *in vivo*: a potential risk factor for human neural tube defects among populations consuming fumonisin-contaminated maize. *The Journal of nutrition*. 134(4):711–716.

Maschietto, V., Colombi, C., Pirona, R., Pea, G., Strozzi, F., Marocco, A., Rossini, L. & Lanubile, A. 2017. QTL mapping and candidate genes for resistance to Fusarium ear rot and fumonisin contamination in maize. *BMC Plant Biology*. 17(1). DOI: 10.1186/s12870-017-0970-1.

Meyer, J., Murray, S.L. & Berger, D.K. 2016. Signals that stop the rot: Regulation of secondary metabolite defences in cereals. *Physiological and Molecular Plant Pathology*. 94:156–166. DOI: 10.1016/j.pmpp.2015.05.011.

Michaelson, J.J., Loguercio, S. & Beyer, A. 2009. Detection and interpretation of expression quantitative trait loci (eQTL). *Methods*. 48(3):265–276. DOI: 10.1016/j.ymeth.2009.03.004.

Moola, N. 2016. An analysis of the terpenoid defence response to *Fusarium verticillioides* infection in an African maize line. Bachelor of Science (Honours) thesis. University of Cape Town.

Munkvold, G.P. 2003a. Epidemiology of Fusarium diseases and their mycotoxins in maize ears. In *Epidemiology of Mycotoxin Producing Fungi*. Springer. 705–713. Available: http://link.springer.com/chapter/10.1007/978-94-017-1452-5_5 [2017, June 30].

Munkvold, G.P. 2003b. Cultural and genetic approaches to managing mycotoxins in maize. *Annual Review of Phytopathology*. 41(1):99–116. DOI: 10.1146/annurev.phyto.41.052002.095510.

Munkvold, G.P. & Desjardins, A.E. 1997. Fumonisins in maize: can we reduce their occurrence? *Plant disease*. 81(6):556–565.

Munkvold, G.P., McGee, D.C. & Carlton, W.M. 1997. Importance of different pathways for maize kernel infection by *Fusarium moniliforme*. *Phytopathology*. 87(2):209–217.

Murillo-Williams, A. & Munkvold, G.P. 2008. Systemic infection by *Fusarium verticillioides* in maize plants grown under three temperature regimes. *Plant disease*. 92(12):1695–1700.

Muthukrishnan, S., Liang, G.H., Trick, H.N. & Gill, B.S. 2001. Pathogenesis-related proteins and their genes in cereals. *Plant Cell, Tissue and Organ Culture*. 64(2):93–114.

Mutiga, S.K., Hoffman, V., Harvey, J.W., Milgroom, M.G. & Nelson, R.J. 2015. Assessment of Aflatoxin and Fumonisin Contamination of Maize in Western Kenya. *Phytopathology*. 105(9):1250–1261.

Navi, S.S. & Yang, X.B. 2008. Foliar symptom expression in association with early infection and xylem colonisation by *Fusarium virguliforme* (formerly *F. solani* f. sp. glycines), the causal agent of soybean sudden death syndrome. *Plant Health Progress*. DOI: 10.1094/PHP-2008-0222-01-RS.

Ncube, E., Flett, B.C., Van den Berg, J., Erasmus, A. & Viljoen, A. 2017. Fusarium ear rot and fumonisins in maize kernels when comparing a Bt hybrid with its non-Bt isohybrid and under conventional insecticide control of *Busseola fusca* infestations. *Crop Protection*. (September). DOI: 10.1016/j.cropro.2017.09.015.

Nicolaisen, M., Supronienė, S., Nielsen, L.K., Lazzaro, I., Spliid, N.H. & Justesen, A.F. 2009. Real-time PCR for quantification of eleven individual *Fusarium* species in cereals. *Journal of Microbiological Methods*. 76(3):234–240. DOI: 10.1016/j.mimet.2008.10.016.

Ntuli, J.F. 2016. Characterisation of Phytoalexin Accumulation in Maize inoculated with *Cercospora zeina*, the causal organism of Grey Leaf Spot Disease. Master of Science thesis. University of Cape Town.

Oerke, E.-C. 2006. Crop losses to pests. *The Journal of Agricultural Science*. 144(1):31. DOI: 10.1017/S0021859605005708.

Oren, L., Ezrati, S., Cohen, D. & Sharon, A. 2003. Early Events in the *Fusarium verticillioides*-Maize Interaction Characterized by Using a Green Fluorescent Protein-Expressing Transgenic Isolate. *Applied and Environmental Microbiology*. 69(3):1695–1701. DOI: 10.1128/AEM.69.3.1695-1701.2003.

Ottenheim, C., Meier, K., Zimmermann, W. & Wu, J.C. 2015. Isolation of Filamentous Fungi Exhibiting High Endoxylanase Activity in Lignocellulose Hydrolysate. *Applied Biochemistry and Biotechnology*. 175(4):2066–2074. DOI: 10.1007/s12010-014-1427-8.

Pamphile, J.A. & Azevedo, J.L. 2002. Molecular characterization of endophytic strains of *F. verticillioides (= Fusarium moniliforme)* from maize (*Zea mays.* L). *World Journal of Microbiology & Biotechnology*. 18:391–396.

Paquis, S., Mazeyrat-Gourbeyre, F., Fernandez, O., Crouzet, J., Clément, C., Baillieul, F. & Dorey, S. 2011. Characterization of a F-box gene up-regulated by phytohormones and upon biotic and abiotic stresses in grapevine. *Molecular Biology Reports*. 38(5):3327–3337. DOI: 10.1007/s11033-010-0438-y.

Patel, J.S., Kharwar, R.N., Singh, H.B., Upadhyay, R.S. & Sarma, B.K. 2017. *Trichoderma asperellum* (T42) and *Pseudomonas fluorescens* (OKC)-Enhances Resistance of Pea against *Erysiphe pisi* through Enhanced ROS Generation and Lignifications. *Frontiers in Microbiology*. 8. DOI: 10.3389/fmicb.2017.00306.

Pavone Maniscalco, D. & Dorta, B. 2015. Diversity of the fungus *Trichoderma* spp. on corn fields in Venezuela. *Interciencia*. 40(1):23–31.

Pechanova, O. & Pechan, T. 2015. Maize-Pathogen Interactions: An Ongoing Combat from a Proteomics Perspective. *International Journal of Molecular Sciences*. 16(12):28429–28448. DOI: 10.3390/ijms161226106.

Pereira, P., Nesci, A. & Etcheverry, M. 2007. Effects of biocontrol agents on *Fusarium verticillioides* count and fumonisin content in the maize agroecosystem: Impact on rhizospheric bacterial and fungal groups. *Biological Control*. 42(3):281–287. DOI: 10.1016/j.biocontrol.2007.05.015.

Pereyra, M.L.G., Alonso, V.A., Sager, R., Morlaco, M.B., Magnoli, C.E., Astoreca, A.L., Rosa, C.A.R., Chiacchiera, S.M., et al. 2008. Fungi and selected mycotoxins from pre- and postfermented corn silage. *Journal of Applied Microbiology*. 104(4):1034–1041. DOI: 10.1111/j.1365-2672.2007.03634.x.

Peters, R.J. 2006. Uncovering the complex metabolic network underlying diterpenoid phytoalexin biosynthesis in rice and other cereal crop plants. *Phytochemistry*. 67(21):2307–2317. DOI: 10.1016/j.phytochem.2006.08.009.

Poland, J.A., Balint-Kurti, P.J., Wisser, R.J., Pratt, R.C. & Nelson, R.J. 2009. Shades of gray: the world of quantitative disease resistance. *Trends in Plant Science*. 14(1):21–29. DOI: 10.1016/j.tplants.2008.10.006.

Reid, L.M., Woldemariam, T., Zhu, X., Stewart, D.W. & Schaafsma, A.W. 2002. Effect of inoculation time and point of entry on disease severity in *Fusarium graminearum, Fusarium verticillioides*, or *Fusarium subglutinans* inoculated maize ears[1]. *Canadian Journal of Plant Pathology*. 24(2):162–167.

Robert-Seilaniantz, A., Grant, M. & Jones, J.D.G. 2011. Hormone Crosstalk in Plant Disease and Defense: More Than Just Jasmonate-Salicylate Antagonism. *Annual Review of Phytopathology*. 49(1):317–343. DOI: 10.1146/annurev-phyto-073009-114447.

Rose, L.J., Okoth, S., Beukes, I., Ouko, A., Mouton, M., Flett, B.C., Makumbi, D. & Viljoen, A. 2017. Determining resistance to *Fusarium verticillioides* and fumonisin accumulation in African maize inbred lines resistant to *Aspergillus flavus* and aflatoxins. *Euphytica*. 213(4). DOI: 10.1007/s10681-017-1883-7.

Saravanakumar, K., Yu, C., Dou, K., Wang, M., Li, Y. & Chen, J. 2016. Biodiversity of *Trichoderma* Community in the Tidal Flats and Wetland of Southeastern China. *PLOS ONE*. 11(12):e0168020. DOI: 10.1371/journal.pone.0168020.

Saravanakumar, K., Li, Y., Yu, C., Wang, Q., Wang, M., Sun, J., Gao, J. & Chen, J. 2017. Effect of *Trichoderma harzianum* on maize rhizosphere microbiome and biocontrol of Fusarium Stalk rot. *Scientific Reports*. 7(1). DOI: 10.1038/s41598-017-01680-w.

Schlenker, W. & Lobell, D.B. 2010. Robust negative impacts of climate change on African agriculture. *Environmental Research Letters*. 5(1):14010. DOI: 10.1088/1748-9326/5/1/014010.

Schmelz, E.A., Kaplan, F., Huffaker, A., Dafoe, N.J., Vaughan, M.M., Ni, X., Rocca, J.R., Alborn, H.T., et al. 2011. Identity, regulation, and activity of inducible diterpenoid phytoalexins in maize. *Proceedings of the National Academy of Sciences*. 108(13):5455–5460. DOI: 10.1073/pnas.1014714108.

Schmelz, E.A., Huffaker, A., Sims, J.W., Christensen, S.A., Lu, X., Okada, K. & Peters, R.J. 2014. Biosynthesis, elicitation and roles of monocot terpenoid phytoalexins. *The Plant Journal*. 79(4):659–678. DOI: 10.1111/tpj.12436.

Schnable, P.S., Ware, D., Fulton, R.S., Stein, J.C., Wei, F., Pasternak, S., Liang, C., Zhang, J., et al. 2009. The B73 maize genome: complexity, diversity, and dynamics. *Science*. 326(5956):1112–1115.

Schnee, C. 2002. The Maize Gene terpene synthase 1 Encodes a Sesquiterpene Synthase Catalyzing the Formation of (*E*)-beta -Farnesene, (*E)*-Nerolidol, and (*E,E*)-Farnesol after Herbivore Damage. *Plant Physiology*. 130(4):2049–2060. DOI: 10.1104/pp.008326.

Schnee, C., Köllner, T.G., Held, M., Turlings, T.C.J., Gershenzon, J. & Degenhardt, J. 2006. The products of a single maize sesquiterpene synthase form a volatile defense signal that attracts natural enemies of maize herbivores. *Proceedings of the National Academy of Sciences*. 103(4):1129–1134. DOI: 10.1073/pnas.0508027103.

Schneider, C.A., Rasband, W.S. & Eliceiri, K.W. 2012. NIH Image to ImageJ: 25 years of image analysis. *Nature methods*. 9(7):671–675.

Schoch, C.L., Seifert, K.A., Huhndorf, S., Robert, V., Spouge, J.L., Levesque, C.A., Chen, W., Fungal Barcoding Consortium, et al. 2012. Nuclear ribosomal internal transcribed spacer (ITS) region as a universal DNA barcode marker for Fungi. *Proceedings of the National Academy of Sciences*. 109(16):6241–6246. DOI: 10.1073/pnas.1117018109.

Sen, T.Z., Harper, L.C., Schaeffer, M.L., Andorf, C.M., Seigfried, T.E., Campbell, D.A. & Lawrence, C.J. (in press). Choosing a genome browser for a Model Organism Database: surveying the Maize community. *Database*. 2010(0):baq007-baq007. DOI: 10.1093/database/baq007.

Shoresh, M. & Harman, G.E. 2008. The Molecular Basis of Shoot Responses of Maize Seedlings to *Trichoderma harzianum* T22 Inoculation of the Root: A Proteomic Approach. *Plant Physiology*. 147(4):2147–2163. DOI: 10.1104/pp.108.123810.

Sikhakolli, U.R., López-Giráldez, F., Li, N., Common, R., Townsend, J.P. & Trail, F. 2012. Transcriptome analyses during fruiting body formation in *Fusarium graminearum* and *Fusarium verticillioides* reflect species life history and ecology. *Fungal Genetics and Biology*. 49(8):663–673. DOI: 10.1016/j.fgb.2012.05.009.

Small, I.M., Flett, B.C., Marasas, W.F.O., McLeod, A., Stander, M.A. & Viljoen, A. 2012. Resistance in maize inbred lines to *Fusarium verticillioides* and fumonisin accumulation in South Africa. *Plant Disease*. 96(6):881–888.

Sobowale, A.A., Cardwell, K.F., Odebode, A.C., Bandyopadhyay, R. & Jonathan, S.G. 2005. Growth inhibition of *Fusarium verticillioides* (Sacc.) Nirenberg by isolates of *Trichoderma pseudokoningii* strains from maize plant parts and its rhizosphere. *Plant Protection Res*. 45(4):249–266.

Sobowale, A.A., Cardwell, K.F., Odebode, A.C., Bandyopadhyay, R. & Jonathan, S.G. 2007. Persistence of *Trichoderma* species within maize stem against *Fusarium verticillioides*. *Archives Of Phytopathology And Plant Protection*. 40(3):215–231. DOI: 10.1080/03235400500424596.

Sobowale, A.A., Odebode, A.C., Cardwell, K.F., Bandyopadhyay, R. & Jonathan, S.G. 2010. Antagonistic potential of *Trichoderma longibrachiatum* and *T. hamatum* resident on maize (*Zea mays*) plant against *Fusarium verticillioides* (Nirenberg) isolated from rotting maize stem. *Archives Of Phytopathology And Plant Protection*. 43(8):744–753. DOI: 10.1080/03235400802175904.

Srivasta, A., Mehta, S., Lindlof, A. & Bhargava, S. 2010. Over-represented promoter motifs in abiotic stress-induced DREB genes of rice and sorghum and their probable role in regulation of gene expression. *Plant Signaling & Behavior*. 5(7):775–784. DOI: 10.4161/psb.5.7.11769.

Steyaert, J.M., Weld, R.J. & Stewart, A. 2010. Isolate-specific conidiation in *Trichoderma* in response to different nitrogen sources. *Fungal Biology*. 114(2–3):179–188. DOI: 10.1016/j.funbio.2009.12.002.

Strange, R.N. & Scott, P.R. 2005. Plant Disease: A Threat to Global Food Security. *Annual Review of Phytopathology*. 43(1):83–116. DOI: 10.1146/annurev.phyto.43.113004.133839.

Sun, G., Wang, S., Hu, X., Su, J., Huang, T., Yu, J., Tang, L., Gao, W., et al. 2007. Fumonisin B_1 contamination of home-grown corn in high-risk areas for esophageal and liver cancer in China. *Food Additives and Contaminants*. 24(2):181–185. DOI: 10.1080/02652030601013471.

Sydenham, E.W., Thiel, P.G., Marasas, W.F., Shephard, G.S., Van Schalkwyk, D.J. & Koch, K.R. 1990. Natural occurrence of some *Fusarium* mycotoxins in corn from low and high esophageal cancer prevalence areas of the Transkei, Southern Africa. *Journal of Agricultural and Food Chemistry*. 38(10):1900–1903.

Tang, D., Wang, G. & Zhou, J.-M. 2017. Receptor Kinases in Plant-Pathogen Interactions: More Than Pattern Recognition. *The Plant Cell*. 29(4):618–637. DOI: 10.1105/tpc.16.00891.

The UniProt Consortium. 2017. UniProt: the universal protein knowledgebase. *Nucleic Acids Research*. 45(D1):D158–D169. DOI: 10.1093/nar/gkw1099.

Thiel, P.G., Marasas, W.F., Sydenham, E.W., Shephard, G.S. & Gelderblom, W.C. 1992. The implications of naturally occurring levels of fumonisins in corn for human and animal health. *Mycopathologia*. 117(1–2):3–9.

Tucci, M., Ruocco, M., De Masi, L., De Palma, M. & Lorito, M. 2011. The beneficial effect of *Trichoderma* spp. on tomato is modulated by the plant genotype: Plant genotype-*Trichoderma* interaction. *Molecular Plant Pathology*. 12(4):341–354. DOI: 10.1111/j.1364-3703.2010.00674.x.

United States Department of Agriculture, Foreign Agricultural Service. 2017. *Grain: World Markets and Trade*. United States Department of Agriculture, Foreign Agricultural Service. Available: https://apps.fas.usda.gov/psdonline/circulars/grain-corn-coarsegrains.pdf [2017, June 26].

VanEtten, H.D., Mansfield, J.W., Bailey, J.A. & Farmer, E.E. 1994. Two Classes of Plant Antibiotics: Phytoalexins versus“ Phytoanticipins”. *The Plant Cell*. 6(9):1191.

Varieties. 2015. Available: http://dtma.cimmyt.org/index.php/varieties/dt-maize-varieties.

Vaughan, M.M., Huffaker, A., Schmelz, E.A., Dafoe, N.J., Christensen, S., Sims, J., Martins, V.F., Swerbilow, J., et al. 2014. Effects of elevated [CO_2] on maize defence against mycotoxigenic *Fusarium verticillioides*. *Plant, Cell & Environment*. 37(12):2691–2706. DOI: 10.1111/pce.12337.

Vaughan, M.M., Christensen, S., Schmelz, E.A., Huffaker, A., Mcauslane, H.J., Alborn, H.T., Romero, M., Allen, L.H., et al. 2015. Accumulation of terpenoid phytoalexins in maize roots is associated with drought tolerance. *Plant, Cell & Environment*. 38(11):2195–2207. DOI: 10.1111/pce.12482.

Vegetative Corn Growth Stages and Scouting Tips. 2017. Available: https://www.pioneer.com/home/site/us/agronomy/crop-management/crop-growth-stages/corn-growth-stages/vegetative/.

Vlot, A.C., Dempsey, D.A. & Klessig, D.F. 2009. Salicylic Acid, a Multifaceted Hormone to Combat Disease. *Annual Review of Phytopathology*. 47(1):177–206. DOI: 10.1146/annurev.phyto.050908.135202.

Vollbrecht, E., Duvick, J., Schares, J.P., Ahern, K.R., Deewatthanawong, P., Xu, L., Conrad, L.J., Kikuchi, K., et al. 2010. Genome-Wide Distribution of Transposed *Dissociation* Elements in Maize. *The Plant Cell*. 22(6):1667–1685. DOI: 10.1105/tpc.109.073452.

Vos, C.M.F., De Cremer, K., Cammue, B.P.A. & De Coninck, B. 2015. The toolbox of *Trichoderma* spp. in the biocontrol of *Botrytis cinerea* disease: *Trichoderma* biocontrol of *Botrytis cinerea* disease. *Molecular Plant Pathology*. 16(4):400–412. DOI: 10.1111/mpp.12189.

Wagacha, J.M. & Muthomi, J.W. 2008. Mycotoxin problem in Africa: Current status, implications to food safety and health and possible management strategies. *International Journal of Food Microbiology*. 124(1):1–12. DOI: 10.1016/j.ijfoodmicro.2008.01.008.

White, T.J., Bruns, T., Lee, S. & Taylor, J. 1990. Amplification and direct sequencing of fungal ribosomal RNA genes for phylogenetics. *PCR protocols: a guide to methods and applications*. 18(1):315–322.

Wighard, S.S. 2017. Characterisation of a maize mutant deficient in antifungal kauralexin accumulation. Master of Science thesis. University of Cape Town.

World of Corn. 2017. *Corn Usage by Segment*. Available: http://www.worldofcorn.com/#corn-usage-by-segment [2017, June 26].

Wu, F. 2006. Mycotoxin Reduction in Bt Corn: Potential Economic, Health, and Regulatory Impacts. *Transgenic Research*. 15(3):277–289. DOI: 10.1007/s11248-005-5237-1.

Xiang, K., Zhang, Z.M., Reid, L.M., Zhu, X.Y., Yuan, G.S., Pan, G.T. & others. 2010. A meta-analysis of QTL associated with ear rot resistance in maize. *Maydica*. 55(3):281.

Xing, H., Pudake, R.N., Guo, G., Xing, G., Hu, Z., Zhang, Y., Sun, Q. & Ni, Z. 2011. Genome-wide identification and expression profiling of auxin response factor (ARF) gene family in maize. *BMC genomics*. 12(1):178.

Yedidia, I., Shoresh, M., Kerem, Z., Benhamou, N., Kapulnik, Y. & Chet, I. 2003. Concomitant Induction of Systemic Resistance to *Pseudomonas syringae* pv. lachrymans in Cucumber by *Trichoderma asperellum* (T-203) and Accumulation of Phytoalexins. *Applied and Environmental Microbiology*. 69(12):7343–7353. DOI: 10.1128/AEM.69.12.7343-7353.2003.

SUPPLEMENTARY DATA

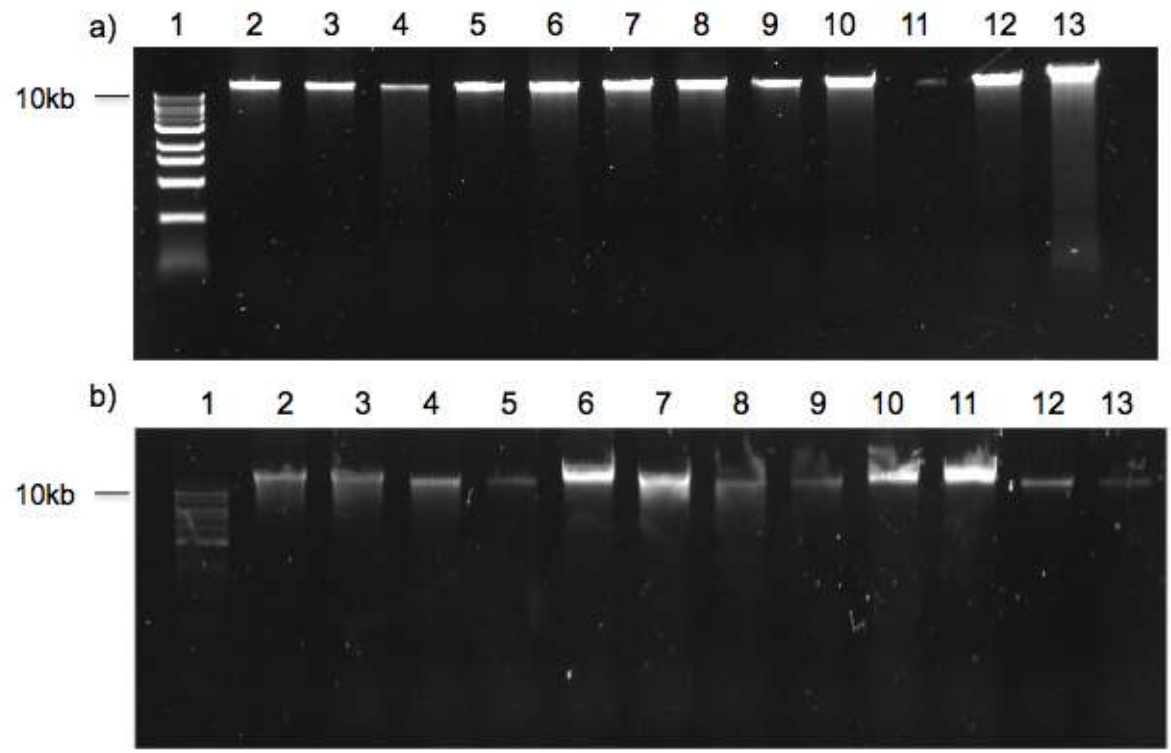

Figure S2.1 Gel electrophoresis of DNA extracted from maize lines. Lane 1: 10kb ladder (New England Biolabs, Ipswich, United States), a) Sample DNA extracted from B73 tissue in the optimisation experiment (lanes 2-5) and time point experiment (lanes 6-13), b) Sample DNA extracted from CML444 (lanes 2-9), CB248 (lanes 10-11) and ZM401 (lanes 12-13).

Table S2.1 Steps taken for analysis of alanyl tRNA synthetase (GRMZM2G140754)

Step	Action	Result
1	RT-qPCR	standard curve failed, lower concentrations not sufficient for detection
2	Repeat RT-qPCR, increased cDNA concentration	standard curve failed, concentration still too low for detection of some points
3	PCR on DNA to ensure that primers bind	expected band size on gel electrophoresis
4	End-point PCR on cDNA	Primer dimers
5	Repeat End-point PCR on cDNA, lowered primer concentration	Less primer dimer, no band

Table S2.2 The calculated M and CV values showing the reference gene stability for each experiment

	Ref genes used	M	CV
B73 optimisation	***ZmLUG/ZmMEP***	0.728	0.261
		0.384	0.133
B73 time point experiment shoots	***ZmLUG/ZmMEP***	1.141	0.395
B73 time point experiment roots	***ZmLUG/ZmMEP***	1.304	0.490
		0.966	0.332
CML444 time point experiment shoots	***ZmGST3/RPOL***	0.808	0.285
		0.961	0.348
CML444 time point experiment roots	***ZmGST3/RPOL***	0.908	0.327
CB248	***ZmLUG/ZmMEP***	0.698	0.239

Table S2.3 The R, R^2 and E values from the standard curves of candidate and reference genes following RT-qPCR

		ZmAn2	*ZmCYP81A1*	*ZmKO*	*ZmKSL2*	*ZmKSL4*	*ZmTPS11*	*ZmGST3*	*ZmLUG*	*ZmMEP*	*ZmRPOL*
B73 optimisation	R		0.95	0.99	0.99		0.98		0.98	0.99	
	R^2		0.90	0.97	0.98		0.96		0.95	0.97	
	E		1.11	0.99	1.10		1.01		1.01	0.97	
	R	0.95				0.99			0.98	0.99	
	R^2	0.90				0.97			0.95	0.98	
	E	1.09				1.13			1.06	1.06	
B73 time point experiment shoots	R	0.97	0.99	1.00	0.99	0.99	0.99		0.98	0.99	
	R^2	0.95	0.98	0.99	0.99	0.98	0.98		0.96	0.98	
	E	0.93	0.94	0.90	0.95	0.94	0.90		1.09	0.92	
B73 time point experiment roots	R	0.98	0.99		1.00		1.00		0.99	0.99	
	R^2	0.96	0.97		1.00		0.99		0.98	0.97	
	E	0.89	1.09		1.10		0.92		0.95	1.16	
	R			0.99		0.99			0.98	0.99	
	R^2			0.98		0.99			0.96	0.98	
	E			1.01		1.06			0.98	0.96	

		ZmAn2	*ZmCYP81A1*	*ZmKO*	*ZmKSL2*	*ZmKSL4*	*ZmTPS11*	*ZmGST3*	*ZmLUG*	*ZmMEP*	*ZmRPOL*
CML444 time point experiment shoots	R	0.98	0.99	0.97	0.96	0.99		1.00			1.00
	R^2	0.96	0.98	0.95	0.92	0.98		1.00			1.00
	E	0.92	0.97	1.00	1.03	1.05		1.07			0.96
	R						0.98	0.99			0.99
	R^2						0.95	0.99			0.98
	E						0.96	0.99			0.99
CML444 time point experiment roots	R	0.99	0.98	0.98	0.99	0.98	0.99	0.99			0.99
	R^2	0.99	0.96	0.96	0.98	0.97	0.97	0.98			0.98
	E	1.05	0.96	1.04	1.04	0.94	0.99	0.90			1.05
CB248	R	0.99	0.99	0.98	0.95	0.97	0.98		0.99	0.98	
	R^2	0.99	0.99	0.97	0.91	0.93	0.97		0.99	0.97	
	E	0.99	0.99	0.94	1.08	0.90	1.05		1.03	0.99	
ZM401	R	0.99	0.99	0.98	0.99	1.00	0.99		0.98		
	R^2	0.99	0.99	0.96	0.98	0.99	0.97		0.97		
	E	1.06	0.91	0.98	0.92	0.92	0.97		1.07		

Where R, R^2 and E values are given in two rows for one tissue type, two sets of cDNA were used. Reference gene expression was reanalysed with every new set of cDNA.

Table S2.4 Accumulation of kauralexin A1, A2, A3, B1, B2, B3 compounds and zealexin A1 and B1 compounds

	Time point	Treatment	KA1 (µg.gFW^{-1})	KA2 (µg.gFW^{-1})	KA3 (µg.gFW^{-1})	KB1 (µg.gFW^{-1})	KB2 (µg.gFW^{-1})	KB3 (µg.gFW^{-1})	ZA1 (µg.gFW^{-1})	ZB1 (µg.gFW^{-1})
B73 shoots	**10 days**	control	0,018	0,000	0,000	0,028	0,000	0,010	0,000	0,008
		F. verticillioides	0,000	0,000	0,000	0,028	0,010	0,000	0,000	0,000
	14 days	control	0,025	0,000	0,018	0,023	0,016	0,027	0,000	0,000
		F. verticillioides	0,032	0,010	0,019	0,069	0,088	0,112	0,000	0,000
B73 roots	**10 days**	control	1,775	0,156	0,544	6,905	0,720	1,498	0,024	0,038
		F. verticillioides	3,544	1,095	4,458	4,704	5,026	4,390	2,168	4,368
	14 days	control	0,015	0,012	0,017	0,039	**0,082**	**0,064**	**0,000**	**0,000**
		F. verticillioides	2,463	1,288	2,645	2,631	**8,364**	**5,045**	**0,376**	**1,100**
CML444 shoots	**10 days**	control	**0,008**	0,040	**0,050**	0,032	0,014	0,035	0,000	0,052
		F. verticillioides	**1,234**	0,844	**7,987**	0,369	0,524	1,575	0,027	0,102
	14 days	control	0,034	0,048	0,246	0,029	0,042	0,094	0,048	0,051
		F. verticillioides	0,605	0,116	2,309	0,281	0,112	**0,617**	0,028	0,057
CML444 roots	**10 days**	control	**0,741**	**0,087**	**1,353**	1,511	0,280	1,802	**0,000**	**0,000**
		F. verticillioides	**5,977**	**2,205**	**14,016**	1,577	0,825	2,207	**2,446**	**8,379**
	14 days	control	**0,191**	**0,065**	**0,760**	0,802	**0,415**	1,274	0,084	0,076
		F. verticillioides	**3,258**	**1,590**	**5,136**	0,960	**0,980**	1,860	0,979	**3,303**
CB248 roots	**10 days**	control	0,853	5,170	0,245	1,227	**0,496**	2,816	0,646	0,081
		F. verticillioides	4,734	5,473	3,015	5,375	**11,767**	10,288	14,715	1,922
ZM401 roots	**10 days**	control	13,693	3,114	0,444	0,186	0,770	**0,155**	2,140	1,935
		F. verticillioides	2,118	2,259	0,903	2,165	8,080	**3,025**	3,575	7,703

Bold, shaded blocks represent control and inoculated samples where phytoalexin compound accumulation is significantly different, green blocks correspond to shoots and brown blocks correspond to roots. An unpaired t test was performed to compare control and inoculated phytoalexin accumulation, $p<0.05$, $n=3$

a) *An2* RT-qPCR sequencing results

```
An2_RT-qPCR      1    GGCGGTGATCCGGAGGACATCATCCACAAGCTACTGAGATCAGCTTGGGCTGAATGGGTC  60
                      ||||||||||||||||||||||||||||||||||||||||||||||||||||||||||||
ZmAn2_mRNA       2684 GGCGGTGATCCGGAGGACATCATCCACAAGCTACTGAGATCAGCTTGGGCTGAATGGGTC  2743

An2_RT-qPCR      61   AGGGAGAAGGCAGATGCAGCAGACAGCGTGTGTAATGGATCCAGTGCTGTGGAACAAGA  119
                      ||||||||||||||||||||||||||||||||||||||||||||||||||||||||||||
ZmAn2_mRNA       2744 AGGGAGAAGGCAGATGCAGCAGACAGCGTGTGTAATGGATCCAGTGCTGTGGAACAAGA  2802
```

b) *KSL2* RT-qPCR sequencing results*

```
KSL2_RT-qPCR     1    GTTGATCAAGCCGCTCCAGATGGGAAGGAGACGAGAAGAAGATCAA  46
                      ||||||||||||||||||||||||||||||||||||||||||||||
uncharac         2355 GTTGATCAAGCCGCTCCAGATGGGAAGGAGACGAGAAGAAGATCAA  2400
```

c) *KO* RT-qPCR sequencing results

```
KO_RT-qPCR       1    AGTTTGCGTGGACGCTCAAGGAAGGCGACGAGGACAAGGACGACACCATCCAGCTTACAA  60
                      ||||||||||||||||||||||||||||||||||||||||||||||||||||||||||||
ZmKO2_mRNA       1503 AGTTTGCGTGGACGCTCAAGGAAGGCGACGAGGACAAGGACGACACCATCCAGCTTACAA  1562

KO_RT-qPCR       61   CCAACAGGCTTTACCCGTTGCATGTGTACCTCA  93
                      |||||||||||||||||||||||||||||||||
ZmKO2_mRNA       1563 CCAACAGGCTTTACCCGTTGCATGTGTACCTCA  1595
```

d) *TPS11* RT-qPCR sequencing results

```
TPS11_RT-qPCR    1    CTGTTGTTTACAACTCCAATTATGATGGTGGTAATTTGGACTTAGTTTCACGCCGATTCT  60
                      ||||||||||||||||||||||||||||||||||||||||||||||||||||||||||||
ZmTPS11_mRNA     290  CTGTTGTTTACAACTCCAATTATGATGGTGGTAATTTGGACTTAGTTTCACGCCGATTCT  349

TPS11_RT-qPCR    61   ATCTTCTGCGTAAATGTGGCTATCATGTT  89
                      |||||||||||||||||||||||||||||
ZmTPS11_mRNA     350  ATCTTCTGCGTAAATGTGGCTATCATGTT  378
```

e) *CYP81A1* RT-qPCR sequencing results

```
CYP81A1_RT-qPCR  1    ACGTAGTAGAATCTTTCCATGGTGGTTCGCTGTGGTGAAGCGGTGGTGATCAGCGTGCGA  60
                      ||||||||||||||||||||||||||||||||||||||||||||||||||||||||||||
ZmCYP81A1_mRNA   131  ACGTAGTAGAATCTTTCCATGGTGGTTCGCTGTGGTGAAGCGGTGGTGATCAGCGTGCGA  72

CYP81A1_RT-qPCR  61   TGAGC  65
                      |||||
ZmCYP81A1_mRNA   71   TGAGC  67
```

Figure S2.2 Sequence alignment of sequenced RT-qPCR products of putative phytoalexin biosynthetic genes in CML444 to NCBI BLASTn results. Top line represents sequencing results and bottom line represents the sequence of BLASTn result. a) *ZmAn2*, b) *ZmKSL2*, c) *ZmKO*, d) *ZmTPS11*, e) *ZmCYP81A1*. * *ZmKSL2* aligned to an uncharacterised gene on NCBI and was checked on Ensembl Plants, where the identity of the sequence was confirmed to be *ZmKSL2*

Table S2.5 Full list of maize lines grown in this study

			Control		Infected	
Maize line	**PR/S**	**Reference**	**Germination frequency (%)**	**Endophyte**	**Germination frequency (%)**	**Endophyte**
B73 (all experiments)	**PR**	**(Baldwin et al., 2014)**	**87,5**	**-**	**87,5**	**-**
CB222	PR	(Rose et al., 2017)	37,5	bacterial-like	12,5	-
CB248	**PR**	**(Rose et al., 2017)**	**65**	**bacterial-like**	**65**	**-**
CML182	PR	(Small et al., 2012)	25	bacterial-like	25	-
CML444 (all experiments)	**PR**	**(Small et al., 2012)**	**93,8**	**-**	**75**	**-**
R119W	PR	(Rose et al., 2017)	12,5	-	0	-
R2565Y	S	(Rose et al., 2017)	62,5	*Trichoderma*-like and bacterial-like	25	*Trichoderma*-like
RO549 W	PR	(Small et al., 2012)	50	bacterial-like	0	-
US2540W	PR	(Rose et al., 2017)	25	*Trichoderma*-like	12,5	*Trichoderma*-like
VO617Y-2	PR	(Small et al., 2012)	75	*Trichoderma*-like	25	-
ZM401	**PR**	("Varieties", 2015)	**75**	***T. asperellum***	**87,5**	**-**

PR = partially resistant, S = susceptible, bold maize lines were used in the study

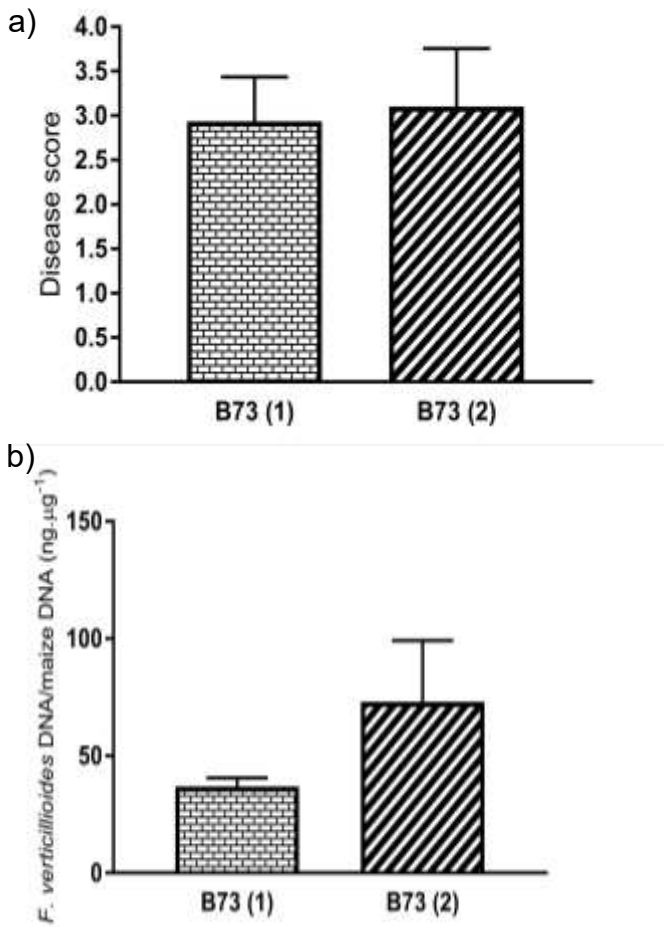

Figure S2.3 *F. verticillioides* inoculated B73 roots at ten dpi. a) Disease scores of inoculated roots, b) *F.* verticillioides growth in the roots, measured using *FvEF1α* and *ZmMEP* for to detect fungal and plant DNA respectively. B73 (1) is B73 grown simultaneously with CB248, B73 (2) is B73 grown simultaneously with ZM401

Table S3.1 NCBI BLASTn results from the *T. asperellum* sequencing reaction showing published *T. asperellum isolates*

Strain	BLASTn score	E value	% identity	Accession	Reference
Trichoderma asperellum isolate C	1020	0.0	100%	KM456217.1	Alvarado-Marchena & Rivera-Méndez, 2016
Trichoderma asperellum isolate B	1020	0.0	100%	KM456216.1	Alvarado-Marchena & Rivera-Méndez, 2016
Trichoderma asperellum isolate A	1020	0.0	100%	KM456214.1	Alvarado-Marchena & Rivera-Méndez, 2016
Trichoderma asperellum strain CHI3	1020	0.0	100%	KR868258.1	Saravanakumar et al., 2016
Trichoderma asperellum strain CHI4	1020	0.0	100%	KR868257.1	Saravanakumar et al., 2016
Trichoderma asperellum strain CHI5	1020	0.0	100%	KR868246.1	Saravanakumar et al., 2016
Trichoderma asperellum strain TBP1-FS03	1020	0.0	100%	KR296906.1	Ottenheim et al., 2015
Trichoderma asperellum strain PUXX-FS08	1020	0.0	100%	KR296889.1	Ottenheim et al., 2015
Trichoderma asperellum strain BPXX-FS02	1020	0.0	100%	KR296855.1	Ottenheim et al., 2015
Trichoderma asperellum strain APXX-FS10	1020	0.0	100%	KR296849.1	Ottenheim et al., 2015
Trichoderma asperellum isolate TV116	1020	0.0	100%	KP263616.1	Pavone Maniscalco & Dorta, 2015
Trichoderma asperellum isolate TV30	1020	0.0	100%	KP263555.1	Pavone Maniscalco & Dorta, 2015
Trichoderma asperellum strain TR696	1020	0.0	100%	KC993073.1	Geraldine et al., 2013

```
consensus          1    TCATTACCGAGTTTACAACTCCCAAACCCAATGTGAACGTTACCAAACTGTTGCCTCGGC  60
                        ||||||||||||||||||||||||||||||||||||||||||||||||||||||||||||
T.asperellumRah4   35   TCATTACCGAGTTTACAACTCCCAAACCCAATGTGAACGTTACCAAACTGTTGCCTCGGC  94

consensus          61   GGGGTCACGCCCCGGGTGCGTCGCAGCCCCGGAACCAGGCGCCCGCCGGAGGAACCAACC  120
                        ||||||||||||||||||||||||||||||||||||||||||||||||||||||||||||
T.asperellumRah4   95   GGGGTCACGCCCCGGGTGCGTCGCAGCCCCGGAACCAGGCGCCCGCCGGAGGAACCAACC  154

consensus          121  AAACTCTTTCTGTAGTCCCCTCGCGGACGTATTTCTTACAGCTCTGAGCAAAAATTCAAA  180
                        ||||||||||||||||||||||||||||||||||||||||||||||||||||||||||||
T.asperellumRah4   155  AAACTCTTTCTGTAGTCCCCTCGCGGACGTATTTCTTACAGCTCTGAGCAAAAATTCAAA  214

consensus          181  ATGAATCAAAACTTTCAACAACGGATCTCTTGGTTCTGGCATCGATGAAGAACGCAGCGA  240
                        ||||||||||||||||||||||||||||||||||||||||||||||||||||||||||||
T.asperellumRah4   215  ATGAATCAAAACTTTCAACAACGGATCTCTTGGTTCTGGCATCGATGAAGAACGCAGCGA  274

consensus          241  AATGCGATAAGTAATGTGAATTGCAGAATTCAGTGAATCATCGAATCTTTGAACGCACAT  300
                        ||||||||||||||||||||||||||||||||||||||||||||||||||||||||||||
T.asperellumRah4   275  AATGCGATAAGTAATGTGAATTGCAGAATTCAGTGAATCATCGAATCTTTGAACGCACAT  334

consensus          301  TGCGCCCGCCAGTATTCTGGCGGGCATGCCTGTCCGAGCGTCATTTCAACCCTCGAACCC  360
                        ||||||||||||||||||||||||||||||||||||||||||||||||||||||||||||
T.asperellumRah4   335  TGCGCCCGCCAGTATTCTGGCGGGCATGCCTGTCCGAGCGTCATTTCAACCCTCGAACCC  394

consensus          361  CTCCGGGGGATCGGCGTTGGGGATCGGGACCCCTCACACGGGTGCCGGCCCCGAAATACA  420
                        ||||||||||||||||||||||||||||||||||||||||||||||||||||||||||||
T.asperellumRah4   395  CTCCGGGGGATCGGCGTTGGGGATCGGGACCCCTCACACGGGTGCCGGCCCCGAAATACA  454

consensus          421  GTGGCGGTCTCGCCGCAGCCTCTCCTGCGCAGTAGTTTGCACAACTCGCACCGGGAGCGC  480
                        ||||||||||||||||||||||||||||||||||||||||||||||||||||||||||||
T.asperellumRah4   455  GTGGCGGTCTCGCCGCAGCCTCTCCTGCGCAGTAGTTTGCACAACTCGCACCGGGAGCGC  514

consensus          481  GGCGCGTCCACGTCCGTAAAACACCCAACTTTCTGAAATGTTGACCTCGGATCAGGTAGG  540
                        ||||||||||||||||||||||||||||||||||||||||||||||||||||||||||||
T.asperellumRah4   515  GGCGCGTCCACGTCCGTAAAACACCCAACTTTCTGAAATGTTGACCTCGGATCAGGTAGG  574

consensus          541  AATACCCGCTGA  552
                        ||||||||||||
T.asperellumRah4   575  AATACCCGCTGA  586
```

Figure S3.1 Sequence alignment of consensus sequence following *ITS1* and *ITS4* PCR product sequencing to NCBI BLASTn results. Top line represents consensus sequence and bottom line represents the sequence of BLASTn result (*T. asperellum* Rah4). The sequence is aligned to a part of the ITS1 region, the 5.8S rDNA and the ITS2 region.

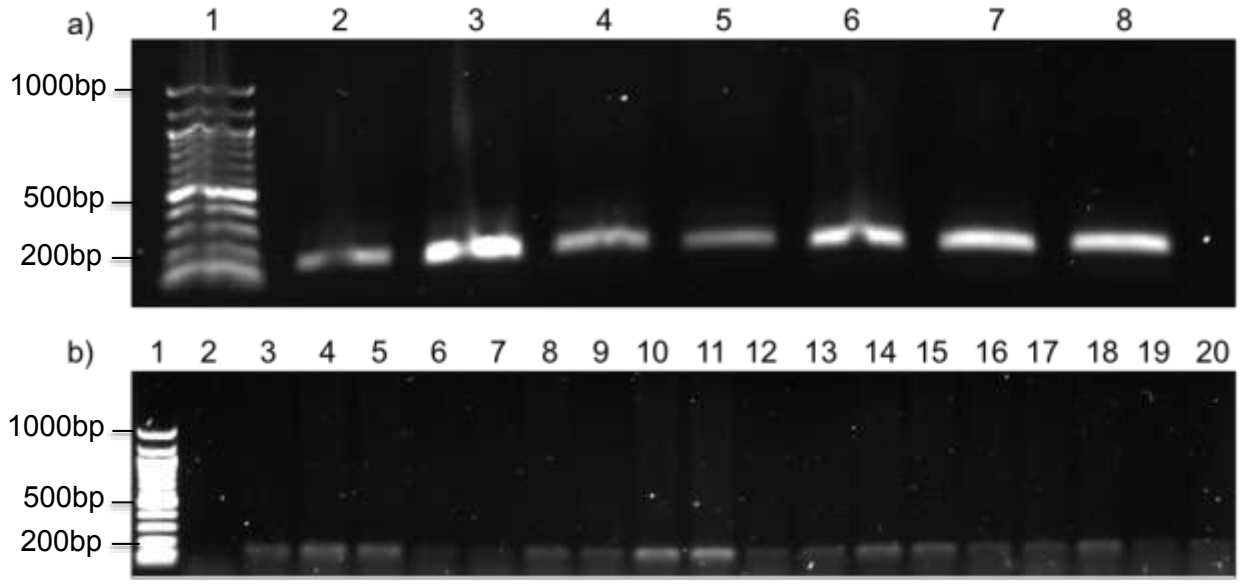

Figure S3.2 Gel elctrophoresis of a) *T. asperellum* and b) *ZmCYP81A1* PCR products. a) Lane 1: 100bp ladder (New England Biolabs (NEB), Ipswich, United States), lanes 2-8: *T. asperellum* DNA, NTC in lane 20 (Figure 3.3), b) lane 1: 100bp ladder (NEB, Ipswich, United States), lane 2: NTC, lane 3-8: B73 DNA, lanes 8-14: CML444 DNA, lanes 15-17: CB248 DNA, lanes 18-20: ZM401

```
T.asp_seq    1    TTCGCTGCGTTCTTCATCGATGCCAGAACCAAGAGATCCGTTGTTGAAAGTTTTGATTCA  60
                  ||||||||||||||||||||||||||||||||||||||||||||||||||||||||||||
T.asp_E465   281  TTCGCTGCGTTCTTCATCGATGCCAGAACCAAGAGATCCGTTGTTGAAAGTTTTGATTCA  222

T.asp_seq    61   TTTTGAATTTTTGCTCAGAGCTGTAAGAAATACGTC  96
                  |||||||||||||||||||||||||||||||||||
T.asp_E465   221  TTTTGAATTTTTGCTCAGAGCTGTAAGAAATACGTC  186
```

Figure S3.3 Sequence alignment of the *T. asperellum* primer sequencing results to NCBI BLASTn results. The top hit aligned to *T. asperellum* isolate E-465